UNIVERSITY OF CALIFORNIA
RIVERSIDE

Mechanical Control of Retinal Vascular Inflammation in Diabetes

A Dissertation submitted in partial satisfaction
of the requirements for the degree of

Doctor of Philosophy

in

Bioengineering

by

Xiao Yang

March 2016

Dissertation Committee:
Dr. Kaustabh Ghosh, Chairperson
Dr. Jiayu Liao
Dr. Ilhem Messaoudi

The Dissertation of Xiao Yang is approved:

_____

_____

_____

Committee Chairperson

University of California, Riverside

Acknowledgements

I would like to express my special appreciation and thanks to my advisor Professor Dr. Kaustabh Ghosh. Dr. Ghosh has been a tremendous mentor. I would like to thank him for encouraging my research, for allowing me to grow as a research scientist, and for motivating me to pursue a successful research career. His advices are invaluable, which have not only helped me on research experiments, but as well as on my future career. I would also like to thank my collaborators, Dr. Timothy S. Kern and Dr. Arup Das, for their support and help on my animal studies. I would also like to acknowledge my committee members, Dr. Jiayu Liao and Dr. Ilhem Messaoudi for serving on my committee and for the time and efforts they put in.

I would also like to thank my laboratory members and colleagues: Harry Scott, Soroush Ardekani, Andrea Cabrera, Arun Bhaskaran, Jun Xu and Shane Eum. I would like to acknowledge them for their constant help with my research experiments. Finally, portion of Chapter 1 and Chapter 2 has been previously published in the *FASEB* journal, and the permission to re-use the work has been granted by the publisher, *Federation of American Societies for Experimental Biology (FASEB)*.

Finally, I would like to express my sincere gratitude to my parents for providing me all the love and supports. Without their constant motivation and help, I would not have been as confident, productive and successful.

ABSTRACT OF THE DISSERTATION

Mechanical Control of Retinal Vascular Inflammation in Diabetes

by

Xiao Yang

Doctor of Philosophy, Bioengineering
University of California, Riverside, March 2016
Dr. Kaustabh Ghosh, Chairperson

The goal of this research was to understand the role of cell- and subendothelial matrix-dependent mechanical cues in retinal endothelial cell (EC) activation associated with diabetes and to identify novel molecular targets for effective suppression of diabetic retinal EC activation. Endothelial activation is a hallmark of high glucose (HG)-induced retinal inflammation associated with diabetic retinopathy. Here I identified that HG-induced upregulation of lysyl oxidase (LOX), a collagen-crosslinking enzyme, in retinal capillary endothelial cells (ECs) leads to subendothelial matrix stiffening that, in turn, promotes retinal EC activation. Further, I showed that (i) HG-induced subendothelial matrix stiffening significantly impairs Transient Receptor Potential Vanilloid 4 (TRPV4, a mechanosensitive Ca^{2+} channel) expression and activity, (ii) TRPV4 impairment alone is sufficient to promote high glucose-induced retinal EC activation, (iii) LOX inhibition prevents high glucose-induced impairment of TRPV4 and, consequently, anti-

inflammatory nitric oxide. Finally, I showed that the effect of matrix stiffening-dependent TRPV4 impairment on retinal EC activation is mediated, at least in part, via the canonical Rho/ROCK mechanotransduction pathway that directly controls EC stiffness. More importantly, there is a feedback mechanism between TRPV4 and Rho/ROCK signaling pathways and it is likely to exacerbate retinal capillary stiffening and inflammation associated with DR. Together, these findings identify a crucial role of TRPV4-mediated Rho/ROCK signaling in diabetic retinal inflammation and implicate TRPV4 as the novel anti-inflammatory target for management of early DR.

Table of Contents

List of Schematics ..…….…. ix

List of Figures ……...…. x

List of Abbreviations …… xiii

CHAPTERS

1. INTRODUCTION……...….. 1

Preface ……..…… 1
Background and Significance…….…….. 2
Pathophysiology of DR …….....…… 2
Current Treatments for DR ……..…… 3
Inflammation and DR ……..……..……... 4
Potential Role of Subendothelial Matrix Stiffening in
EC Activation …… 5
Hypothesis…….... 6
Schematics 1.1 -1.2 ……..……..... 7
References ……..……..… 9

2. Basement Membrane Stiffening Promotes Retinal Endothelial Activation
Associated with Diabetes ……..…… 13

Preface ……..…..... 13
Introduction …….. 14
Materials and Methods …….……. 16
Results ……..…. 24
Discussion …….…. 29
Conclusion …… 34
Figures 2.1 – 2.10 …….…. 36
References ……..…. 49

3. Loss of Mechanosensitive TRPV4 Mediates Mechanical Control of
Diabetic Retinal Endothelial Activation ……... 55

Preface …….. 55

Introduction …….. 56
Materials and Methods …… 57
Results …… 65
Discussion …… 71
Conclusion …… 74
Figures 3.1 – 3.10 …… 75
References …… 87

4. TRPV4-mediated Rho/ROCK Signaling in Diabetes-induced Retinal Endothelial Activation ..…… ……..… 91

Preface …….. 91
Introduction …….. 92
Materials and Methods …… 92
Results ……...…….. 96
Discussion …… 99
Conclusion …… 102
Figures 4.1 – 4.6…….. 104
References …… 110

5. CONCLUSION ……..… 112
Working Model ……..……..…… 113
Future Directions ……..……..……. 116
Schematic 5.1 ……..……..…… 120
References ……..……..……..…… 121

List of Schematics

Schematic 1.1. Illustration of DR progression ……..... 7

Schematic 1.2. Alterations in Matrix Stiffness and Associated Mechanotransduction Govern Endothelial Function ……... 8

Schematic 5.1. Illustration of mechanisms in subendothelial matrix stiffness-dependent EC activation ……... 120

List of Figures

Figure 2.1. Retinal endothelial activation is a chief characteristic of diabetes …… 36

Figure 2.2. Diabetes is associated with significant increase in retinal subendothelial matrix crosslinking and stiffening ……..… 38

Figure 2.3. HG enhances LOX activity in retinal ECs ……...… 40

Figure 2.4. Inhibition of HG-induced retinal subendothelial matrix stiffening prevents monocyte-EC adhesion …… 41

Figure 2.5. Inhibition of LOX activity prevents HG-induced retinal subendothelial matrix thickening …….....……..... 42

Figure 2.6. LOX inhibition reverses the inflammatory effects of HG-induced subendothelial matrix stiffening …….....……..... 43

Figure 2.7. Inhibition of HG-induced subendothelial matrix stiffening prevents NF-κB activation and restores endothelial NO production ……..... 44

Figure 2.8. HG-induced subendothelial matrix stiffening alone can promote retinal EC activation …….. …… 45

Figure 2.9. Subendothelial matrix stiffening is sufficient to enhance endothelial NF-κB activation …….. 46

Figure 2.10. Subendothelial matrix stiffening is necessary and sufficient for HG-induced retinal EC activation ……..…... 47

Figure 3.1. Diabetes induces retinal EC activation ……... 75

Figure 3.2. Diabetes leads to loss of mechanosensitive TRPV4 in retinal ECs …… 76

Figure 3.3. Downregulation of mechanosensitive TRPV4 is associated with HG-induced retinal EC activation ……...…… 77

Figure 3.4. Inhibition of LOX-dependent subendothelial matrix stiffening rescues loss of TRPV4 under high glucose conditions ……... 78

Figure 3.5. Subendothelial matrix stiffening alone is sufficient to inhibit TRPV4 activity ……..……. 80

Figure 3.6. Increase in TRPV4 activity mediates the anti-inflammatory effects of LOX inhibition on HG-treated ECs ……. 82

Figure 3.7. Inhibition of retinal capillary and subendothelial matrix stiffening prevents retinal endothelial TRPV4 impairment and retinal EC activation …….….. 83

Figure 3.8. Pharmacological enhancement of TRPV4 activity reverses the effect of subendothelial matrix stiffness on endothelial NO production ……..…… 84

Figure 3.9. Pharmacological enhancement of TRPV4 activity reverses the effect of subendothelial matrix stiffness on retinal EC activation ……...……..… 85

Figure 3.10. Pharmacological enhancement of TRPV4 activity reverses the effect of matrix stiffness-dependent retinal EC activation ……...……. 86

Figure 4.1. HG treatment increases EC stiffness ……..… 104

Figure 4.2. Rho/ROCK2 and TRPV4 is upregulated in HG-treated ECs …… 105

Figure 4.3. Pharmacological enhancement of TRPV4 activity inhibits Rho activity and EC stiffening in HG-treated ECs ……..……..... 106

Figure 4.4. Inhibition of ROCK2 restores TRPV4 activity in HG-treated ECs ….. 107

Figure 4.5. Inhibition of Rho/ROCK restores NO production in HG-treated ECs via an increase in TRPV4 ……..... 108

Figure 4.6. Inhibition of Rho/ROCK suppresses activation of HG-treated ECs via an increase in TRPV4 …….. 109

List of Abbreviations

AFM	Atomic force microscope
BM	Basement membrane
BAPN	β-aminopropionitrile
CAM	Cell adhesion molecules
DR	Diabetic retinopathy
EC	Endothelial cell
eNOS	Endothelial nitric oxide synthase
FA	Focal adhesion
FBS	Fetal bovine serum
GSK	GSK1016790A
HG	High glucose
ICAM-1	Intercellular cell adhesion molecules 1
LOX	Lysyl oxidase
NO	Nitric oxide
PFA	Paraformaldehyde
PBMs	Peripheral blood monocytes
ROCK	Rho-associated Kinase
RN	RN1734
STZ	Streptozotocin
TNF-α	Tumor necrosis factor-α

VEGF	Vascular endothelial growth factor
Y27	Y27632
HIF-1	Hypoxia inducible factor-1
CaM	Calmodulin
CaMKII	Calmodulin kinase II
IKK	Inhibitory κB kinase
GEF	Guanine nucleotide exchange factor

CHAPTER 1

INTRODUCTION

Preface

This Chapter discusses the role of subendothelial matrix stiffness in EC function and implicates its role in diabetic retinal inflammation. The global aim of this doctoral research is to understand the role of cell- and extracellular matrix-dependent mechanical cues in retinal vascular inflammation associated with diabetes and to identify novel molecular targets for effective suppression of diabetic retinal vascular inflammation.

Background and Significance

Diabetic retinopathy (DR) is a prevalent and debilitating microvascular complication of diabetes that leads to progressive loss of vision. It is the leading cause of blindness in the working-age population (20-64 years old), affecting nearly 40% of all individuals with diabetes (1-4). Given that diabetes has reached epidemic proportions, the number of individuals expected to suffer from DR is expected to rise astronomically. Yet, despite numerous efforts, DR management has been difficult to achieve. A better understanding of DR pathophysiology is thus essential to develop new and more effective therapies for this debilitating condition.

Pathophysiology of DR

DR is a microvascular disease resulting from abnormal changes in retinal capillaries (Schematic 1.1). The early stage of DR is characterized by an increase in leukocyte adhesion to retinal blood vessels (leukostasis) that, in turn, leads to capillary degeneration (5). The adherent leukocytes subsequently release pro-inflammatory and vascular permeability factors, such as TNF-α, IL-1β, IL-6, IL-8 and endothelial growth factor (VEGF), that together disrupt the blood-retinal barrier, leading to an increase in vascular permeability that culminates in macular edema (nonproliferative DR) (5, 6). Further, leukostasis-mediated EC apoptosis leads to the formation of acellular capillaries that eventually regress (6, 7). The resulting local retinal ischemia, in turn, leads to compensatory vessel multiplication (proliferative DR) (8). Notably, both macular edema

and excessive vessel multiplication (neovascularization) are characteristics of advanced stages of DR and are common causes for vision loss in DR.

Current Treatments for DR

Clinically there are several therapeutic approaches to inhibit the development or progression of the DR. For the earlier stages of DR, the main approach is to manage by control hyperglycemia (9, 10), blood pressure and lipids (10-12). However, it has been very difficult to maintain normal metabolic control in many diabetic patients. Recent studies have also challenged the beneficial effect of lipid or blood pressure control (13, 14).

Current pharmacological treatments for advanced stages of DR focus predominantly on the inhibition of vascular endothelial growth factor (VEGF), a potent hyperpermeability and neovascularization factor that is significantly elevated in DR subjects (15). VEGF also stimulates increased leukostasis in retinal microvessels where the adherent leukocytes release cytokines and toxic factors to enhance endothelial permeability and cause retinal EC death (5). Despite these critical roles of VEGF in DR pathogenesis, anti-VEGF therapies are effective in treating proliferative DR, they only produce transient benefit in individuals with diabetic macular edema (16). Intravitreal injection of steriods have been found to work well in DR patients with late-stage macular edema, however, steroids exert side effects such as increased intraocular pressure and cataract formation (17, 18).

Alternative nonpharmacological approaches for DR management include laser photocoagulation and vitrectomy, which aim to surgically eliminate abnormal blood vessels, reduce fluid leakage in the retina, and remove blood in case of severe bleeding (19, 20). However, these treatments have a major limitation in that they may reduce color and night vision (20). Collectively, these limitations of current DR therapies emphasize the need to better understand the mechanisms governing DR so that more effective therapeutic approaches can be developed.

Inflammation and DR

Growing evidence indicates that DR is a multifactorial condition that is strongly regulated by retinal inflammation (5, 15). A critical early step in diabetic retinal inflammation is the activation of retinal capillary endothelial cells (EC) (5, 21). Activated retinal ECs upregulate cell adhesion molecules (CAMs) such as intercellular CAM (ICAM-1) to promote leukocyte-EC adhesion (leukostasis).

Recent *in vivo* studies have implicated EC activation as a critical early step in DR pathogenesis (6). Specifically, blocking endothelial ICAM-1 alone prevents diabetic retinal leukostasis and vascular hyperpermeability in animal models of DR (21), thereby implicating retinal EC activation as a major determinant of DR pathogenesis. Thus, while anti-ICAM-1 therapies are currently being explored for DR treatment, a deeper understanding of the mechanisms regulating EC activation is required so additional molecular targets can be identified for effective DR management.

Potential Role of Subendothelial Matrix Stiffening in EC Activation

Past studies aimed at understanding diabetic retinal EC activation have focused largely on the role of abnormal epigenetic, metabolic, and inflammatory factors (5, 22). However, a recent study reported that diabetic rat retinal ECs express increased levels of lysyl oxidase (LOX) (23), a copper-dependent enzyme that crosslinks collagen and enhances extracellular matrix stiffness (24). Notably, LOX overexpression and associated increase in extracellular matrix stiffness have been shown to promote endothelial dysfunction resulting in lung vascular hyperpermeability (25). Whether LOX upregulation in diabetic retinal ECs leads to subendothelial matrix stiffening and EC activation, however, remains unknown.

It is important to examine this previously-unknown role of subendothelial matrix stiffening in leukocyte-retinal EC adhesion because subendothelial matrix stiffness alone can govern EC fate and function (26). This is because EC adhesion to the underlying subendothelial matrix generates cytoskeletal tension that is exerted on and balanced by cell-matrix adhesions whose strength, in turn, is proportional to subendothelial matrix stiffness (Schematic 1.2A). The ensuing force balance at cell-matrix adhesion complexes initiates mechanotransduction (Schematic 1.2B), the process by which mechanical cues are transduced into intracellular biochemical signaling to produce a global cellular response (Schematic 1.2C) (27). Indeed, alterations in subendothelial matrix stiffness alone have been shown to cause lung vascular hyperpermeability and edema (25, 28), atherosclerosis (29), and tumor growth and metastasis (30). These findings, together with the observation

that diabetic aortas that exhibit extensive leukocyte adhesion also undergo significant BM stiffening (31), raise the intriguing possibility of a causal relationship between aberrant subendothelial matrix stiffening and increased EC activation associated with DR.

Hypothesis

Based on these findings, **the working hypothesis** of this doctoral dissertation is that diabetes-induced retinal capillary stiffening and associated mechanotransduction actively contribute to retinal endothelial activation and inflammation associated with DR.

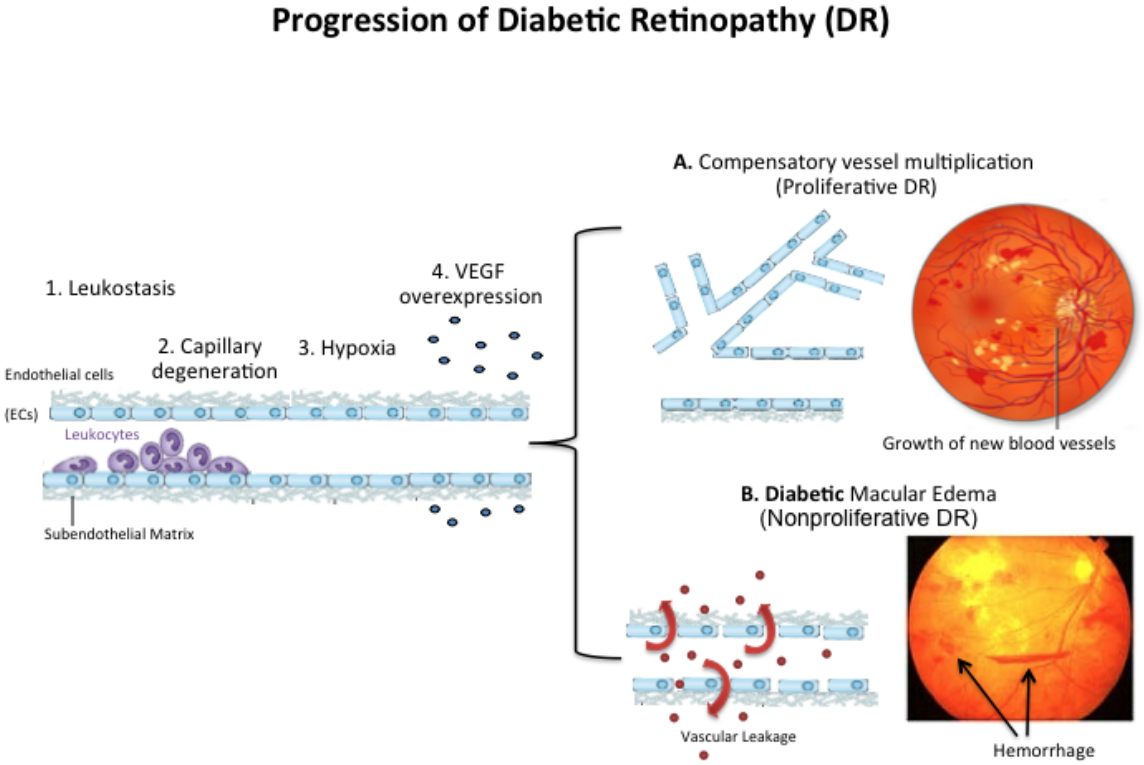

Schematic 1.1: Illustration of DR progression. In the early stage of DR, excessive leukocyte adhesion to retinal endothelial cells (leukostasis) leads to retinal capillary degeneration**,** which results in local ischemia. Further, these events lead to upregulation of VEGF and other pro-inflammatory factors, which can cause (A) compensatory vessel multiplication (proliferative DR) or (B) diabetic macular edema (nonproliferative DR).

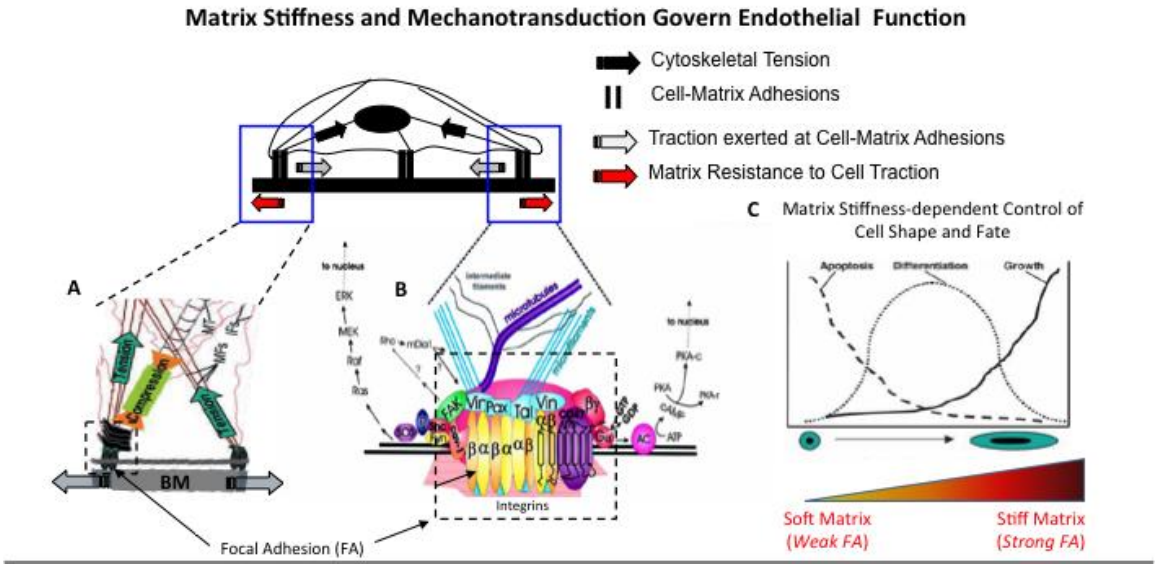

Schematic 1.2: Alterations in matrix stiffness and associated mechanotransduction govern endothelial function: (A) ECs adhere to underlying matrix using integrin-dependent focal adhesions (FAs). These FAs facilitate the development of a cell-matrix force equilibrium where the tension in actin filaments is balanced by the sum of compression borne by microtubules and the strength of FAs. The strength of FAs, in turn, is dictated by matrix stiffness where stiffer matrices produce stronger FAs and vice versa. (B) Various cytoskeletal adaptor proteins and cell signaling molecules are also recruited to FAs. Thus, by actively controlling FA strength, BM stiffness plays an important role in cellular mechanotransduction. (C) The biochemical signaling pathways elicited by matrix stiffness-dependent mechanotransduction converge in the nucleus to govern global cell function such that cells on soft matrices round up and die (apoptosis), those on stiff matrices spread fully and proliferate while cells on intermediate stiffness undergo partial retraction and differentiation.

References

1. (1996) From the Centers for Disease Control and Prevention. Blindness caused by diabetes--Massachusetts, 1987-1994. *JAMA : the journal of the American Medical Association* **276**, 1865-1866

2. Aiello, L. M. (2003) Perspectives on diabetic retinopathy. *American journal of ophthalmology* **136**, 122-135

3. Ciulla, T. A., Amador, A. G., and Zinman, B. (2003) Diabetic retinopathy and diabetic macular edema: pathophysiology, screening, and novel therapies. *Diabetes care* **26**, 2653-2664

4. Klein, R., Klein, B. E., Moss, S. E., and Cruickshanks, K. J. (1998) The Wisconsin Epidemiologic Study of Diabetic Retinopathy: XVII. The 14-year incidence and progression of diabetic retinopathy and associated risk factors in type 1 diabetes. *Ophthalmology* **105**, 1801-1815

5. Tang, J., and Kern, T. S. (2011) Inflammation in diabetic retinopathy. *Progress in retinal and eye research* **30**, 343-358

6. Lutty, G. A. (2013) Effects of diabetes on the eye. *Investigative ophthalmology & visual science* **54**, ORSF81-87

7. Veenstra, A. A., Tang, J., and Kern, T. S. (2013) Antagonism of CD11b with neutrophil inhibitory factor (NIF) inhibits vascular lesions in diabetic retinopathy. *PloS one* **8**, e78405

8. Kohner, E. M., and Henkind, P. (1970) Correlation of fluorescein angiogram and retinal digest in diabetic retinopathy. *American journal of ophthalmology* **69**, 403-414

9. (1993) The effect of intensive treatment of diabetes on the development and progression of long-term complications in insulin-dependent diabetes mellitus. The Diabetes Control and Complications Trial Research Group. *The New England journal of medicine* **329**, 977-986

10. (1998) Tight blood pressure control and risk of macrovascular and microvascular complications in type 2 diabetes: UKPDS 38. UK Prospective Diabetes Study Group. *Bmj* **317**, 703-713

11. Chaturvedi, N., Sjolie, A. K., Stephenson, J. M., Abrahamian, H., Keipes, M., Castellarin, A., Rogulja-Pepeonik, Z., and Fuller, J. H. (1998) Effect of lisinopril on progression of retinopathy in normotensive people with type 1 diabetes. The

EUCLID Study Group. EURODIAB Controlled Trial of Lisinopril in Insulin-Dependent Diabetes Mellitus. *Lancet* **351**, 28-31

12. Mauer, M., Zinman, B., Gardiner, R., Suissa, S., Sinaiko, A., Strand, T., Drummond, K., Donnelly, S., Goodyer, P., Gubler, M. C., and Klein, R. (2009) Renal and retinal effects of enalapril and losartan in type 1 diabetes. *The New England journal of medicine* **361**, 40-51

13. Mancia, G. (2010) Effects of intensive blood pressure control in the management of patients with type 2 diabetes mellitus in the Action to Control Cardiovascular Risk in Diabetes (ACCORD) trial. *Circulation* **122**, 847-849

14. Mitka, M. (2010) Aggressive lipid, hypertension targeting yields no benefit for some with diabetes. *JAMA : the journal of the American Medical Association* **303**, 1681-1683

15. Rangasamy, S., McGuire, P. G., and Das, A. (2012) Diabetic retinopathy and inflammation: novel therapeutic targets. *Middle East African journal of ophthalmology* **19**, 52-59

16. Elman, M. J., Aiello, L. P., Beck, R. W., Bressler, N. M., Bressler, S. B., Edwards, A. R., Ferris, F. L., 3rd, Friedman, S. M., Glassman, A. R., Miller, K. M., Scott, I. U., Stockdale, C. R., and Sun, J. K. (2010) Randomized trial evaluating ranibizumab plus prompt or deferred laser or triamcinolone plus prompt laser for diabetic macular edema. *Ophthalmology* **117**, 1064-1077 e1035

17. O'Day, R. F., Barthelmes, D., Zhu, M., Wong, T. Y., McAllister, I. L., Arnold, J. J., and Gillies, M. C. (2014) Intraocular pressure rise is predictive of vision improvement after intravitreal triamcinolone acetonide for diabetic macular oedema: a retrospective analysis of data from a randomised controlled trial. *BMC ophthalmology* **14**, 123

18. Das, A., McGuire, P. G., and Rangasamy, S. (2015) Diabetic Macular Edema: Pathophysiology and Novel Therapeutic Targets. *Ophthalmology*

19. Simo, R., and Hernandez, C. (2009) Advances in the medical treatment of diabetic retinopathy. *Diabetes care* **32**, 1556-1562

20. Mohamed, Q., Gillies, M. C., and Wong, T. Y. (2007) Management of diabetic retinopathy: a systematic review. *JAMA : the journal of the American Medical Association* **298**, 902-916

21. Miyamoto, K., Khosrof, S., Bursell, S. E., Rohan, R., Murata, T., Clermont, A. C., Aiello, L. P., Ogura, Y., and Adamis, A. P. (1999) Prevention of leukostasis and

vascular leakage in streptozotocin-induced diabetic retinopathy via intercellular adhesion molecule-1 inhibition. *Proceedings of the National Academy of Sciences of the United States of America* **96**, 10836-10841

22. Kowluru, R. A., Kowluru, A., Mishra, M., and Kumar, B. (2015) Oxidative Stress and Epigenetic Modifications in the Pathogenesis of Diabetic Retinopathy. *Progress in retinal and eye research*

23. Chronopoulos, A., Tang, A., Beglova, E., Trackman, P. C., and Roy, S. (2010) High glucose increases lysyl oxidase expression and activity in retinal endothelial cells: mechanism for compromised extracellular matrix barrier function. *Diabetes* **59**, 3159-3166

24. Kagan, H. M., and Li, W. (2003) Lysyl oxidase: properties, specificity, and biological roles inside and outside of the cell. *J Cell Biochem* **88**, 660-672

25. Mammoto, A., Mammoto, T., Kanapathipillai, M., Wing Yung, C., Jiang, E., Jiang, A., Lofgren, K., Gee, E. P., and Ingber, D. E. (2013) Control of lung vascular permeability and endotoxin-induced pulmonary oedema by changes in extracellular matrix mechanics. *Nature communications* **4**, 1759

26. Ghosh, K., and Ingber, D. E. (2007) Micromechanical control of cell and tissue development: implications for tissue engineering. *Advanced drug delivery reviews* **59**, 1306-1318

27. Ingber, D. E. (2002) Mechanical signaling and the cellular response to extracellular matrix in angiogenesis and cardiovascular physiology. *Circulation research* **91**, 877-887

28. Huynh, J., Nishimura, N., Rana, K., Peloquin, J. M., Califano, J. P., Montague, C. R., King, M. R., Schaffer, C. B., and Reinhart-King, C. A. (2011) Age-related intimal stiffening enhances endothelial permeability and leukocyte transmigration. *Science translational medicine* **3**, 112ra122

29. Kothapalli, D., Liu, S. L., Bae, Y. H., Monslow, J., Xu, T., Hawthorne, E. A., Byfield, F. J., Castagnino, P., Rao, S., Rader, D. J., Pure, E., Phillips, M. C., Lund-Katz, S., Janmey, P. A., and Assoian, R. K. (2012) Cardiovascular protection by ApoE and ApoE-HDL linked to suppression of ECM gene expression and arterial stiffening. *Cell reports* **2**, 1259-1271

30. Levental, K. R., Yu, H., Kass, L., Lakins, J. N., Egeblad, M., Erler, J. T., Fong, S. F., Csiszar, K., Giaccia, A., Weninger, W., Yamauchi, M., Gasser, D. L., and Weaver, V. M. (2009) Matrix crosslinking forces tumor progression by enhancing integrin signaling. *Cell* **139**, 891-906

31. To, M., Goz, A., Camenzind, L., Oertle, P., Candiello, J., Sullivan, M., Henrich, P. B., Loparic, M., Safi, F., Eller, A., and Halfter, W. (2013) Diabetes-induced morphological, biomechanical, and compositional changes in ocular basement membranes. *Experimental eye research* **116**, 298-307

CHAPTER 2

Basement Membrane Stiffening Promotes Retinal Endothelial Activation Associated with Diabetes

Preface

This Chapter explores the role of subendothelial basement membrane (BM) stiffening in retinal EC activation associated with diabetic retinopathy.

Adapted from manuscript*	:	Figures 2.1-2.2B, 2.2D-2.10
In collaboration	:	Data for Figures 2.2C

Introduction

Diabetic retinopathy (DR) is an important microvascular complication of diabetes and the leading cause of blindness in the working-age population (1). Growing evidence indicates that DR is a multifactorial condition that is strongly regulated by retinal inflammation (2, 3). A critical early step in diabetic retinal inflammation is the activation of retinal capillary endothelial cells (EC) (3, 4). Activated retinal ECs upregulate cell adhesion molecules (CAMs) such as intercellular CAM (ICAM-1) to promote leukocyte-EC adhesion (leukostasis). The adherent leukocytes subsequently release pro-inflammatory and vascular permeability factors that together disrupt the blood-retinal barrier, leading to an increase in vascular permeability that culminates in macular edema (3, 5). Importantly, blocking endothelial ICAM-1 alone prevents diabetic retinal leukostasis and vascular hyperpermeability in animal models of DR (4), thereby implicating retinal EC activation as a major determinant of DR pathogenesis.

Studies aimed at understanding diabetic retinal EC activation have focused primarily on the role of abnormal epigenetic, metabolic, and inflammatory factors (3, 6). However, a recent study reported that diabetic rat retinal ECs express increased levels of lysyl oxidase (LOX) (7), a copper-dependent enzyme that crosslinks collagen and enhances extracellular matrix stiffness (8). Notably, LOX overexpression and associated increase in extracellular matrix stiffness have been shown to promote endothelial dysfunction resulting in lung vascular hyperpermeability (9). Whether LOX upregulation in diabetic retinal ECs leads to subendothelial basement membrane (BM) stiffening and EC activation, however, remains unknown.

It is important to understand the role of subendothelial BM stiffening in diabetic retinal EC activation and inflammation as it can modulate the efficacy of existing and new anti-inflammatory DR therapies that commonly target soluble factors and their signaling pathways. This is because changes in extracellular matrix stiffness is known to independently regulate intracellular biochemistry, and thereby cell response to soluble cues, via alteration in cytoskeletal tension and cell-matrix adhesion strength (10). This conversion of matrix stiffness-dependent mechanical cues into intracellular biochemical signaling (termed mechanotransduction) plays an important role in regulating tissue function and disease. For instance, abnormal subendothelial matrix stiffness and associated alterations in intracellular mechanical signaling has been strongly implicated in vascular malformations (11), loss of capillary ECs (12), pulmonary edema (9), and atherosclerosis (13). Thus, I hypothesized that LOX upregulation in diabetic retinas promotes increased crosslinking and stiffening of retinal subendothelial BM that, in turn, actively contributes to retinal inflammation seen in DR.

Using atomic force microscopy, I show that high glucose (HG), the major risk factor for DR, causes significant increase in the stiffness of retinal EC-secreted matrix *in vitro*, which correlates with increased subendothelial collagen IV deposition, LOX upregulation, NF-κB-dependent retinal EC activation, and monocyte-EC adhesion. These findings are consistent with in vivo observations where diabetic mouse retinal inflammation correlated with higher levels of LOX and BM collagen IV. Finally, by pharmacological inhibition of LOX and development of synthetic matrices, I show that

HG-induced subendothelial matrix stiffening is necessary and sufficient for diabetic retinal EC activation.

Materials and Methods

Animal Model. All animal studies were performed as per Association for Research in Vision and Ophthalmology (ARVO) guidelines and in compliance with IACUC protocols approved by UC, Riverside, and University of New Mexico. Adult (8 week-old) male C57BL6/J mice (Jackson Labs) were injected with streptozotocin (STZ; 60 mg/kg body weight; Sigma) in 10 mM citrate buffer (pH 4.5) daily for five consecutive days. Animals with fasting blood glucose greater than 300 mg/dL were considered diabetic and were studied at four months' duration of diabetes. Age-matched mice receiving no STZ injection were used as non-diabetic control.

Retinal Whole Mount Immunofluorescence. Enucleated eyes from diabetic and control mice were fixed in 4% paraformaldehyde (PFA; Electron Microscopy Sciences, PA) for 4h prior to retinal isolation. Next, isolated retinas were permeabilized in 1% Triton X-100 and labeled with rabbit anti-collagen IV antibody (Abcam, MA, Cat#ab6586) followed by fluorescently-labeled anti-rabbit IgG (Vector Laboratories, Cat#DI-1488). Retinal capillaries were counterstained with isolectin GS-IB_4 (Life Technologies, Cat#I21412) and imaged using a Leica SP5 confocal microscope. To confirm the specificity of anti-collagen

IV immunostaining, some retinal whole mounts were labeled with secondary antibody alone.

Cell Culture and Glucose Treatment. Human retinal ECs, monkey chorioretinal ECs (RF/6A), and human monocytic cells (U937) were purchased from Cell Systems (Kirkland, WA) and ATCC, respectively. Human retinal ECs were grown in MCDB131 medium (Mediatech, VA) supplemented with 10% fetal bovine serum (FBS; Fisherbrand), 2 mM L-Glutamine (Life Technologies), 0.03 mg/mL Endothelial Cell Growth Supplement (Sigma), 1x antimycotic/antibiotic mixture (Life Technologies), 10 ng/ml human EGF (Millipore), 1 μg/ml hydrocortizone, and 0.09 mg/ml heparin (Sigma). Monkey chorioretinal ECs were grown in EMEM (ATCC) supplemented with 10% FBS and 1x antimycotic/antibiotic mixture. U937 monocytes were grown in RPMI-1640 medium (GE Healthcare) supplemented with 10% FBS, 2 mM L-Glutamine, 1.5 mg/ml sodium bicarbonate (Life Technologies), 1x antimycotic/antibiotic mixture, 1 mM sodium pyruvate (Life Technologies), and 4.5 mg/ml glucose (Sigma). Human $CD14^+$ peripheral blood monocytes (PBMs) were freshly isolated by centrifuging peripheral blood (Zenbio, NC) in Ficoll-Paque (GE Healthcare) to obtain buffy coat, which was subsequently spun down, decanted, resuspended in PBS buffer (containing 1% BSA and 2mM EDTA) at $250x10^6$ cells/ml, and mixed with 20 uL of $CD14^+$ magnetic microbeads (Miltenyi Biotec, CA) per $10x10^6$ cells for 20 min at 4 ℃. Finally, cell/bead suspension was spun down, decanted, suspended in PBS buffer and subjected to magnet-activated cell sorting.

For in vitro studies, EC monolayers were cultured in regular growth medium containing normal glucose (NG, 5.5 mM) or high glucose (HG, 30 mM) ± LOX inhibitor β-aminopropionitrile (BAPN;$C_3H_6N_2$ $0.5C_4H_4O_4$; 0.1 mM; ≥98% purity; Sigma), and supplemented with ascorbic acid (200 μg/mL; Sigma) to facilitate BM deposition. BAPN is a specific and irreversible inhibitor of LOX enzymatic activity (7, 14, 15). After 9 days, culture medium was replaced with low serum (2.5% FBS) medium (with all other components at original concentration) and monolayers allowed to grow overnight prior to specific assay.

Western Blot. To detect LOX, ICAM-1, and CD11b expression in vivo, mouse retinas were perfused, isolated, and homogenized in ice-cold RIPA lysis buffer (containing protease and phosphatase inhibitors). To detect LOX expression in cultured ECs, cells were grown in medium containing NG or HG ±BAPN for 10d, followed by lysis in RIPA lysis buffer. Supernatants from centrifuged retinal and EC culture lysates were subjected to Western Blotting using nitrocellulose membrane, which was probed with antibodies against LOX (Novus Biologicals, Cat#NB110-59729), CD11b (Novus Biologicals, Cat#NB110-89474) and ICAM-1 (Santa Cruz Biotech, Cat#SC-1511) followed by appropriate HRP-conjugated secondary antibodies (Vector Laboratories, Cat#DI-1488). GAPDH (Sigma, Cat#G9545) or β-tubulin (Abcam, Cat#ab6046) were used as loading controls. Western Blot protein bands were visualized using a camera-based imaging system (Biospectrum AC Imaging System) that automatically adjusts exposure time to avoid pixel saturation. ImageJ was used to perform densitometric analysis, and the measurements

(within the 10-250 pixel intensity range) were normalized with respect to corresponding loading controls.

EC-secreted Subendothelial Matrix. Decellularized (cell-free) subendothelial matrix was obtained using a technique that others and I have reported before (12, 16). Briefly, ECs in NG or HG±BAPN medium were grown on glass cover slips coated with glutaraldehyde-crosslinked gelatin for 10d, followed by decellularization of EC monolayers using a mild detergent composed of 20mM ammonium hydroxide (Sigma) and 0.5% Triton X-100 (Sigma) and fixation of the resultant subendothelial matrix with 1% PFA. Decellularized BM were labeled with rabbit anti-collagen IV (Abcam, Cat#ab6586) and fluorescein-conjugated anti-rabbit secondary antibody (Vector Laboratories, Cat#DI-1488) and imaged with a Leica SP5 confocal microscope. Subendothelial matrix thickness (n=3 per condition) was analyzed from xzy-plane images using ImageJ.

Measurement of Mouse Retinal Capillary and Subendothelial Matrix Stiffness. The stiffness of isolated normal and diabetic mouse retinal capillaries and unfixed decellularized subendothelial matrices obtained from NG- or HG±BAPN-treated EC cultures was measured using a biological-grade atomic force microscope (AFM; Veeco Instruments, NY) operated in tapping mode using a ~40 nm silicon nitride tip (glass bead for retinal capillaries) attached to a 140 μm-long microcantilever (MLCT, Bruker) with bending spring constant of 0.1 N/m. The maximum indentation force applied to sample was ~8 nN. Measurements were made in force-curve mode, and the cantilever deflection

was measured through the photodiode difference signal (S_{def}, volts). For each region, ~25 force curves were measured and only the linear region of force curves were considered for matrix stiffness analysis. Sample stiffness is calculated as $k_{sample} = F/ z_s$, where F is the applied force and z_s the sample deformation. Average stiffness was obtained from indentations in at least 9 different regions across the subendothelial matrix samples.

Real-time PCR. Total RNA was isolated from cells (Direct-zol RNA MiniPrep; Zymo Research, Irvine, CA), converted to cDNA using High Capacity cDNA Reverse Transcription (Applied Biosystems, Foster City, CA), and amplified with the appropriate TaqMan assay for ICAM-1 (Applied Biosystems, CA, Cat#4331182) in the Applied Biosystems 7500 Fast system. Relative mRNA levels were determined by the comparative Ct method with normalization to GAPDH.

Flow Cytometry. ECs were detached and labeled with rabbit anti-ICAM-1 antibody (Santa Cruz Biotech, SC-107) followed by fluorescently-labeled anti-mouse IgG (Vector Laboratories, Catalog# DI-2488). Next, ECs were fixed with 1% PFA, detected by a Cell Lab Quanta SC flow cytometer (Beckman Coulter, CA), and analyzed by FlowJo (Treestar Inc, CA).

Synthetic Matrix Fabrication. Thin (~100 μm-thick), elastic synthetic matrices of varying stiffness were prepared by mixing polyacrylamide and bis-acrylamide at different mass ratios, as reported previously (17, 18). Polyacrylamide gels have been extensively

used to study extracellular matrix mechanosensing because they can be synthesized over a broad range of stiffness through simple variation in bis-acrylamide (crosslinker) concentration, in addition to permitting a chemically-activated surface for covalent conjugation of any cell-binding matrix protein. Synthetic matrices were prepared at 1000 Pa, which mimics the average stiffness of normal subendothelial matrix (19), as well as 2000 Pa and 4000 Pa to mimic progressive matrix stiffening. To promote EC spreading, synthetic matrix surfaces were activated using sulfo-SANPAH prior to covalently conjugating human plasma fibronectin (BD Bioscience) at ~3 $\mu g/cm^2$ for 2h at 37°C. Retinal ECs grown under NG or HG±BAPN conditions for 10d were detached and re-plated on fibronectin-coated synthetic matrices in low serum medium and incubated overnight prior to use in assays.

Monocyte-EC Adhesion. ECs were cultured in NG or HG±BAPN medium for 10d prior to addition of fluorescently-labeled human PBMs or U937 cells (125,000 cells/cm^2) for 30 minutes at 37°C. Following rinsing with PBS, adherent monocytes were fixed with 1% PFA, imaged using Nikon Eclipse Ti microscope fitted with a Nikon DS-Qi1Mc camera, and counted using ImageJ (≥10 images per condition). To confirm the effect of subendothelial matrix stiffness on monocyte-EC adhesion, NG- and HG-treated ECs were grown on synthetic matrices of normal (1000 Pa) or higher (2000 Pa, 4000 Pa) stiffness in low serum medium and subjected to monocyte-EC adhesion assay, as described above.

NF-κB Activation. ECs grown in NG or HG±BAPN medium for 10d were detached and re-plated (in low serum medium containing NG or HG±BAPN) on decellularized subendothelial matrices obtained from parallel NG or HG±BAPN cultures. 6h post-plating, cells were fixed with 1% PFA, permeabilized, blocked with 2% BSA, and labeled with rabbit anti-NF-κB p65 antibody (Santa Cruz Biotech, Cat#SC-109) followed by fluorescently-labeled anti-rabbit IgG (Vector Laboratories, Cat#DI-1488). Cells were counter-stained with DAPI to label nuclei and imaged using Nikon Eclipse Ti microscope. NF-κB activation was determined by quantifying the fraction of cells (expressed as percent of total) that exhibit significant nuclear NF-κB p65 staining ($n \geq 20$ cells per condition), as previously reported (20). To confirm the effect of HG-induced subendothelial matrix stiffening on NF-κB activation, NG-treated ECs were plated (in low serum medium) on the corresponding decellularized matrices for 6h prior to assessment of NF-κB activation. ECs treated with tumor necrosis factor-α (TNF-α; 25 ng/ml; 5h), an inflammatory cytokine that induces NF-kB activation (21), served as positive control while antibody specificity was confirmed by labeling some samples with secondary antibody alone.

Intracellular Nitric Oxide (NO) Production. Retinal ECs grown in NG or HG±BAPN medium for 10d were detached and re-plated on the corresponding decellularized subendothelial matrices in low serum medium containing NG or HG±BAPN. After overnight incubation, cells were loaded with fluorescent NO-sensitive dye DAF-FM diacetate (2 μM; Life Technologies), as per manufacturer's protocol. After excess dye was rinsed off and cells recovered in NG or HG±BAPN medium, the medium was replaced

with Krebs–Henseleit buffer. Dye-loaded cells were imaged using Nikon Eclipse Ti microscope and intracellular net fluorescence intensity was quantified using ImageJ in the aforementioned manner ($n \geq 20$ cells per condition). To confirm the effect of subendothelial matrix stiffness on intracellular NO, NG- or HG-treated ECs were grown overnight on synthetic matrices of normal (1000 Pa) or high (4000 Pa) stiffness in low serum medium and subjected to intracellular NO measurement.

LOX Activity Assay. Retinal ECs were cultured in NG or HG ±BAPN medium for 9d, followed by overnight starvation in NG or HG ±BAPN-containing phenol red-free medium. LOX activity was determined by the conventional Amplex Red fluorescence assay (22, 23). Briefly, culture supernatants were incubated (at 1:1 ratio) with a reaction buffer (37 ℃; 30 min) containing 10 μM Amplex Red Reagent (Life Technologies) and the LOX activity was determined by measuring emitted fluorescence (540/590 nm), resulting from hydrogen peroxide produced by active LOX, with a fluorescence spectrophotometer ($n \geq 8$) and comparing it with a standard curve generated from serially-diluted hydrogen peroxide solution.

Statistics. All data were obtained from multiple replicates and expressed as mean ±SEM. For studies involving three experimental conditions, statistical significance was determined by analysis of variance (ANOVA; GraphPad Instat®), followed by Tukey's post-hoc analysis. For studies involving two experimental conditions, statistical significance was determined by both unpaired t-test (GraphPad Instat®), followed by Welch correction, as

well as Pearson's correlation analysis (SPSS Statistics, IBM, Inc.). Results were considered significant if $p<0.05$.

Results

Retinal endothelial activation is a chief characteristic of diabetes

Activated ECs express ICAM-1, a key endothelial cell adhesion molecule that promotes adhesion of circulating leukocytes. Predictably, I found that retinal ECs in diabetic mice exhibit ~70% higher ($p<0.01$) ICAM-1 expression than non-diabetic controls (Fig. 2.1A). This significant increase in retinal ICAM-1 expression correlated with a markedly (~50%; $p<0.05$) greater accumulation of CD11b+ monocytes/macrophages in diabetic retinas than in non-diabetic controls.

Consistent with the *in vivo* observations, HG treatment caused significantly greater activation of cultured human retinal ECs, as judged by ~1.6-fold higher ($p<0.01$) ICAM-1 mRNA expression in HG-treated ECs than in NG-treated counterparts (Fig. 2.1B). This increase in ICAM-1 mRNA levels under HG conditions correlated with ~2-fold higher number of HG-treated ECs expressing high surface ICAM-1-expression than NG-treated cells (Fig. 2.1C). Further, consistent with a significant increase in monocyte accumulation in diabetic retinas, HG-treated ECs exhibited ~4-fold greater binding ($p<0.001$) of fluorescently-labeled U937 human monocytic cells than NG-treated ECs (Fig. 2.1D). Human peripheral blood monocytes (PBMs) freshly isolated from whole blood also exhibited preferential binding to HG-treated ECs (Fig. 2.1E), thereby indicating that U937

cells mimic human circulating monocytes with regards to their ability to differentially adhere to normal versus diabetic retinal ECs.

To further understand the mechanism underlying higher endothelial ICAM-1 expression on HG-treated stiffer subendothelial matrix, I looked at the activation of NF-κB, the major transcriptional factor that upregulates various inflammatory genes including ICAM-1 (21). Immunostaining for NF-κB p65 and subsequent quantitative analysis revealed an approximately two-fold greater ($p<0.05$) incidence of its nuclear translocation, an indicator of NF-κB activation (20), in HG-treated cells than in NG-treated cells (Fig. 2.1F).

Diabetes is associated with significant increase in retinal subendothelial matrix crosslinking and stiffening

To test our hypothesis that BM stiffening actively contributes to retinal EC activation associated with DR, I examined retinas of diabetic mice for levels of LOX, a collagen-crosslinking enzyme, and BM collagen IV that, together, confer stiffness to capillary BM. LOX expression was found to be significantly higher (1.6-fold; $p<0.05$) in diabetic retinas than in non-diabetic controls (Fig. 2.2A). Further, whole mount retinal immunofluorescent staining revealed that diabetic retinal capillaries also exhibit markedly greater BM collagen IV deposition than their non-diabetic counterparts (Fig. 2.2B), likely due to greater LOX-mediated collagen crosslinking in diabetic retinas. More importantly, AFM force indentation on isolated mouse retinal capillaries showed a significant increase

(~3-fold; $p<0.01$) in the stiffness of diabetic retinal capillaries compared to their non-diabetic counterparts (Fig. 2.2C).

ECs cultured under NG and HG conditions (for 10d) exhibited a similar trend in LOX expression and collagen IV deposition. Specifically, HG-treated cells were found to exhibit two-fold higher ($p<0.001$) LOX expression than NG-treated cells (Fig. 2.2D), which correlated with a similar two-fold increase ($p<0.001$) in LOX activity in HG-treated ECs (Fig. 2.3). Immunofluorescent staining of decellularized retinal EC monolayers for collagen IV showed a significant increase ($p<0.001$) in the density and thickness of subendothelial collagen IV matrix secreted under HG conditions (Fig. 2.2E), which correlates with HG-induced LOX upregulation.

To determine whether higher levels of LOX and collagen IV observed in diabetic retinas and HG-treated EC cultures are associated with retinal subendothelial matrix stiffening, AFM force indentation was performed on matrices obtained from decellularized NG- and HG-treated EC cultures. Quantitative analysis of multiple ($n\approx25$) AFM force indentation curves revealed that the subendothelial matrix deposited by HG-treated ECs is two-fold stiffer ($p<0.001$) than that produced by NG-treated cells (Fig. 2.2F).

Inhibition of subendothelial matrix stiffening prevents HG-induced retinal EC activation

To determine whether HG-induced subendothelial matrix stiffening actively contributes to retinal EC activation, I suppressed LOX crosslinking in HG-treated cells using a pharmacological LOX inhibitor BAPN. AFM force indentations of decellularized

matrices indicated that inhibition of LOX crosslinking completely prevented HG-induced subendothelial matrix stiffening (Fig. 2.4A). This inhibition of matrix stiffening correlated with reduced matrix deposition by HG-treated cells, as judged by immunofluorescent staining of collagen IV (Fig. 2.5). More importantly, suppression of HG-induced subendothelial matrix stiffening by BAPN prevented the increase in U937 cell adhesion to HG-treated ECs (Fig. 2.4B). Notably, BAPN exerted comparable anti-inflammatory effect when added 10d after the onset of HG treatment (Fig. 2.6), thereby indicating that the pro-inflammatory effects of subendothelial matrix stiffening are reversible.

The anti-inflammatory effect produced by inhibition of subendothelial matrix stiffening was associated with significant suppression of NF-κB activation (nuclear translocation) (Fig. 2.7A). Notably, NF-κB activation is regulated upstream by endothelial nitric oxide (NO), a potent anti-inflammatory factor that suppresses NF-κB activation and ICAM-1-mediated leukocyte-EC adhesion (24-26). Thus, I looked to see whether BM stiffness-dependent mechanical control of NF-κB activation correlated inversely with endothelial NO production. Quantitative analyses of cells labeled with NO-sensitive dye revealed that, indeed, HG-mediated EC activation was associated with a significant (~40%; $p<0.001$) reduction in intracellular NO, which was prevented by suppression of subendothelial matrix stiffening (Fig. 2.7B). Taken together, these findings strongly implicate subendothelial BM stiffening as a critical determinant of diabetic retinal EC activation.

Subendothelial matrix stiffening is necessary and sufficient for HG-induced retinal EC activation

In addition to increasing subendothelial matrix stiffness, hyperglycemia also exerts biochemical effects that lead to increased oxidative stress and inflammation (3). Thus, to determine the extent to which LOX-mediated subendothelial matrix stiffening alone causes HG-induced retinal EC activation, I plated fresh, NG-treated retinal ECs on decellularized matrices obtained from preceding NG- and HG±BAPN-treated EC cultures and examined monocyte-EC adhesion and endothelial NO production (Fig. 2.8A). Under these conditions where the effects of LOX is conveyed only via matrix stiffness, retinal ECs plated on HG-treated (stiffer) subendothelial matrix exhibited significantly greater U937 cell adhesion than those plated on NG- or HG+BAPN-treated matrices (Fig. 2.8B). These differential levels of monocyte-EC adhesion on decellularized matrices were inversely related to the levels of endothelial NO, with ECs plated on HG-treated matrix producing ~40% lower NO ($p<0.001$) than those on NG- or HG+BAPN-treated matrices (Fig. 2.8C). Expectedly, the reduction in endothelial NO on HG-treated matrix correlated with greater NF-κB activation (Fig. 2.9). Thus, these findings indicate that LOX-dependent subendothelial matrix stiffening that occurs under HG conditions is alone sufficient to cause retinal EC activation.

To unequivocally confirm the pivotal role of subendothelial matrix stiffening in retinal EC activation, NG-treated cells were grown on synthetic matrices of progressively increasing stiffness. Counting of adherent U937 cells revealed a progressive increase in monocyte-EC adhesion on stiffer synthetic matrices (Fig. 2.10A), which correlated

inversely with endothelial NO production (Fig. 2.10B). Given that these significant differences in monocyte-EC adhesion and NO production are observed under NG conditions, these data corroborate the findings from decellularized matrices that subendothelial matrix stiffening is sufficient to cause retinal EC activation.

Further, when ECs grown in NG and HG medium were detached and plated on synthetic matrices of low (normal) stiffness for 24h in corresponding NG or HG medium, both monocyte-EC adhesion and NO production were found to be comparable (Figs. 2.10C,D). Since 24h is insufficient time for ECs to deposit a robust matrix, these data confirm our initial observation (Figs. 2.4, 2.7) that subendothelial matrix stiffening is also necessary to promote HG-induced retinal EC activation.

Discussions

Retinal inflammation plays a crucial role in DR pathogenesis. Past studies have demonstrated that retinal EC activation is a rate-limiting step in diabetic retinal inflammation (3, 4). Efforts aimed at understanding how retinal EC activation is regulated have revealed an important role of epigenetic, metabolic and inflammatory factors (2, 3, 6). Our findings are the first to implicate mechanical cues in the form of subendothelial BM stiffening as an important determinant of diabetic retinal EC activation. Using cultured retinal ECs, I further show that subendothelial matrix stiffening, caused by HG-induced LOX upregulation, is alone sufficient to activate retinal ECs. By highlighting the critical yet previously unrecognized role of subendothelial matrix stiffening in HG-induced retinal

EC activation, this study creates a new paradigm for the understanding of diabetic retinal inflammation and provides a strong rationale for detailed preclinical studies to evaluate BM stiffness normalization as a potential anti-inflammatory DR therapy either alone or in conjunction with existing DR treatment strategies. Further, since matrix stiffening triggers mechanotransduction pathways that can independently control cell function (10), a deeper mechanistic understanding of the mechanical control of diabetic retinal EC activation may lead to the identification of new therapeutic targets for effective DR management.

Vascular inflammation is a hallmark of diabetic complications such as retinopathy and cardiovascular diseases. Indeed, our mouse model of DR and HG-treated retinal EC cultures demonstrated significant increase in endothelial ICAM-1 expression and monocyte-EC binding, which is consistent with EC activation observed in diabetic aortas/arteries (27, 28). Notably, diabetes is also associated with significant stiffening of large vessels such as arteries and aorta (29, 30) and independent studies have implicated aortic/arterial subendothelial matrix stiffening in increased vascular permeability and monocyte accumulation associated with atherosclerosis (13, 31). Thus, here I asked whether diabetes also leads to an increase in retinal subendothelial matrix stiffness and, if so, whether matrix stiffening actively contributes to retinal EC activation associated with DR.

I found that EC activation and inflammation *in vitro* and in diabetic mouse retina correlate with higher expression and activity of the collagen-crosslinking enzyme LOX, which is consistent with LOX upregulation reported in diabetic rat retinal capillaries (7). Since past studies have implicated LOX upregulation in the stiffening of lung and tumor

extracellular matrix (9, 32), I asked whether LOX enhances retinal subendothelial matrix stiffness. To address this question, I used a biological-grade AFM to perform force indentation measurements on decellularized subendothelial matrix obtained from retinal EC cultures. AFM offers a unique, sensitive, quantitative, and reliable technique to measure micromechanical properties (e.g. cell/matrix stiffness, intermolecular bond forces) of myriad biological materials such as DNA, proteins, cells, and tissues (33-35). Our AFM force measurements confirmed that HG treatment significantly increases LOX-dependent retinal subendothelial matrix stiffness. These AFM measurements, which are the first to quantify retinal subendothelial matrix or BM stiffness *in vitro* or *in vivo*, formed the basis for examining the mechanical control of diabetic retinal EC activation. To this end, I showed that HG-induced retinal EC activation depends strongly on the increase in LOX-dependent subendothelial matrix stiffness. It must be noted that the subendothelial matrix deposited by retinal EC cultures is similar, but not identical, to the BM deposited in retinal capillaries, with the presence of interstitial matrix proteins (e.g. collagen I and VI) in subendothelial matrices in vitro being a major distinction (36, 37). Since the retinal capillary BM in vivo is regulated by both ECs and pericytes, co-culturing these cells in vitro may lead to the deposition of a matrix that more closely resembles the in vivo BM. Nonetheless, together with a past study that implicated HG-induced LOX upregulation in retinal vascular hyperpermeability (7), our findings implicate a crucial role of LOX-dependent BM stiffening in diabetic retinal inflammation.

Owing to its collagen-crosslinking property, LOX upregulation in HG-treated ECs and diabetic mouse retinas predictably correlated with increased collagen IV deposition in

subendothelial matrix and BM, respectively. This observation agrees well with past reports of increased BM collagen IV accumulation in retinal vessels of diabetic rats and humans with DR (7, 38-40). Notably, other BM components such as fibronectin, tenascin-C and collagen XIII are also deposited in excessive amounts in diabetic retinal capillary BMs (39-41). Among these, fibronectin is particularly important as it interacts with both collagen IV and LOX via specific molecular domains within its N- and C-terminal domains, respectively (23, 42), and is implicated in regulating LOX activity (23). Thus, it is possible that, in addition to increasing retinal capillary BM thickness, excessive fibronectin also contributes to LOX-dependent BM stiffening and associated retinal inflammation. DR is also associated with upregulation of plasminogen activator-inhibitor 1 (PAI-1) in retinal ECs (43, 44). Since plasminogen activation leads to degradation of BM fibronectin (45), upregulation of PAI-1 in DR may also, at least indirectly, contribute to BM stiffening via increased fibronectin/LOX interaction.

In addition to increasing LOX-mediated subendothelial matrix stiffening, hyperglycemia causes other biochemical alterations such as increased polyol and hexosamine pathway flux, glycation of plasma biomolecules, and formation of advanced glycation end-products (AGE) that contribute to oxidative stress and inflammation (46). Thus, it may be possible that the inflammatory effects of HG reported here result from dual effects of aberrant matrix stiffness-dependent mechanical *and* HG-dependent biochemical cues. Remarkably, however, our findings revealed that LOX-mediated subendothelial matrix stiffening alone is sufficient to promote retinal EC activation independent of the effects of HG-induced biochemical modifications. This is an important finding because it

implicates BM stiffening as an independent regulator of diabetic retinal inflammation. To unequivocally confirm this, I cultured NG-treated ECs on synthetically-engineered matrices made of polyacrylamide gels of increasing stiffness. Polyacrylamide gels have been widely used to examine the role of BM/matrix stiffness in endothelial permeability (31), transcriptional control of angiogenesis (47), atheroprotective effects of apoE (13), and tumor vascular dysfunction (11). Here, I leveraged them to confirm that subendothelial matrix stiffening *alone* promotes activation of NG-treated ECs, thereby consolidating the observations made on decellularized matrices.

To determine the inflammatory pathway by which subendothelial matrix stiffening activates retinal ECs, I focused on the NO/NF-κB axis. NO is a potent endogenous anti-inflammatory factor that suppresses EC activation by inhibiting the activity of NF-κB (25, 26), a key transcriptional factor that promotes ICAM-1-dependent leukocyte-EC adhesion in DR (48-50). Indeed, diabetic vascular inflammation is associated with impaired endothelial NO (51). Further, genetic knockout of endothelial nitric oxide synthase (eNOS), the primary enzyme that produces endothelial NO, has been shown to accelerate DR pathogenesis (52). Consistent with these reports, I found that the inflammatory effects of HG-induced subendothelial matrix stiffening result from impaired retinal endothelial NO and associated increase in NF-κB activation. The underlying mechanotransduction pathway by which matrix stiffening regulates inflammatory processes, however, remains to be examined.

Current anti-inflammatory treatments for DR are limited to the use of steroids (53, 54). Although they work well in DR patients with late-stage macular edema, steroids exert

side effects such as increased intraocular pressure and cataract formation (53, 55). Thus, there is an unmet need to identify new anti-inflammatory targets and therapies for more effective DR management. By highlighting the crucial role of subendothelial matrix stiffening in retinal EC activation, this study provides new mechanistic insights into the pathophysiology of inflammation associated with DR. These findings also form the basis for carrying out detailed *in vivo* studies that examine BM stiffness as a potential anti-inflammatory target for DR treatment. These animal studies will help determine the extent to which inhibition of BM stiffening suppresses diabetic retinal inflammation both alone and in conjunction with existing DR therapies. Furthermore, future studies that examine the mechanotransduction pathways underlying the mechanical control of diabetic retinal inflammation may lead to the identification of entirely new class of molecular targets for more effective anti-inflammatory DR therapies.

Conclusion

Diabetic mice exhibiting 70% and 50% increase in retinal ICAM-1 expression and leukocyte accumulation, respectively, demonstrated a two-fold increase in the levels of BM collagen IV and LOX, key determinants of capillary BM stiffness. Using atomic force microscopy, I confirmed that HG significantly enhances LOX-dependent subendothelial matrix stiffness *in vitro*, which correlated with ~2.5-fold increase in endothelial ICAM-1 expression, four-fold greater monocyte-EC adhesion, and ~two-fold alteration in endothelial nitric oxide (decrease) and NF-κB activation (increase). Importantly, inhibition

of LOX-dependent subendothelial matrix stiffening alone suppressed HG-induced retinal EC activation. Finally, using synthetic matrices of tunable stiffness, I demonstrate that subendothelial matrix stiffening is necessary and sufficient to promote EC activation.

These findings implicate BM stiffening as a critical determinant of HG-induced retinal EC activation and provides rationale to examine BM stiffness and underlying mechanotransduction pathways as therapeutic targets for diabetic retinopathy.

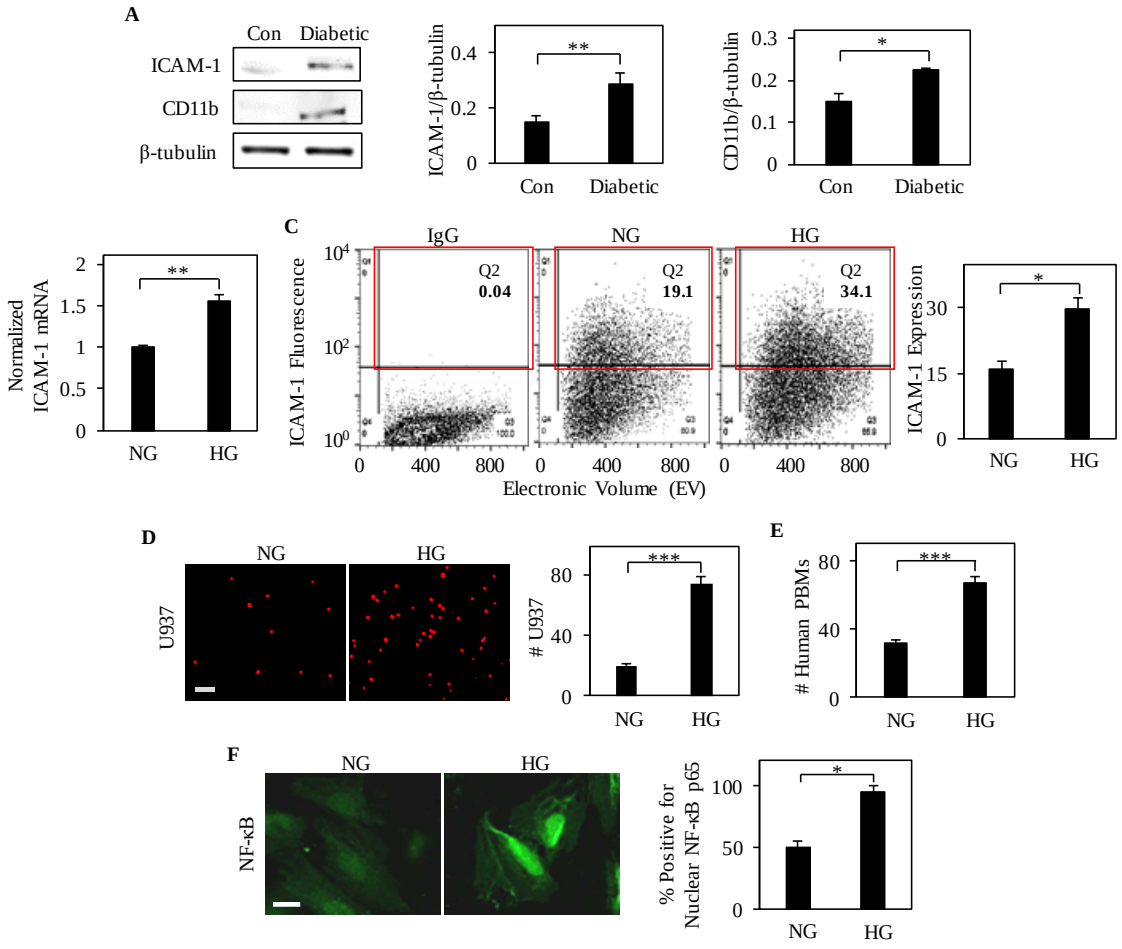
A
Con
Diabetic
ICAM-1
CD11b
β-tubulin
ICAM-1/β-tubulin
CD11b/β-tubulin
**
*
C
IgG
NG
HG
Q2
0.04
Q2
19.1
Q2
34.1
ICAM-1 Fluorescence
Electronic Volume (EV)
Normalized ICAM-1 mRNA
ICAM-1 Expression
D
U937
U937
E
Human PBMs
***
F
NF-κB
% Positive for Nuclear NF-κB p65

FIGURE 2.1. Retinal endothelial activation is a chief characteristic of diabetes. (A) Representative Western blot bands and their densitometric analyses (bar graphs) together reveal that the levels of endothelial ICAM-1 and $CD11b^+$ monocyte/macrophage are significantly higher (*, $p<0.05$; **, $p<0.01$) in diabetic mouse retinas when compared with control retinas (n=5). ICAM-1, and $CD11b^+$ levels were normalized with respect to the corresponding levels of β-tubulin (loading control). (B) Real-time RT-PCR analysis shows that HG-treated retinal EC cultures exhibit 60% increase (**, $p<0.01$) in ICAM-1 mRNA expression than NG-treated cells. ICAM-1 mRNA levels were normalized with respect to NG levels. (C) Surface expression of endothelial ICAM-1 was determined by flow cytometry. Quantitative analysis of representative fluorescence vs size (electronic volume) dot plots indicates that HG treatment produces an ~2-fold increase in the number of high ICAM-1-expressing ECs (red box) than NG treatment. (D, E) Fluorescently-labeled U937 cells or freshly-isolated human peripheral blood monocytes (PBMs) were added to EC monolayer for 30 min. Representative fluorescent images of adherent U937 cells or human PBMs and subsequent cell count indicate a significant (2.1- to 3.5-fold; ***, $p<0.001$) increase in monocyte-EC adhesion under HG conditions. Bar graph indicates average ± SEM (per mm^2) from multiple ($n\geq10$) images of monocyte-EC co-cultures. Scale bar: 100 μm. PBM: peripheral blood monocytes. (F) Representative fluorescent images of NG- and HG-treated ECs labeled with anti-NF-κB p65 and quantification of percent total cells (bar graph; $n\geq20$ cells) with NF-κB p65 nuclear translocation reveal significantly greater (***, $p<0.001$) incidence of NF-κB activation in HG-treated ECs than in their NG-treated counterparts. Significance was determined by unpaired t-test, followed by Welch correction, and confirmed by Pearson's correlation analysis. Scale bar: 20 μm. NG: normal glucose; HG: high glucose. *, $p<0.05$; **, $p<0.01$; ***, $p<0.001$.

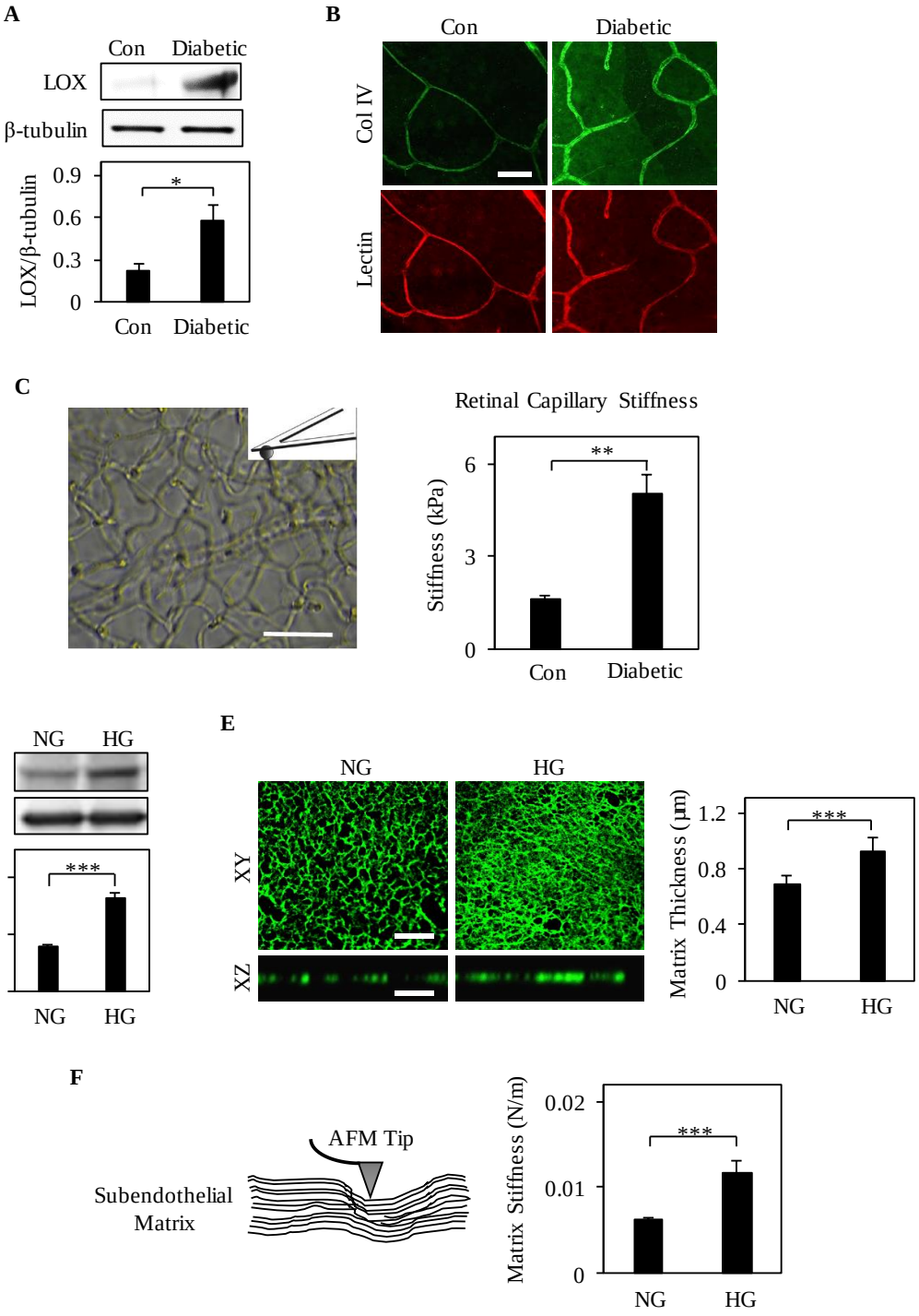
A
Con
Diabetic
LOX
β-tubulin
LOX/β-tubulin
0.9
0.6
0.3
0
*
Con
Diabetic
B
Con
Diabetic
Col IV
Lectin
C
Retinal Capillary Stiffness
Stiffness (kPa)
6
3
0
**
Con
Diabetic
D
NG
HG
LOX
GAPDH
LOX/GAPDH
0.4
0.2
0
***
NG
HG
E
NG
HG
XY
XZ
Matrix Thickness (μm)
1.2
0.8
0.4
0
***
NG
HG
F
AFM Tip
Subendothelial
Matrix
Matrix Stiffness (N/m)
0.02
0.01
0
***
NG
HG

FIGURE 2.2. Diabetes is associated with significant increase in retinal subendothelial matrix crosslinking and stiffening. (A) Representative Western blot bands and their densitometric analyses (bar graph) together reveal that LOX expression is significantly higher (*, $p<0.05$) in diabetic mouse retinas when compared with control retinas. LOX levels were normalized with respect to the corresponding levels of β-tubulin (loading control). (B) Representative fluorescent images ($n \geq 15$) of non-diabetic control and diabetic mouse retinas immunostained with anti-collagen IV indicate that diabetes leads to marked increase in collagen IV deposition in retinal capillary BM. Scale bar: 50 μm. (C) Stiffness of isolated mouse retinal capillaries was measured by an atomic force microscope (AFM) fitted with a ~5 μm glass bead tip (schematic). Quantitative analysis of multiple ($n \geq 13$) force indentation measurements revealed a 3-fold (***, $p<0.001$) increase in retinal capillary stiffness in diabetic mouse retinal capillaries than in non-diabetic control condition. (D) Representative Western blot bands and their densitometric analyses (bar graph) together reveal that HG-treated retinal ECs express two-fold higher (***, $p<0.001$) levels of lysyl oxidase (LOX) than NG-treated cells. LOX levels were normalized with respect to the corresponding levels of GAPDH (loading control). (E) Decellularized matrices obtained from NG- and HG-treated human retinal EC cultures were immunostained with anti-collagen IV. Representative top (XY plane) and cross-sectional (XZ plane) views of the collagen IV network shows that, compared to NG-treated ECs, those treated with HG deposit a markedly denser and thicker matrix. Matrix thickness was quantified from multiple ($n=3$) samples and plotted as average ± SEM (bar graph). Scale bar: 10 μm. (F) Stiffness of EC-secreted matrix was measured by an atomic force microscope (AFM) fitted with a ~40 nm pyramidal silicon nitride tip (schematic). Quantitative analysis of multiple ($n \geq 25$) force indentation measurements (bar graph) revealed a two-fold (***, $p<0.001$) increase in subendothelial matrix stiffness under HG conditions than in NG conditions. Significance was determined by unpaired t-test, followed by Welch correction, and confirmed by Pearson's correlation analysis. **, $p<0.01$; ***, $p<0.001$.

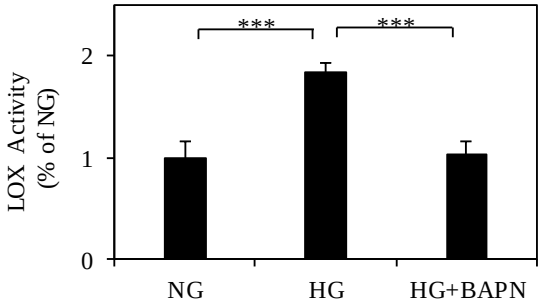

FIGURE 2.3. HG enhances LOX activity in retinal ECs. LOX activity assay shows that HG-treated retinal ECs exhibit a ~two-fold greater (***, $p<0.001$) LOX activity than NG-treated cells. The HG-induced increase in LOX activity was suppressed by BAPN (0.1 mM), a specific and irreversible inhibitor of LOX activity. LOX activity levels were normalized with respect to NG levels. Significance was determined by ANOVA, followed by Tukey's post-hoc analysis. ***, $p<0.001$.

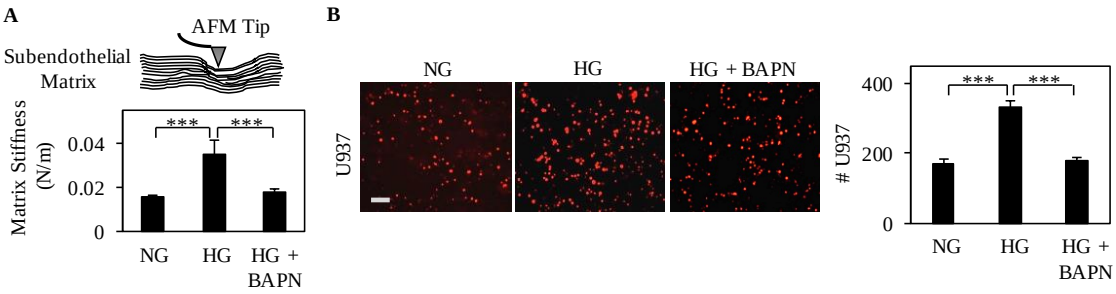

FIGURE 2.4. Inhibition of HG-induced retinal subendothelial matrix stiffening prevents monocyte-EC adhesion. (A) AFM force indentation measurements of decellularized EC-secreted matrix confirms that pharmacological inhibition of LOX activity (by BAPN) in HG-treated ECs prevents HG-induced subendothelial matrix stiffening. Bar graph indicates average ± SEM from multiple ($n \geq 25$) force curves (***, $p<0.001$). (B) Fluorescently-labeled U937 cells were added to EC monolayers for 30 min. Representative fluorescent images of adherent U937 cells and subsequent cell count indicate that the significant increase in monocyte adhesion to HG-treated ECs can be prevented by suppressing LOX-dependent subendothelial matrix stiffening. Bar graph indicates average ± SEM (per mm^2) from multiple ($n \geq 10$) images of monocyte-EC co-cultures (***, $p<0.001$). Significance was determined by ANOVA, followed by Tukey's post-hoc analysis. Scale bar: 100 μm. ***, $p<0.001$.

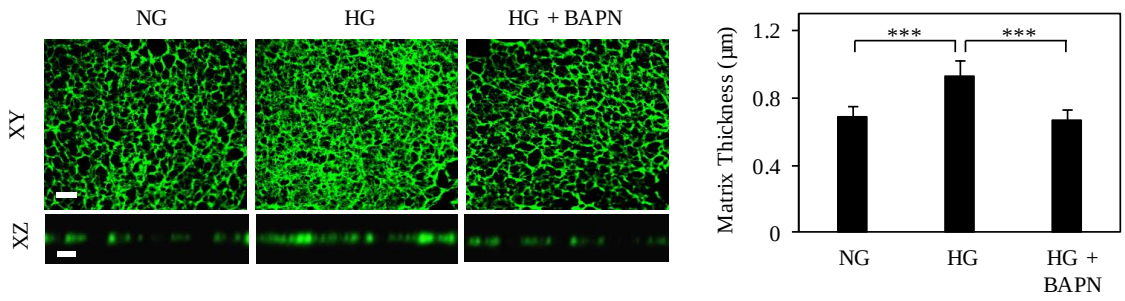

FIGURE 2.5. Inhibition of LOX activity prevents HG-induced retinal subendothelial matrix thickening. The representative top (XY plane) and cross-sectional (XZ plane) views of EC-secreted matrix labeled with anti-collagen IV reveal that pharmacological inhibition of LOX activity (by BAPN) in HG-treated ECs reduces matrix deposition. Subendothelial matrix thickness was quantified from multiple (n=3) samples and plotted as average ± SEM (bar graph). Significance was determined by ANOVA, followed by Tukey's post-hoc analysis. Scale bar: 5 μm. ***, $p<0.001$.

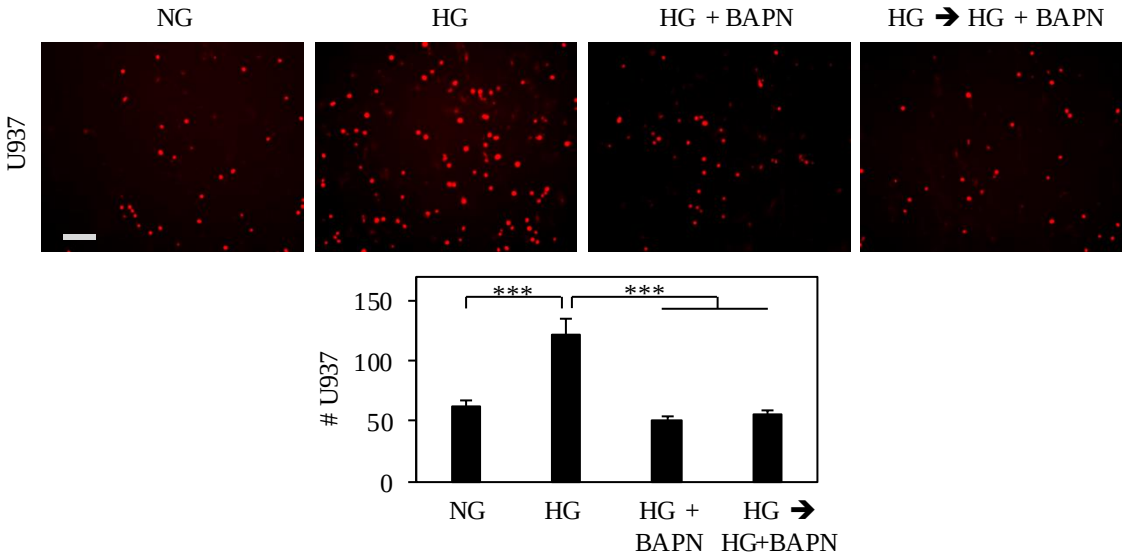

FIGURE 2.6. LOX inhibition reverses the inflammatory effects of HG-induced subendothelial matrix stiffening. LOX inhibitor BAPN was added to HG-treated ECs either at the onset of HG culture (HG+BAPN) or 10d after the onset of HG culture (HG➔HG+BAPN) prior to the addition of fluorescently-labeled U937 cells for 30 min. Representative fluorescent images of adherent U937 cells and subsequent cell count (bar graph) indicate that the significant increase in monocyte adhesion to HG-treated ECs can be successfully reversed upon LOX inhibition in 10d-old HG cultures. Bar graph indicates average ± SEM from multiple ($n \geq 10$) images of monocyte-EC co-cultures. Significance was determined by ANOVA, followed by Tukey's post-hoc analysis. Scale bar: 100 μm. ***, $p<0.001$.

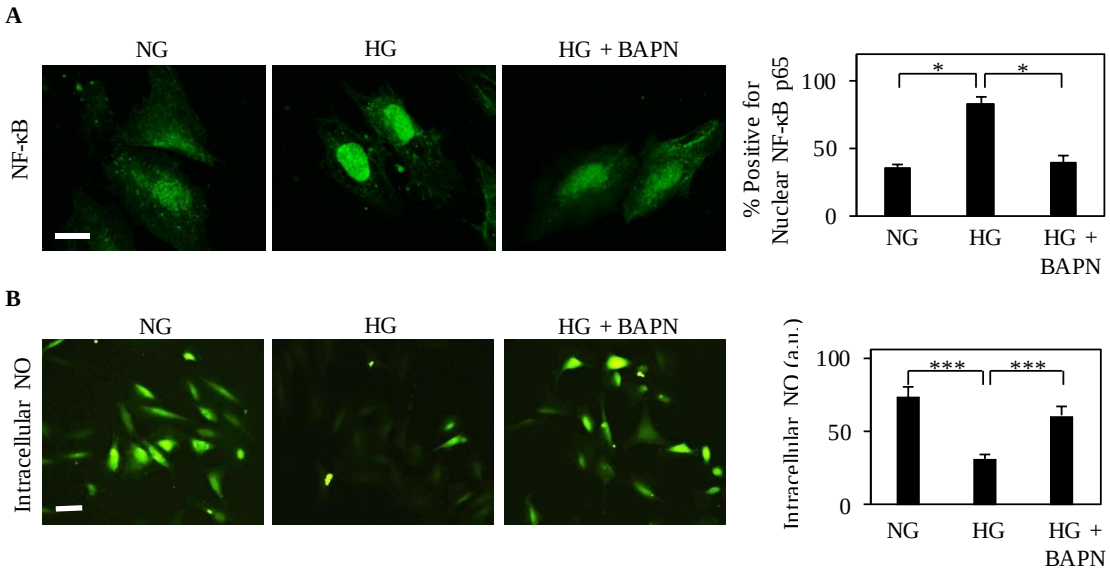

FIGURE 2.7. Inhibition of HG-induced subendothelial matrix stiffening prevents NF-κB activation and restores endothelial NO production. (A) Representative fluorescent images of ECs labeled with anti-NF-κB p65 and subsequent quantitative analysis from multiple (n≈35) cells (bar graph) indicate that the significant increase in the incidence of NF-κB nuclear translocation (activation) seen in HG-treated ECs is effectively (*, $p<0.05$) prevented by BAPN-mediated LOX inhibition. Scale bar: 20 μm. (B) Representative fluorescent images of ECs labeled with DAF-FM diacetate, a NO-sensitive dye, and subsequent intensity measurements from multiple (n≥30) cells (bar graph) reveal that the loss of NO production caused by HG treatment is prevented by BAPN-mediated inhibition of subendothelial matrix stiffening (***, $p<0.001$). Significance was determined by ANOVA, followed by Tukey's post-hoc analysis. Scale bar:100 μm. *, $p<0.05$; ***, $p<0.001$.

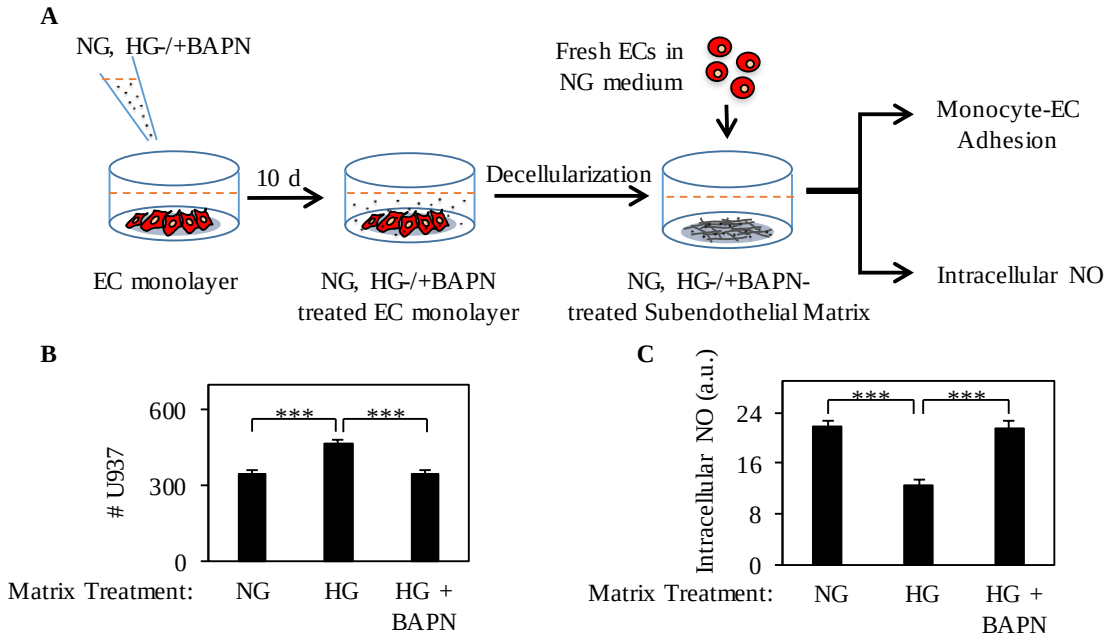

FIGURE 2.8. HG-induced subendothelial matrix stiffening alone can promote retinal EC activation. (A) Schematic depiction of the experimental procedure to examine the direct effect of modified BM on normal ECs. (B) Fluorescently-labeled U937 cells were added (for 30 min) to NG-treated EC monolayers grown on decellularized matrices obtained from preceding NG, HG or HG+BAPN cultures. Counting of adherent U937 cells (per mm^2) from multiple ($n \geq 10$) images of monocyte-EC co-cultures indicate that HG-treated stiff matrix alone causes significant (***, $p<0.001$) increase in monocyte-EC adhesion, which did not occur on 'normalized' matrix obtained from BAPN-treated cultures. (C) The lack of increase in monocyte-EC adhesion on 'normalized' HG+BAPN-treated matrix correlates strongly with a lack of decrease in endothelial NO production on these matrices, as indicated by fluorescent intensity measurement from multiple ($n \geq 30$) ECs labeled with the NO-sensitive dye DAF-FM diacetate (***, $p<0.001$). Significance was determined by ANOVA, followed by Tukey's post-hoc analysis. ***, $p<0.001$.

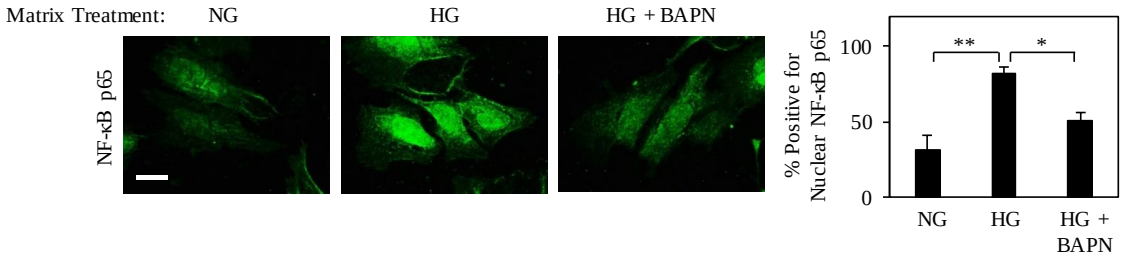

FIGURE 2.9. Subendothelial matrix stiffening is sufficient to enhance endothelial NF-κB activation. Representative fluorescent images show NG-treated ECs grown on decellularized matrices obtained from preceding NG, HG or HG+BAPN cultures and immunostained with anti-NF-κB p65. Subsequent quantitative analysis (bar graph) from multiple ($n \geq 25$) cells indicates that the significant increase in the incidence of NF-κB nuclear translocation (activation) seen on HG-treated matrix is effectively (***, $p<0.001$) prevented on BAPN-treated 'normalized' matrix. Significance was determined by ANOVA, followed by Tukey's post-hoc analysis. Scale bar: 20 μm. *, $p<0.05$; **, $p<0.01$.

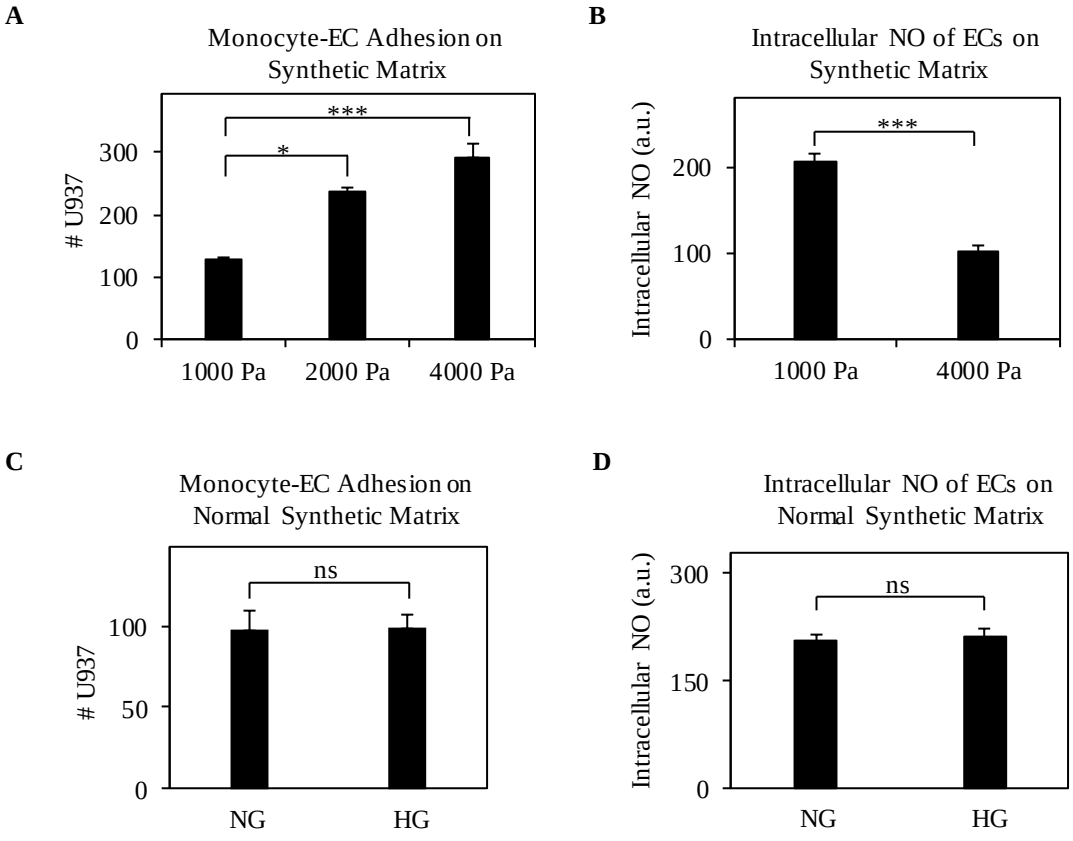
A
Monocyte-EC Adhesion on Synthetic Matrix
U937
300
200
100
0
***
*
1000 Pa
2000 Pa
4000 Pa
B
Intracellular NO of ECs on Synthetic Matrix
Intracellular NO (a.u.)
200
100
0
***
1000 Pa
4000 Pa
C
Monocyte-EC Adhesion on Normal Synthetic Matrix
U937
100
50
0
ns
NG
HG
D
Intracellular NO of ECs on Normal Synthetic Matrix
Intracellular NO (a.u.)
300
150
0
ns
NG
HG

FIGURE 2.10. Subendothelial matrix stiffening is necessary and sufficient for HG-induced retinal EC activation. (A) Fresh NG-treated ECs were plated on synthetic matrices of normal (1000 Pa) or increasing (2000 Pa and 4000 Pa) stiffness and evaluated for U937 cell adhesion. Counting of adherent U937 cells indicates that, under NG conditions, ECs grown on stiffer synthetic matrix exhibit a progressive increase in monocyte-EC adhesion. Bar graph indicates average ± SEM (per mm^2) from multiple ($n \geq 10$) images of monocyte-EC co-cultures (*, $p<0.05$; ***, $p<0.001$). Significance was determined by ANOVA, followed by Tukey's post-hoc analysis. (B) Increase in monocyte-EC adhesion on stiffer synthetic matrix correlates with a significant decrease in endothelial NO production, as indicated by fluorescent intensity measurement of multiple ($n \geq 30$) ECs labeled with NO-sensitive dye DAF-FM diacetate. (C, D) ECs grown in NG or HG medium for 10d were detached and re-plated on synthetic matrix of normal (1000 Pa) stiffness for evaluation of U937 cell adhesion and intracellular NO production. Counting of adherent U937 cells indicates no significant difference ($p>0.05$) in monocyte adhesion to NG- and HG-treated ECs grown on synthetic matrix of normal stiffness (C). This is consistent with the similar levels of intracellular NO observed in these cells, as judged by fluorescence intensity measurement of DAF-FM diacetate-labeled ECs (D). For B-D, significance was determined by unpaired t-test, followed by Welch correction, and confirmed by Pearson's correlation analysis. *, $p<0.05$; ***, $p<0.001$; ns, no significance.

References

1. Antonetti, D. A., Klein, R., and Gardner, T. W. (2012) Diabetic retinopathy. *The New England journal of medicine* **366**, 1227-1239

2. Rangasamy, S., McGuire, P. G., and Das, A. (2012) Diabetic retinopathy and inflammation: novel therapeutic targets. *Middle East African journal of ophthalmology* **19**, 52-59

3. Tang, J., and Kern, T. S. (2011) Inflammation in diabetic retinopathy. *Progress in retinal and eye research* **30**, 343-358

4. Miyamoto, K., Khosrof, S., Bursell, S. E., Rohan, R., Murata, T., Clermont, A. C., Aiello, L. P., Ogura, Y., and Adamis, A. P. (1999) Prevention of leukostasis and vascular leakage in streptozotocin-induced diabetic retinopathy via intercellular adhesion molecule-1 inhibition. *Proceedings of the National Academy of Sciences of the United States of America* **96**, 10836-10841

5. Lutty, G. A. (2013) Effects of diabetes on the eye. *Investigative ophthalmology & visual science* **54**, ORSF81-87

6. Kowluru, R. A., Kowluru, A., Mishra, M., and Kumar, B. (2015) Oxidative Stress and Epigenetic Modifications in the Pathogenesis of Diabetic Retinopathy. *Progress in retinal and eye research*

7. Chronopoulos, A., Tang, A., Beglova, E., Trackman, P. C., and Roy, S. (2010) High glucose increases lysyl oxidase expression and activity in retinal endothelial cells: mechanism for compromised extracellular matrix barrier function. *Diabetes* **59**, 3159-3166

8. Kagan, H. M., and Li, W. (2003) Lysyl oxidase: properties, specificity, and biological roles inside and outside of the cell. *J Cell Biochem* **88**, 660-672

9. Mammoto, A., Mammoto, T., Kanapathipillai, M., Wing Yung, C., Jiang, E., Jiang, A., Lofgren, K., Gee, E. P., and Ingber, D. E. (2013) Control of lung vascular permeability and endotoxin-induced pulmonary oedema by changes in extracellular matrix mechanics. *Nature communications* **4**, 1759

10. Ghosh, K., and Ingber, D. E. (2007) Micromechanical control of cell and tissue development: implications for tissue engineering. *Advanced drug delivery reviews* **59**, 1306-1318

11. Ghosh, K., Thodeti, C. K., Dudley, A. C., Mammoto, A., Klagsbrun, M., and Ingber, D. E. (2008) Tumor-derived endothelial cells exhibit aberrant Rho-mediated mechanosensing and abnormal angiogenesis in vitro. *Proceedings of the National Academy of Sciences of the United States of America* **105**, 11305-11310

12. Yang, X., Scott, H. A., Ardekani, S., Williams, M., Talbot, P., and Ghosh, K. (2014) Aberrant cell and basement membrane architecture contribute to sidestream smoke-induced choroidal endothelial dysfunction. *Investigative ophthalmology & visual science* **55**, 3140-3147

13. Kothapalli, D., Liu, S. L., Bae, Y. H., Monslow, J., Xu, T., Hawthorne, E. A., Byfield, F. J., Castagnino, P., Rao, S., Rader, D. J., Pure, E., Phillips, M. C., Lund-Katz, S., Janmey, P. A., and Assoian, R. K. (2012) Cardiovascular protection by ApoE and ApoE-HDL linked to suppression of ECM gene expression and arterial stiffening. *Cell reports* **2**, 1259-1271

14. Ito, H., Akiyama, H., Iguchi, H., Iyama, K., Miyamoto, M., Ohsawa, K., and Nakamura, T. (2001) Molecular cloning and biological activity of a novel lysyl oxidase-related gene expressed in cartilage. *The Journal of biological chemistry* **276**, 24023-24029

15. Bondareva, A., Downey, C. M., Ayres, F., Liu, W., Boyd, S. K., Hallgrimsson, B., and Jirik, F. R. (2009) The lysyl oxidase inhibitor, beta-aminopropionitrile, diminishes the metastatic colonization potential of circulating breast cancer cells. *PloS one* **4**, e5620

16. Beacham, D. A., Amatangelo, M. D., and Cukierman, E. (2007) Preparation of extracellular matrices produced by cultured and primary fibroblasts. *Curr Protoc Cell Biol* **Chapter 10**, Unit 10 19

17. Wang, Y. L., and Pelham, R. J., Jr. (1998) Preparation of a flexible, porous polyacrylamide substrate for mechanical studies of cultured cells. *Methods in enzymology* **298**, 489-496

18. Yeung, T., Georges, P. C., Flanagan, L. A., Marg, B., Ortiz, M., Funaki, M., Zahir, N., Ming, W., Weaver, V., and Janmey, P. A. (2005) Effects of substrate stiffness on cell morphology, cytoskeletal structure, and adhesion. *Cell motility and the cytoskeleton* **60**, 24-34

19. Scott, H. A., Yang, X., Ardekani, S., Cabrera, A., Wilson, R., Messaoudi-Powers, I., and Ghosh, K. TRPV4-mediated Biphasic Matrix-dependent Mechanical Control of Endothelial Activation. *Journal of cell science* **Submitted**

20. Orr, A. W., Sanders, J. M., Bevard, M., Coleman, E., Sarembock, I. J., and Schwartz, M. A. (2005) The subendothelial extracellular matrix modulates NF-

kappaB activation by flow: a potential role in atherosclerosis. *The Journal of cell biology* **169**, 191-202

21. Pober, J. S., and Sessa, W. C. (2007) Evolving functions of endothelial cells in inflammation. *Nature reviews. Immunology* **7**, 803-815

22. Palamakumbura, A. H., and Trackman, P. C. (2002) A fluorometric assay for detection of lysyl oxidase enzyme activity in biological samples. *Anal Biochem* **300**, 245-251

23. Fogelgren, B., Polgar, N., Szauter, K. M., Ujfaludi, Z., Laczko, R., Fong, K. S., and Csiszar, K. (2005) Cellular fibronectin binds to lysyl oxidase with high affinity and is critical for its proteolytic activation. *The Journal of biological chemistry* **280**, 24690-24697

24. Lefer, D. J., Jones, S. P., Girod, W. G., Baines, A., Grisham, M. B., Cockrell, A. S., Huang, P. L., and Scalia, R. (1999) Leukocyte-endothelial cell interactions in nitric oxide synthase-deficient mice. *The American journal of physiology* **276**, H1943-1950

25. Peng, H. B., Libby, P., and Liao, J. K. (1995) Induction and stabilization of I kappa B alpha by nitric oxide mediates inhibition of NF-kappa B. *The Journal of biological chemistry* **270**, 14214-14219

26. De Caterina, R., Libby, P., Peng, H. B., Thannickal, V. J., Rajavashisth, T. B., Gimbrone, M. A., Jr., Shin, W. S., and Liao, J. K. (1995) Nitric oxide decreases cytokine-induced endothelial activation. Nitric oxide selectively reduces endothelial expression of adhesion molecules and proinflammatory cytokines. *The Journal of clinical investigation* **96**, 60-68

27. Hartge, M. M., Unger, T., and Kintscher, U. (2007) The endothelium and vascular inflammation in diabetes. *Diabetes & vascular disease research* **4**, 84-88

28. Shirwany, N. A., and Zou, M. H. (2012) Vascular inflammation is a missing link for diabetes-enhanced atherosclerotic cardiovascular diseases. *Front Biosci (Landmark Ed)* **17**, 1140-1164

29. Chang, K. C., Tseng, C. D., Chou, T. F., Cho, Y. L., Chi, T. C., Su, M. J., and Tseng, Y. Z. (2006) Arterial stiffening and cardiac hypertrophy in a new rat model of type 2 diabetes. *European journal of clinical investigation* **36**, 1-7

30. Oxlund, H., Rasmussen, L. M., Andreassen, T. T., and Heickendorff, L. (1989) Increased aortic stiffness in patients with type 1 (insulin-dependent) diabetes mellitus. *Diabetologia* **32**, 748-752

31. Huynh, J., Nishimura, N., Rana, K., Peloquin, J. M., Califano, J. P., Montague, C. R., King, M. R., Schaffer, C. B., and Reinhart-King, C. A. (2011) Age-related intimal stiffening enhances endothelial permeability and leukocyte transmigration. *Science translational medicine* **3**, 112ra122

32. Levental, K. R., Yu, H., Kass, L., Lakins, J. N., Egeblad, M., Erler, J. T., Fong, S. F., Csiszar, K., Giaccia, A., Weninger, W., Yamauchi, M., Gasser, D. L., and Weaver, V. M. (2009) Matrix crosslinking forces tumor progression by enhancing integrin signaling. *Cell* **139**, 891-906

33. Goldsbury, C. S., Scheuring, S., and Kreplak, L. (2009) Introduction to atomic force microscopy (AFM) in biology. *Current protocols in protein science / editorial board, John E. Coligan ... [et al.]* **Chapter 17**, Unit 17 17 11-19

34. Trache, A., and Meininger, G. A. (2008) Atomic force microscopy (AFM). *Current protocols in microbiology* **Chapter 2**, Unit 2C 2

35. Lehenkari, P. P., Charras, G. T., Nesbitt, S. A., and Horton, M. A. (2000) New technologies in scanning probe microscopy for studying molecular interactions in cells. *Expert reviews in molecular medicine* **2**, 1-19

36. Halfter, W., Oertle, P., Monnier, C. A., Camenzind, L., Reyes-Lua, M., Hu, H., Candiello, J., Labilloy, A., Balasubramani, M., Henrich, P. B., and Plodinec, M. (2015) New concepts in basement membrane biology. *FEBS J*

37. Davis, G. E., and Senger, D. R. (2005) Endothelial extracellular matrix: biosynthesis, remodeling, and functions during vascular morphogenesis and neovessel stabilization. *Circulation research* **97**, 1093-1107

38. Roy, S., Maiello, M., and Lorenzi, M. (1994) Increased expression of basement membrane collagen in human diabetic retinopathy. *J Clin Invest* **93**, 438-442

39. Ljubimov, A. V., Burgeson, R. E., Butkowski, R. J., Couchman, J. R., Zardi, L., Ninomiya, Y., Sado, Y., Huang, Z. S., Nesburn, A. B., and Kenney, M. C. (1996) Basement membrane abnormalities in human eyes with diabetic retinopathy. *J Histochem Cytochem* **44**, 1469-1479

40. Chronopoulos, A., Trudeau, K., Roy, S., Huang, H., Vinores, S. A., and Roy, S. (2011) High glucose-induced altered basement membrane composition and structure increases trans-endothelial permeability: implications for diabetic retinopathy. *Current eye research* **36**, 747-753

41. To, M., Goz, A., Camenzind, L., Oertle, P., Candiello, J., Sullivan, M., Henrich, P. B., Loparic, M., Safi, F., Eller, A., and Halfter, W. (2013) Diabetes-induced

morphological, biomechanical, and compositional changes in ocular basement membranes. *Experimental eye research* **116**, 298-307

42. Shimizu, M., Minakuchi, K., Moon, M., and Koga, J. (1997) Difference in interaction of fibronectin with type I collagen and type IV collagen. *Biochimica et biophysica acta* **1339**, 53-61

43. Grant, M. B., Ellis, E. A., Caballero, S., and Mames, R. N. (1996) Plasminogen activator inhibitor-1 overexpression in nonproliferative diabetic retinopathy. *Experimental eye research* **63**, 233-244

44. Azad, N., Agrawal, L., Emanuele, N. V., Klein, R., Bahn, G. D., McCarren, M., Reaven, P., Hayward, R., Duckworth, W., and Group, V. S. (2014) Association of PAI-1 and fibrinogen with diabetic retinopathy in the Veterans Affairs Diabetes Trial (VADT). *Diabetes care* **37**, 501-506

45. Marchina, E., and Barlati, S. (1996) Degradation of human plasma and extracellular matrix fibronectin by tissue type plasminogen activator and urokinase. *The international journal of biochemistry & cell biology* **28**, 1141-1150

46. Brownlee, M. (2005) The pathobiology of diabetic complications: a unifying mechanism. *Diabetes* **54**, 1615-1625

47. Mammoto, A., Connor, K. M., Mammoto, T., Yung, C. W., Huh, D., Aderman, C. M., Mostoslavsky, G., Smith, L. E., and Ingber, D. E. (2009) A mechanosensitive transcriptional mechanism that controls angiogenesis. *Nature* **457**, 1103-1108

48. Zheng, L., Howell, S. J., Hatala, D. A., Huang, K., and Kern, T. S. (2007) Salicylate-based anti-inflammatory drugs inhibit the early lesion of diabetic retinopathy. *Diabetes* **56**, 337-345

49. Iliaki, E., Poulaki, V., Mitsiades, N., Mitsiades, C. S., Miller, J. W., and Gragoudas, E. S. (2009) Role of alpha 4 integrin (CD49d) in the pathogenesis of diabetic retinopathy. *Investigative ophthalmology & visual science* **50**, 4898-4904

50. Palenski, T. L., Sorenson, C. M., and Sheibani, N. (2013) Inflammatory cytokine-specific alterations in retinal endothelial cell function. *Microvascular research* **89**, 57-69

51. Kolluru, G. K., Siamwala, J. H., and Chatterjee, S. (2010) eNOS phosphorylation in health and disease. *Biochimie* **92**, 1186-1198

52. Li, Q., Verma, A., Han, P. Y., Nakagawa, T., Johnson, R. J., Grant, M. B., Campbell-Thompson, M., Jarajapu, Y. P., Lei, B., and Hauswirth, W. W. (2010)

Diabetic eNOS-knockout mice develop accelerated retinopathy. *Investigative ophthalmology & visual science* **51**, 5240-5246

53. Das, A., McGuire, P. G., and Rangasamy, S. (2015) Diabetic Macular Edema: Pathophysiology and Novel Therapeutic Targets. *Ophthalmology*

54. Bandello, F., Preziosa, C., Querques, G., and Lattanzio, R. (2014) Update of intravitreal steroids for the treatment of diabetic macular edema. *Ophthalmic research* **52**, 89-96

55. O'Day, R. F., Barthelmes, D., Zhu, M., Wong, T. Y., McAllister, I. L., Arnold, J. J., and Gillies, M. C. (2014) Intraocular pressure rise is predictive of vision improvement after intravitreal triamcinolone acetonide for diabetic macular oedema: a retrospective analysis of data from a randomised controlled trial. *BMC ophthalmology* **14**, 123

CHAPTER 3

Loss of Mechanosensitive TRPV4 Mediates Mechanical Control of Diabetic Retinal Endothelial Activation

Preface

This Chapter explores the role of mechanosensitive TRPV4 in diabetic retinal EC activation and implicates TRPV4 as a novel anti-inflammatory target for management of early DR.

Original contribution : Data for Figures 3.2B - 3.3, 3.5, 3.6A, 3.7B-C, 3.8, 3.9

In collaboration : Data for Figures 3.1, 3.2A, 3.4, 3.6B, 3.7A, 3.10

Introduction

Studies in Chapter 2 have shown that high glucose (HG) causes significant LOX-mediated stiffening of retinal subendothelial matrix *in vitro*, which is necessary and sufficient to promote retinal EC activation, as judged by impaired constitutive NO production, increased NF-κB activation and greater monocyte-EC adhesion (1). However, the molecular mechanism behind this subendothelial matrix stiffness-induced retinal EC activation and inflammation remains unknown.

To identify the mechanosensitive mechanism implicated in this subendothelial matrix stiffening-dependent retinal EC activation, I looked at the role of mechanosensitive TRPV4 (Transient Receptor Potential Vanilloid 4) Ca^{2+} channel. TRPV4 is a member of the transmembrane TRP family of Ca^{2+} channels that are ubiquitously expressed in ECs and known to be sensitive to mechanical forces such as shear stress and cyclic stretch (2, 3). Notably, my collaborative work on atherosclerosis has recently shown that TRPV4 mediates matrix stiffness sensitivity in aortic endothelial (4), which is consistent with the role of TRPV4 is matrix stiffness sensing in cardiac myocytes and tumor-derived ECs (5, 6). Further, TRPV4 is also known to enhance eNOS (endothelial nitric oxide synthase) activation, (7, 8) which leads to the production of anti-inflammatory NO. Since diabetes and HG treatment lead to both increased subendothelial matrix stiffness and impaired endothelial NO production (Chapter 2), I hypothesized that HG-induced subendothelial matrix stiffening impairs TRPV4-mediated mechanotransduction that, in turn, leads to

impaired retinal endothelial NO production (EC activation) and increased monocyte-EC adhesion.

By uncovering the previously unknown link between subendothelial matrix stiffening, TRPV4-mediated mechanotransduction and EC activation, I here show that HG causes significant increase in the stiffness of retinal EC-secreted subendothelial matrix *in vitro*, which correlates with TRPV4-mediated retinal EC activation and monocyte-EC adhesion. These findings are consistent with *in vivo* observations where diabetic retinal inflammation correlates with lower TRPV4 expression. Finally, I show that HG-induced retinal EC activation and monocyte-EC adhesion can be suppressed by pharmacological enhancement of TRPV4.

Materials and Methods

Animal Model. All animal studies were performed as per Association for Research in Vision and Ophthalmology (ARVO) guidelines and in compliance with IACUC protocols approved by UC, Riverside, and University of New Mexico. Adult (8 week-old) male C57BL6/J mice (Jackson Labs) were injected with streptozotocin (STZ; 60 mg/kg body weight; Sigma) in 10 mM citrate buffer (pH 4.5) daily for five days. Animals with fasting blood glucose greater than 300 mg/dL were considered diabetic. Once the animals were considered diabetic, a group of mice was treated with LOX inhibitor β-aminopropionitrile (BAPN; 3 mg/kg; drinking water; Sigma) for three months. Studies were performed at three

months' duration of diabetes. Age-matched mice receiving no STZ injection were used as non-diabetic control.

Retinal Whole Mount Immunofluorescence. Enucleated eyes from diabetic and control mice were fixed in 4% paraformaldehyde (PFA; Electron Microscopy Sciences, PA) 4h prior to retinal isolation. 1% Triton X-100 was used to permeabilize the isolated retinas. Next, permeabilized retinas were labeled with rabbit anti-TRPV4 antibody (Alomone Labs, Isreal) followed by FITC-labeled anti-rabbit IgG (Life Technologies). Retinal vessels were counterstained with isolectin GS-IB_4 (Life Technologies) and imaged with a Leica SP5 confocal microscope. TRPV4 expression was quantified using ImageJ (NIH) and expressed as fluorescence intensity per unit vessel area ($n \geq 15$ vessels per condition). For semi-quantitative analysis of TRPV4 levels in retinal capillaries, I first measured the background fluorescence intensity from an empty surrounding region with an area identical to that of the retinal vessel and then subtracted this value from the fluorescence intensity obtained directly from the vessel. Data was expressed as fluorescence intensity per unit vessel area ($n \geq 15$ vessel segments per condition).

Retinal Capillary Isolation. Enucleated eyes from control, diabetic ± BAPN mice were fixed in 5% formalin (Sigma) overnight prior to retinal isolation. Next, isolated retinas were digested with 1.5% Trypsin (1:250; Amresco) and washed in ddH_2O to obtain retinal capillaries for stiffness analysis. Retinal capillaries from three mice were isolated per condition.

Cell Culture and Glucose Treatment. Human retinal ECs and human monocytic cells (U937) were purchased from Cell Systems (Kirkland, WA) and ATCC, respectively. Human retinal ECs were grown in MCDB131 medium (Mediatech, VA) supplemented with 10% fetal bovine serum (FBS; Fisherbrand), 2 mM L-Glutamine (Life Technologies), 0.03 mg/mL Endothelial Cell Growth Supplement (Sigma), 1x antimycotic/antibiotic mixture (Life Technologies), 10 ng/ml human EGF (Millipore), 1 μg/ml hydrocortizone, and 0.09 mg/ml heparin (Sigma). U937 monocytes were grown in RPMI-1640 medium (GE Healthcare) supplemented with 10% FBS, 2 mM L-Glutamine, 1.5 mg/ml sodium bicarbonate (Life Technologies), 1x antimycotic/antibiotic mixture, 1 mM sodium pyruvate (Life Technologies), and 4.5 mg/ml glucose (Sigma).

For *in vitro* studies, EC monolayers were cultured in regular growth medium containing normal glucose (NG, 5.5 mM) or high glucose (HG, 30 mM) ± BAPN (0.1 mM; Sigma), and supplemented with ascorbic acid (200 μg/mL; Sigma) to facilitate subendothelial matrix deposition. BAPN is a specific and irreversible inhibitor of LOX enzymatic activity (9-11). After 9 days, culture medium was replaced with low serum (2.5% FBS) medium (with all other components at original concentration) and cells were incubated overnight prior to specific assay.

LOX Activity Assay. Retinal ECs were cultured in NG or HG ±BAPN medium for 9d, followed by overnight starvation in NG or HG ±BAPN-containing phenol red-free medium.

LOX activity was determined by the conventional Amplex Red fluorescence assay (12, 13). Briefly, culture supernatants were incubated (at 1:1 ratio) with a reaction buffer (37 ℃; 30 min) containing 10 μM Amplex Red Reagent (Life Technologies) and the LOX activity was determined by measuring emitted fluorescence (540/590 nm), resulting from hydrogen peroxide produced by active LOX, with a fluorescence spectrophotometer ($n \geq 8$) and comparing it with a standard curve generated from serially-diluted hydrogen peroxide solution.

EC-secreted Subendothelial Matrix. Decellularized (cell-free) subendothelial matrix was obtained using a technique as previously reported(14, 15). Briefly, ECs in NG or HG±BAPN medium were grown on glass cover slips coated with glutaraldehyde-crosslinked gelatin for 10d, followed by decellularization of EC monolayers using a mild detergent composed of 20mM ammonium hydroxide (Sigma) and 0.5% Triton X-100 (Sigma). Retinal ECs grown under NG or HG±BAPN conditions for 10d were detached and re-plated on decellularized subendothelial matrices in low serum medium and incubated overnight prior to use in assays.

Western Blot. To detect eNOS expression *in vivo*, mouse retinas were perfused, isolated, and homogenized in ice-cold RIPA lysis buffer (containing protease and phosphatase inhibitors). To detect TRPV4 expression *in vivo*, mouse retinal capillaries were isolated and homogenized in ice-cold RIPA lysis buffer. To detect TRPV4 expression in cultured ECs, cells were grown in medium containing NG or HG±BAPN for 10d, followed by lysis

in RIPA buffer. Retinal and EC culture lysates were centrifuged and supernatants were subjected to Western Blotting using nitrocellulose membrane, which was probed with antibodies against eNOS (BD Bioscience), CD11b (Novus Biologicals) and TRPV4 (Alomone Labs) followed by appropriate HRP-conjugated secondary antibodies (Vector Labs). GAPDH (Sigma) or β-tubulin (Abcam) was used as the loading control. Western Blot protein bands were visualized using a camera-based imaging system (Biospectrum AC Imaging System) that automatically adjusts exposure time to avoid pixel saturation. ImageJ was used to perform densitometric analysis, and the measurements (within the 10-250 pixel intensity range) were normalized with respect to corresponding loading controls.

Flow Cytometry. ECs were detached and labeled with anti-ICAM-1 antibody (Santa Cruz Biotech), or detached, permeabilized, and then labeled with rabbit anti-eNOS p1117 antibody (Santa Cruz Biotech) followed by fluorescently-labeled anti-rabbit secondary IgG (Vector Laboratories). To detect $CD11b^+$ monocyte/macrophage accumulation *in vivo*, mouse retinas were isolated, and labeled with rabbit anti-$CD11b^+$ antibody followed by fluorescently-labeled anti-rabbit IgG. Next, ECs and mouse retinal cells were fixed with 1% PFA, detected by a Cell Lab Quanta SC flow cytometer (Beckman Coulter, CA), and analyzed by FlowJo (Treestar Inc, CA).

Measurement of Retinal Capillary and Subendothelial Matrix Stiffness. The stiffness of isolated mouse retinal capillaries and unfixed decellularized subendothelial matrix obtained from NG- or HG±BAPN-treated EC cultures was measured using a biological-

grade atomic force microscope (AFM; Veeco Instruments, NY) operated in tapping mode using a ~5 μm glass bead or ~40 nm silicon nitride tip attached to a 140 μm-long microcantilever (MLCT, Bruker) with bending spring constant of 0.1 N/m. The maximum indentation force applied to sample was ~8 nN. Measurements were made in force-curve mode, and the cantilever deflection was measured through the photodiode difference signal (S_{def}, volts). For each region, ~25 force curves were measured and only the linear region of force curves were considered for subendothelial matrix stiffness analysis. Sample stiffness is calculated as $k_{sample} = F/ z_s$, where F is the applied force and z_s the sample deformation. Average stiffness was obtained from indentations in at least 8 different regions across the mouse retinal capillaries and the subendothelial matrix samples.

Synthetic Matrix Fabrication. Thin (~100 μm-thick), elastic synthetic matrices of varying stiffness were prepared by mixing polyacrylamide and bis-acrylamide at different mass ratios, as previously reported (16, 17). Polyacrylamide gels have been extensively used to study extracellular matrix mechanosensing because they can be synthesized over a broad range of stiffness through simple variation in bis-acrylamide (crosslinker) concentration, in addition to permitting a chemically-activated surface for covalent conjugation of any cell-binding matrix protein. Synthetic matrices were prepared at 1000 Pa, which mimics the average stiffness of normal subendothelial matrix (4), as well as 4000 Pa to mimic subendothelial matrix stiffening. To promote EC spreading, synthetic matrix surfaces were activated using sulfo-SANPAHprior to covalently conjugating human plasma fibronectin (BD Bioscience) at ~3 μg/cm^2 for 2h at 37^{o}C. Retinal ECs grown under

NG or HG±BAPN conditions for 10d were detached and re-plated on fibronectin-coated synthetic matrices in low serum medium and incubated overnight prior to use in assays.

Monocyte-EC Adhesion. ECs were cultured in NG or HG±BAPN medium for 10 days prior to addition of fluorescently-labeled U937 cells (125,000 cells/cm^2) for 30 minutes at 37^{o}C. Following rinsing with PBS, adherent monocytes were fixed with 1% PFA, imaged using Nikon Eclipse Ti microscope fitted with a Nikon DS-Qi1Mc camera, and counted using ImageJ (≥10 images per condition). To confirm the effect of TRPV4 on monocyte-EC adhesion, HG-treated ECs were grown on corresponding decellularized subendothelial matrices in low serum medium and subjected to TRPV4 activation through pharmacological agonist (GSK1016790A; 50 nM) for 3h. To further confirm TRPV4's role in monocyte-EC adhesion, cells were grown on stiff (4000 Pa) synthetic matrix in low serum medium and subjected to TRPV4 activation through agonist GSK1016790A (50 nM) for 3h. Next, monocyte-EC adhesion assay was performed, as described above.

Intracellular Nitric Oxide (NO) Production. Retinal ECs grown in NG or HG±BAPN medium for 10 days were detached and re-plated on the corresponding decellularized BM in low serum medium containing NG or HG±BAPN. After overnight incubation, cells were loaded with fluorescent NO-sensitive dye DAF-FM diacetate (2 μM; Life Technologies), as per manufacturer's protocol. After excess dye was rinsed off and cells recovered in NG or HG±BAPN medium, the medium was replaced with Krebs–Henseleit buffer. Dye-loaded cells were imaged using Nikon Eclipse Ti microscope and intracellular fluorescence

intensities were quantified using ImageJ (n ≥20 cells per condition). To unequivocally confirm the effect of subendothelial matrix stiffness on intracellular NO, NG- or HG-treated ECs were grown overnight on synthetic matrix of normal (1000 Pa) or high (4000 Pa) stiffness in low serum medium and subjected to intracellular NO measurement. To test the mediator's role of TRPV4, retinal ECs grown under HG ± BAPN conditions or plated on stiffer (4000 Pa) synthetic matrix were treated without or with selective TRPV4 antagonist RN1734 (8) (25 μM, 5h; Sigma-Aldrich) or agonist GSK1016790A (50 nM; 3h; Sigma-Aldrich), and then subjected to intracellular NO measurement.

Calcium Imaging. Retinal ECs grown in NG or HG±BAPN medium for 10 days were detached and re-plated on the corresponding decellularized subendothelial matrices in low serum medium containing NG or HG ±BAPN. Next day, ECs were loaded with fluorescent Ca^{2+}-sensitive dye Fluo-4 AM (1 μM; Life Technologies) in Ca^{2+} buffer containing 136 mM Sodium Chloride, 4.7 mM potassium chloride, 1.2 mM magnecium sulfate, 1.1 mM calcium chloride, 1.2 mM potassium phosphate monobasic, 5 mM sodium bicarbonate, 5.5 mM glucose and 20mM HEPES (Sigma). Excess dye was then rinsed off and cells recovered in Ca^{+} Buffer for 30 minutes. To detect TRPV4 activity, dye-loaded cells were imaged with time-lapse function every 3 seconds using Nikon Eclipse Ti microscope and after one minute of time-lapse imaging, cells were stimulated with TRPV4 agonist GSK-1016790A (300 nM) and imaged for an additional 5 min. To unequivocally confirm the effect of subendothelial matrix stiffness on TRPV4 activity, NG-treated ECs were grown overnight on synthetic matrices of normal (1000 Pa) or high (4000 Pa) stiffness in low

serum medium and subjected to TRPV4 activity measurement. Intracellular Ca^{2+} was quantified by measuring net intracellular fluorescence intensity (n ≥20 cells per condition; using ImageJ), as previously described (2).

Real-time PCR. Total RNA was isolated from control, diabetic ± BAPN mice retinal capillaries (Direct-zol RNA MiniPrep; Zymo Research, Irvine, CA), converted to cDNA using High Capacity cDNA Reverse Transcription (Applied Biosystems, Foster City, CA), and amplified with the appropriate TaqMan assay for ICAM-1 (Applied Biosystems, CA) in the Applied Biosystems 7500 Fast system. Relative mRNA levels were determined by the comparative Ct method with normalization to GAPDH.

Statistics. All data were obtained from multiple replicates (n ≥ 3) and expressed as mean±SEM or histogram, as indicated in the respective experiments. Statistical significance was determined using analysis of variance (ANOVA; GraphPad Instat®), followed by Tukey's post-hoc analysis. Results were considered significant if $p<0.05$.

Results

Diabetes induces retinal EC activation

Chapter 2 showed that diabetic retinal capillary is significantly stiffer compared to non-diabetic mouse retinal capillaries (Fig. 2.2C). As expected, this significant increase in retinal capillary stiffness correlated with ~2-fold ($p<0.05$) greater accumulation of $CD11b^{+}$

monocytes/macrophages in diabetic retinas than in non-diabetic controls (Fig. 3.1A). This significant increase in monocyte accumulation within diabetic retinas correlated strongly with a marked inhibition in the levels of both eNOS phosphorylation (activation) and expression (3- and ~3.5-fold lower, respectively; $p<0.01$), with the relative levels of eNOS phosphorylation (p-eNOS/eNOS) also undergoing a 3-fold decrease ($p<0.01$) in diabetic retinas compared to non-diabetic controls (Fig. 3.1B).

Diabetes leads to loss of mechanosensitive TRPV4 in retinal ECs

Activation of TRPV4, a member of the transmembrane TRP family of Ca^{2+} channels, is known to enhance NO production through both Ca^{2+}/Calmodulin-dependent eNOS activation (18, 19), and activation of Calmodulin kinase II which phosphorylates eNOS on Ser1177 (20). Since eNOS phosphorylation was impaired in diabetic mouse retinas, here I looked at the expression of mechanosensitive TRPV4 in normal and diabetic mouse retinas. Whole mount retinal immunofluorescence and quantitative image analysis revealed that diabetic mouse retinal capillaries exhibit ~70% decrease ($p<0.01$) in TRPV4 expression when compared to their non-diabetic counterparts (Fig. 3.2A).

Consistent with our *in vivo* observations, HG treatment caused significant downregulation of TRPV4 in cultured human retinal ECs, as judged by ~70% lower ($p<0.01$) TRPV4 expression in HG-treated ECs than in NG-treated counterparts (Fig. 3.2B). Further, to determine TRPV4 activity, NG- and HG-treated retinal ECs were loaded with Ca^{2+}-sensitive Fluo-4/AM dye and Ca^{2+} influx was recorded in response to a selective TRPV4 agonist GSK1016790A. Predictably, HG-treated retinal ECs exhibited ~40%

decrease ($p<0.001$) in both baseline and peak Ca^+ influx levels (Fig. 3.2C). Importantly, this decrease in TRPV4 activity was not due to difference in osmotic pressure, as indicated by the lack of increase in Ca^+ influx in mannitol-treated ECs (osmotic control).

Further, I looked to see whether HG-induced downregulation of TRPV4 was associated with impaired eNOS phosphorylation in cultured ECs. Quantitative analyses of cells labeled with phospho-eNOS (p-eNOS) antibody revealed that HG-treated ECs produce an ~77% decrease in the number of high p-eNOS-expressing ECs than NG-treated cells (Fig. 3.3A). HG-induced p-eNOS downregulation was associated with impaired endothelial NO production and enhanced monocyte-EC adhesion. Quantitative analysis of ECs labeled with NO-sensitive dye revealed that, HG-treated ECs exhibit a ~30% decrease ($p<0.001$) in intracellular NO levels compared to NG-treated ECs, and this HG-induced decrease in NO levels was associated with 2.5-fold increase ($p<0.001$) in monocyte-EC adhesion (Fig. 3.3B, C). Notably, these observed differences in monocyte-EC adhesion were not due to differences in osmotic pressure as mannitol-treated ECs (osmotic control) showed no difference in monocyte-EC adhesion compared to NG-treated ECs.

Inhibition of LOX-dependent subendothelial matrix stiffening rescues loss of TRPV4 under high glucose conditions

Consistent with our previous *in vivo* and *in vitro* observations (Chapter 2), HG-treated ECs exhibit ~1.7-fold increase ($p<0.001$) in LOX expression along with ~2-fold increase ($p<0.001$) in LOX activity (Fig. 3.4A, B). Quantitative analysis of AFM force indentation curves revealed that increase in LOX activity correlates with ~1.7-fold increase

($p<0.001$) in stiffness of subendothelial matrix deposited by HG-treated ECs, and inhibition of LOX activity in HG-treated ECs using a pharmacological LOX inhibitor BAPN suppresses HG-induced subendothelial matrix stiffening (Fig. 3.4C).

To confirm whether subendothelial matrix stiffening can independently regulate TRPV4, LOX activity in HG-treated cells was pharmacologically inhibited using BAPN and the corresponding effects on TRPV4 activity and expression were measured. Importantly, inhibition of LOX activity (by BAPN) in HG-treated ECs prevented HG-induced suppression of both TRPV4 expression and activity (Fig. 3.4D,E).

Subendothelial matrix stiffening alone is sufficient to inhibit TRPV4 activity and promote retinal EC activation

Previously, I showed that subendothelial matrix stiffening is necessary and sufficient to promote retinal EC activation. However, whether this subendothelial matrix stiffening-dependent inflammatory effect was mediated through inhibition of TRPV4 activity remains unknown. Thus, to determine the extent to which LOX-mediated subendothelial matrix stiffening alone causes HG-induced inhibition of TRPV4 activity, fresh, NG-treated retinal ECs were plated on decellularized subendothelial matrices obtained from NG- and HG ± BAPN-treated EC cultures and examined TRPV4 activity and endothelial NO production (Fig. 3.5A). Under these conditions where the effects of LOX is conveyed only via subendothelial matrix stiffness, retinal ECs plated on HG-treated (stiffer) subendothelial matrix exhibited significantly lower TRPV4 activation than those plated on NG- or HG+BAPN-treated subendothelial matrix, as determined by the

fluorescent intensities of baseline and peak Ca^{2+} levels in the cells (Fig. 3.5B). Thus, these findings indicate that LOX-dependent subendothelial matrix stiffening that occurs under HG conditions is alone sufficient to cause TRPV4 downregulation.

To unequivocally confirm the pivotal role of subendothelial matrix stiffening in HG-induced suppression of TRPV4 activity, NG-treated cells were grown on normal and stiff synthetic matrices. Quantitative measurement of Ca^{2+} influx revealed that ECs on stiffer matrix exhibit a significant decrease in both baseline and peak Ca^{2+} levels (Fig. 3.5C). These findings clearly indicate that subendothelial matrix stiffening is sufficient to cause TRPV4 downregulation.

Increase in TRPV4 activity mediates the anti-inflammatory effects of LOX inhibition on HG-treated ECs

To confirm whether the anti-inflammatory effects of LOX inhibition on HG-treated ECs are mediated through TRPV4, pharmacological antagonist of TRPV4, RN1734 (RN) was used and endothelial NO production and ICAM-1 expression were measured. Quantitative analyses of ECs labeled with NO-sensitive dye revealed that, HG-treated ECs exhibit ~80% decrease ($p<0.001$) in intracellular NO levels compared to NG-treated ECs, and this decrease in NO levels was restored with suppression of BM stiffening by BAPN (Fig. 3.6A). However, with suppression of TRPV4 activity, the restoration of NO levels was significantly diminished ($p<0.001$). Importantly, quantitatively analyses of cells labeled with ICAM-1 antibody revealed that HG-treated ECs exhibit a ~1.5-fold increase in the number of high ICAM-1-expressing ECs than NG-treated cells and suppression of

subendothelial matrix stiffness significantly inhibited ICAM-1 expression in HG-treated cells (Fig. 3.6B). Further, the number of high ICAM-1-expressing cells in HG+BAPN-treated ECs were significantly increased by TRPV4 inhibition with RN1734. Together, these data suggest that the anti-inflammatory effects of LOX inhibition on HG-treated ECs is mediated via an increase in TRPV4 activity.

Inhibition of retinal capillary and subendothelial matrix stiffening prevents retinal endothelial TRPV4 impairment and retinal EC activation

In Chapter 2, I have shown that LOX-mediated crosslinking contributes to subendothelial matrix stiffening seen in HG-treated retinal ECs and diabetic mouse retinas exhibit significantly increased LOX expression and increased capillary stiffness. Here I show that pharmacological inhibition of LOX activity (using BAPN) in diabetic mice significantly inhibited ($p<0.001$) diabetes-induced retinal capillary stiffening (Fig. 3.7A). Crucially, this inhibition in diabetic retinal capillary stiffening prevented the loss of TRPV4 in retinal capillaries (Fig. 3.7B) that, in turn, correlated with suppression of retinal endothelial ICAM-1 (Fig. 3.7C).

Pharmacological enhancement of TRPV4 activity reverses the effect of subendothelial matrix stiffness on retinal EC activation

To determine whether HG-induced retinal EC activation can be inhibited by direct TRPV4 activation, TRPV4-selective *agonist* (GSK1016790) was added to HG-treated retinal ECs. Remarkably, pharmacologically enhance TRPV4 activity (using

GSK1016790) in HG-treated retinal ECs significantly restored ($p<0.001$) the production level of constitutive endothelial NO (Fig. 3.8). Further, pharmacological enhancement of TRPV4 activity also suppressed the number of high ICAM-1-expressing cells in HG-treated ECs which, in turn, inhibited monocyte-EC adhesion (Fig. 3.9A, B).

To confirm the pivotal role of subendothelial matrix stiffening-mediated TRPV4 impairment in retinal EC activation, NG-treated cells were grown on synthetic matrices of normal (1000 Pa) or higher (4000 Pa) stiffness and treated with TRPV4-selective *agonist* (GSK1016790). Consistent with the result from the native subendothelial matrix, retinal ECs plated on the synthetic matrix exhibit the same trend, where addition of TRPV4 agonist to ECs grown on stiffer matrix significantly enhanced (~2.7-fold; $p<0.001$) endothelial NO levels and reduced (65%; $p<0.001$) monocyte adhesion (Fig. 3.10A, B). Together, these findings indicate that TRPV4 acts as a pivotal mechanical 'control switch' in subendothelial matrix stiffening-dependent control of diabetic retinal EC activation.

Discussion

Retinal inflammation is a major characteristic of DR pathogenesis, where retinal EC activation is acting as the rate-limiting step in diabetic retinal inflammation (21, 22). Although many studies have revealed that epigenetic, metabolic and inflammatory factors play an important role in regulation of retinal EC activation (22-24), our recent findings indicated that LOX-mediated subendothelial matrix stiffening alone is necessary and sufficient to cause HG-induced retinal ECs activation (1). However, the molecular

mechanism behind this subendothelial matrix stiffening-mediated retinal EC activation has remained unclear. Our current findings revealed that subendothelial matrix stiffening-dependent retinal EC activation is mediated by TRPV4, a mechanosensitive Ca^{+} ion channel. Crucially, pharmacological inhibition of LOX-dependent BM stiffening in diabetic mice caused a significant rescue of TRPV4 loss and associated decrease in ICAM-1 expression in retinal capillaries. I further show that inhibition of TRPV4 activity alone is sufficient to activate retinal ECs. By highlighting the critical yet previously unrecognized role of TRPV4 in HG-induced retinal EC activation, this study creates a new paradigm for the understanding of diabetic retinal inflammation and provides a strong rationale for detailed preclinical studies to evaluate TRPV4 as a potential therapeutic target for anti-inflammatory DR therapy either alone or in conjunction with existing DR treatment strategies.

Vascular inflammation is a hallmark of diabetic retinopathy and is associated with impaired endothelial NO (25). Further, DR pathogenesis has been shown to accelerate with genetic knockout of endothelial nitric oxide synthase (eNOS), the primary enzyme that produces endothelial NO (26). Consistent with these reports, I found that our mouse model of DR and HG-treated retinal EC cultures demonstrated significant decrease in phosphorylated eNOS (p-eNOS) expression. Notably, the impairment of p-eNOS was associated with LOX-mediated subendothelial matrix stiffening and increased monocyte-EC adhesion in HG-treated retinal EC cultures.

To elucidate the mechanism underlying BM stiffness-dependent retinal endothelial activation, I looked at the role of mechanosensitive TRPV4 Ca^{2+} channel. I focused on

endothelial TRPV4 because firstly, it has been shown to be activated by physical cues such as subendothelial matrix stiffness, cyclic stretch, shear stress and osmotic pressure (2-4), and secondly, its activation enhances endothelial NO production not only through Ca^{2+}/Calmodulin-dependent eNOS activation (18, 19), but also through activation of Calmodulin kinase II which phosphorylates eNOS on Ser1177 (20). Importantly, I showed that the expression of TRPV4 is significantly downregulated in diabetic mouse retinas, which is consistent with what had been found in diabetic rat retina (27). Our current findings are the first to identify subendothelial matrix stiffening as an independent regulator of TRPV4, as confirmed by the *in vitro* studies where suppression of LOX-dependent subendothelial matrix stiffening restored TRPV4 levels in HG-treated ECs. Thus, it is plausible that the decrease in TRPV4 level observed in diabetic mouse retinal capillaries results, at least in part, from diabetic-induced stiffening of subendothelial BM.

In the current study, downregulation of TRPV4 activity and expression on HG-induced stiffer subendothelial matrix correlated directly with p-eNOS/NO levels and inversely with monocyte-EC adhesion. Thus, I looked to see whether retinal endothelial TRPV4 activation is sufficient to regulate NO-dependent control of monocyte-EC adhesion. Indeed, pharmacological enhancement of TRPV4 in HG-treated retinal EC cultures alone increased eNOS phosphorylation and NO production, and suppressed ICAM-1 expression and monocyte-EC adhesion. Together, these new findings confirm that loss of TRPV4 activity contributes greatly to subendothelial matrix stiffening-dependent mechanical control of diabetic retinal endothelial activation, thus, confirming the pivotal role of TRPV4 in DR pathogenesis.

Although steroids have been used for anti-inflammatory treatments of DR (28, 29), they exert side effects such as increased intraocular pressure and cataract formation (28, 30). Thus, there is an unmet need to identify new anti-inflammatory targets and therapies for more effective DR management. By highlighting the crucial role of mechanosensitive TRPV4 in retinal EC activation, this study implicates TRPV4 as a novel anti-inflammatory target for management of early DR. Future studies that uncover the mechanotransduction pathways linking BM stiffening, TRPV4 and retinal EC activation may lead to the identification of new anti-inflammatory targets for more effective DR management.

Conclusion

In summary, I here show that TRPV4 expression was markedly impaired in diabetic mouse retinal capillaries, which correlates with enhanced ICAM-1, impaired eNOS, and increased $CD11b^+$ leukocyte accumulation. Notably, inhibition of LOX-dependent subendothelial matrix stiffening alone caused significant recovery of TRPV4 expression/activity and endothelial NO production. Further, and more importantly, pharmacological enhancement of TRPV4 alone suppressed the inflammatory effects of HG-induced BM stiffening in vitro.

These findings identify a crucial role of mechanosensitive TRPV4 in diabetic retinal inflammation and implicate TRPV4 as a novel anti-inflammatory target for management of early DR.

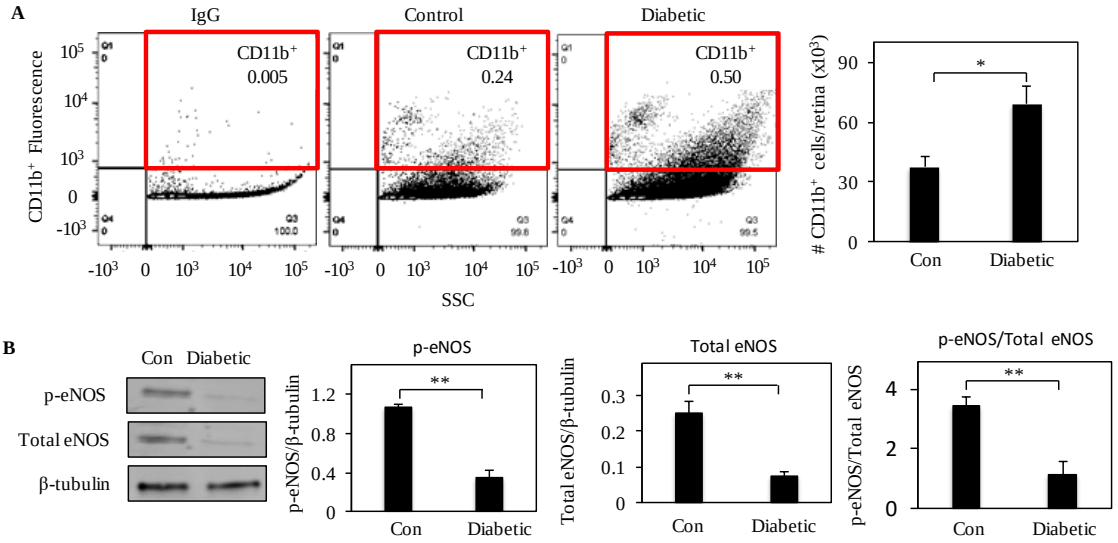

FIGURE 3.1. Diabetes induces retinal EC activation. (A) Levels of $CD11b^+$ monocytes/macrophages accumulated in mouse retinas were determined by flow cytometry. Quantitative analysis of representative vs fluor. vs SSC dot plots indicates that diabetic mouse retinas exhibit ~2.1-fold greater accumulation of $CD11b^+$ monocytes/macrophages (red box) than in non-diabetic controls. (B) Representative Western blot bands and their densitometric analyses (bar graphs) together reveal that both phosphorylated eNOS (p-eNOS) and total eNOS expression is significantly higher (**, $p<0.01$) in diabetic mouse retinas when compared with control retinas. Bar graphs indicate average ± SEM from five retinas per condition. p-eNOS levels were normalized with respect to the corresponding levels of β-tubulin (loading control) or total eNOS. *, $p<0.05$; **, $p<0.01$.

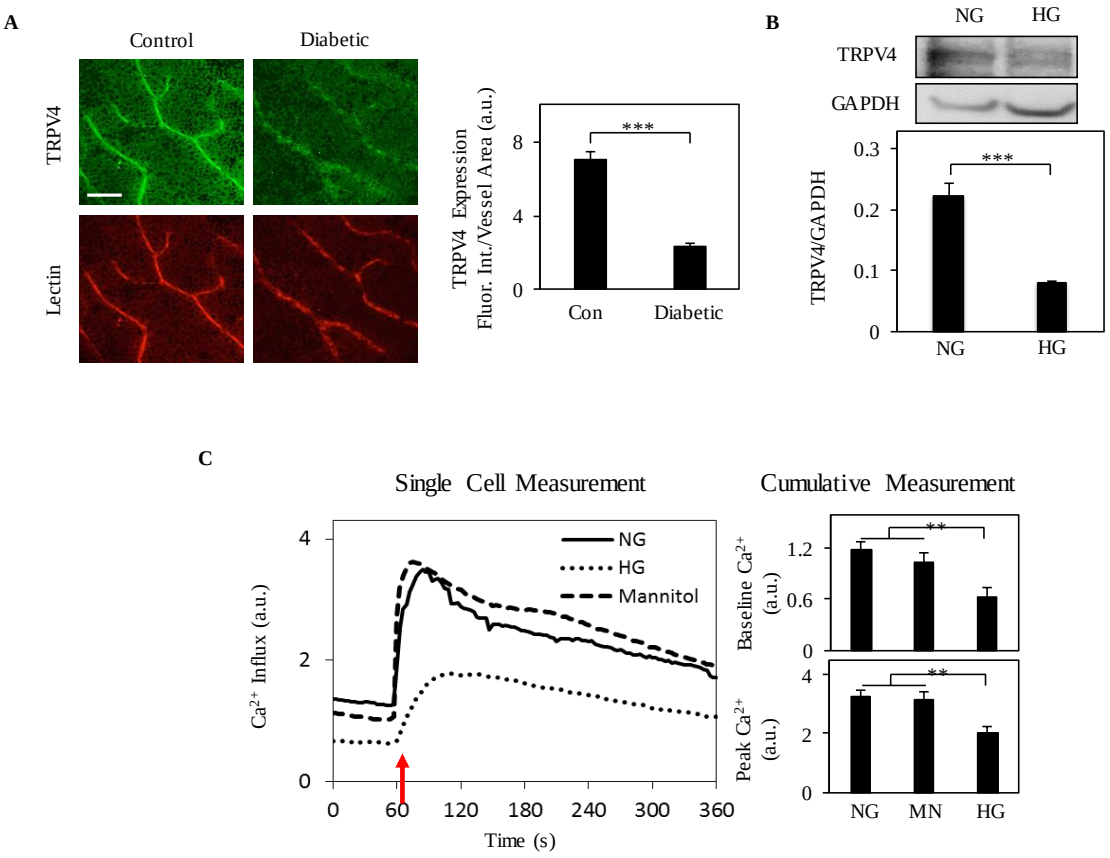

FIGURE 3.2. Diabetes leads to loss of mechanosensitive TRPV4 in retinal ECs. (A) Representative fluorescent images of non-diabetic control and diabetic mouse retinas immunostained with anti-TRPV4 and subsequent fluorescence intensity measurements reveal that diabetes leads to a ~70% decrease (***, $p<0.001$) in TRPV4 expression in retinal capillaries. Average fluorescence intensity/unit vessel area was determined from multiple ($n \geq 15$) retinal capillaries. Scale bar: 50 µm. (B) Representative Western blot bands (from three repeats) and their densitometric analyses (bar graph) together reveal that HG-treated retinal ECs exhibit ~70% (***, $p<0.001$) decrease in TRPV4 expression than NG-treated cells. TRPV4 levels were normalized with respect to the corresponding levels of GAPDH (loading control). (C) Calcium microfluorimetry was performed in Fluo4-AM-loaded HRECs cultured in medium containing NG, HG or mannitol (osmotic control). Line graph from a representative cell and bar graph (average ± SEM) from multiple ($n \geq 20$) cells reveal that HG treatment significantly inhibits TRPV4 activity, as indicated by a ~40% decrease (**, $p<0.01$) in both baseline Ca^{2+} and peak Ca^{2+} influx levels. Arrow indicates the moment selective TRPV4 agonist GSK1016790A was added to cells. HREC: Human Retinal Microvascular Endothelial Cells; NG: Normal Glucose, 5.5 mM; HG: High Glucose, 30 mM; MN: Mannitol, 30mM. **, $p<0.01$; ***, $p<0.001$.

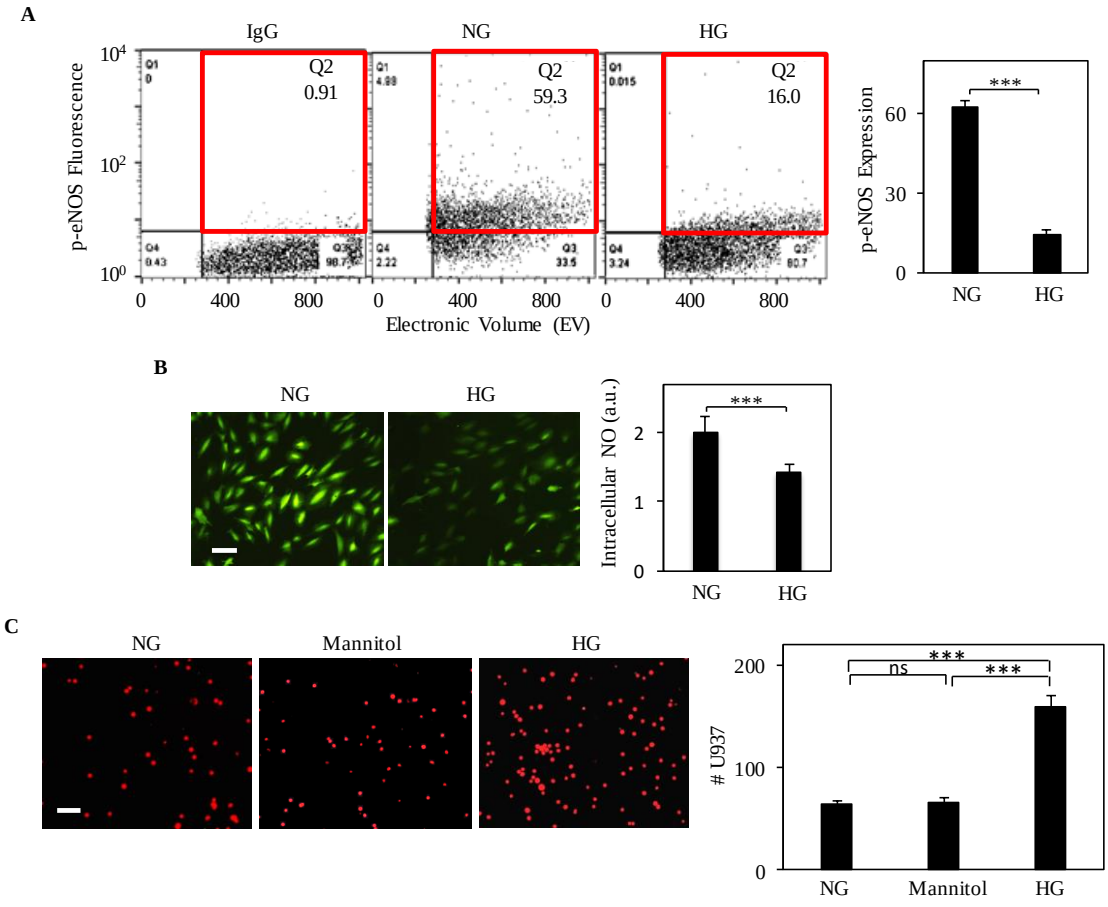

FIGURE 3.3. Downregulation of mechanosensitive TRPV4 is associated with HG-induced retinal EC activation. (A) Intracellular expression of phosphorylated eNOS (p-eNOS) was determined by flow cytometry. Quantitative analysis of representative fluorescence vs size (electronic volume) dot plots (red box) indicates that HG treatment produces an ~77% decrease in the number of high p-eNOS-expressing ECs (bar graph) than NG treatment. (B) Representative fluorescent images of HRECs labeled with DAF-FM diacetate, a NO-sensitive dye, and their subsequent intensity measurements ($n \geq 25$ cells) indicate a ~30% (***, $p<0.001$) reduction of constitutive NO production in HG-treated ECs. (C) Fluorescently-labeled U937 cells were added to EC monolayers for 30 min. Representative fluorescent images of adherent U937 cells and subsequent cell count of adherent U937 cells (bar graph) indicate a significant (2.5-fold; ***, $p<0.001$) increase in monocyte-EC adhesion under HG conditions. Bar graph indicates average ± SEM (per mm^2) from multiple ($n \geq 10$) images of monocyte-EC co-cultures. Scale bar: 100 μm. ***, $p<0.001$; ns, no significance.

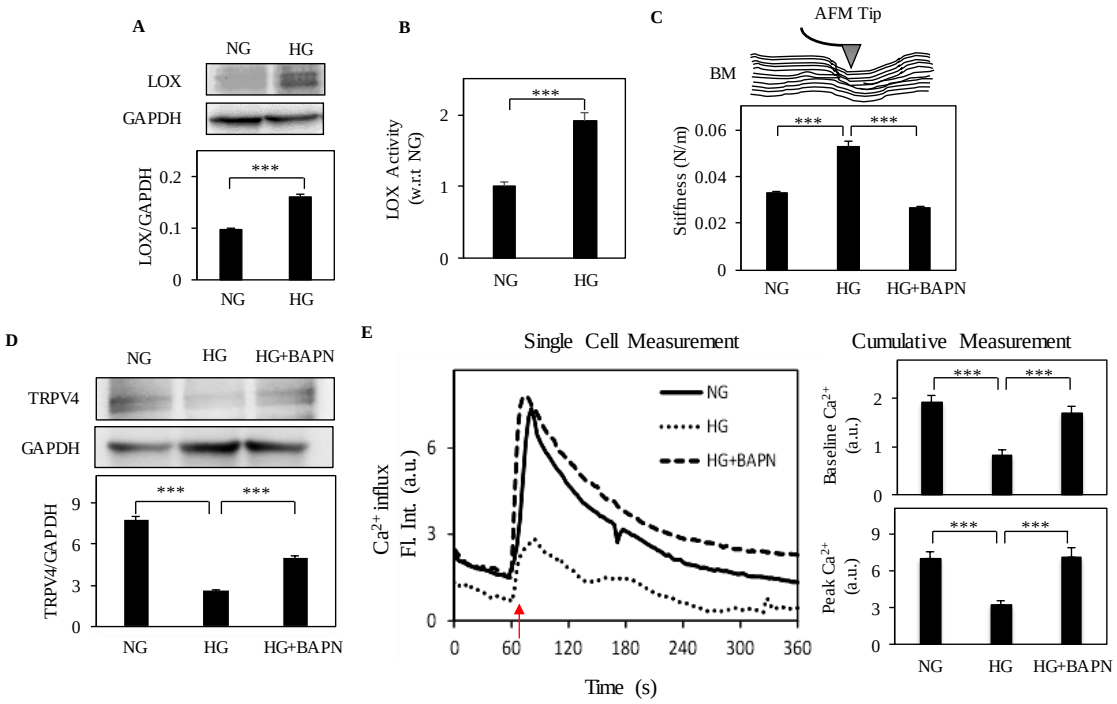
A
NG
HG
LOX
GAPDH
LOX/GAPDH
0
0.1
0.2
***
NG
HG
B
LOX Activity
(w.r.t NG)
0
1
2
***
NG
HG
C
AFM Tip
BM
Stiffness (N/m)
0
0.02
0.04
0.06
***
***
NG
HG
HG+BAPN
D
NG
HG
HG+BAPN
TRPV4
GAPDH
TRPV4/GAPDH
0
3
6
9
***
***
NG
HG
HG+BAPN
E
Single Cell Measurement
Cumulative Measurement
NG
HG
HG+BAPN
Ca2+ influx
Fl. Int. (a.u.)
0
3
6
0
60
120
180
240
300
360
Time (s)
Baseline Ca2+
(a.u.)
0
1
2
***
***
Peak Ca2+
(a.u.)
0
3
6
9
***
***
NG
HG
HG+BAPN

FIGURE 3.4. Inhibition of LOX-dependent subendothelial matrix stiffening rescues loss of TRPV4 under high glucose conditions. (A) Western blot bands and their densitometric analyses (bar graph) together reveal that lysyl oxidase (LOX) expression by retinal ECs increases significantly (~1.7-fold: ***, $p<0.001$) upon treatment with HG. LOX levels were normalized with respect to the corresponding levels of GAPDH, which served as the loading control. (B) LOX activity assay indicates that HG-treated retinal ECs exhibit a two-fold increase (***, $p<0.001$) in LOX activity compared with NG-treated cells. LOX activity levels were normalized with respect to NG levels. The increase in HG-mediated LOX expression correlated directly with a corresponding increase in LOX activity, as measured by a LOX activity kit and quantified in the bar graph. (C) Stiffness of HREC-secreted subendothelial matrix was measured by an atomic force microscope (AFM) fitted with a ~40 nm pyramidal silicon nitride tip (schematic). Quantitative analysis of multiple ($n\geq10$) force indentation measurements revealed a 1.7-fold (***, $p<0.001$) increase in subendothelial matrix stiffness under HG conditions than in NG conditions. Importantly, inhibition of LOX activity in HG-treated ECs (by BAPN) prevents HG-induced subendothelial matrix stiffening. (C) Representative Western blot bands (from three repeats) and their densitometric analyses (bar graph) together reveal that HG-induced downregulation of TRPV4 expression was prevented by inhibition of LOX activity. TRPV4 levels were normalized with respect to the corresponding levels of GAPDH (loading control). ***, $p<0.001$. (D) LOX inhibition restores TRPV4 activity, as indicated by recovery of Ca^{2+} influx in HG-treated ECs following stimulation with selective TRPV4 agonist GSK1016790A (red arrow; line graph of a representative cell). Bar graphs indicate both baseline and peak Ca^{2+} levels in HG-treated ECs were restored with LOX inhibition. BAPN: β-amino-propionitrile (0.1 mM). ***, $p<0.001$.

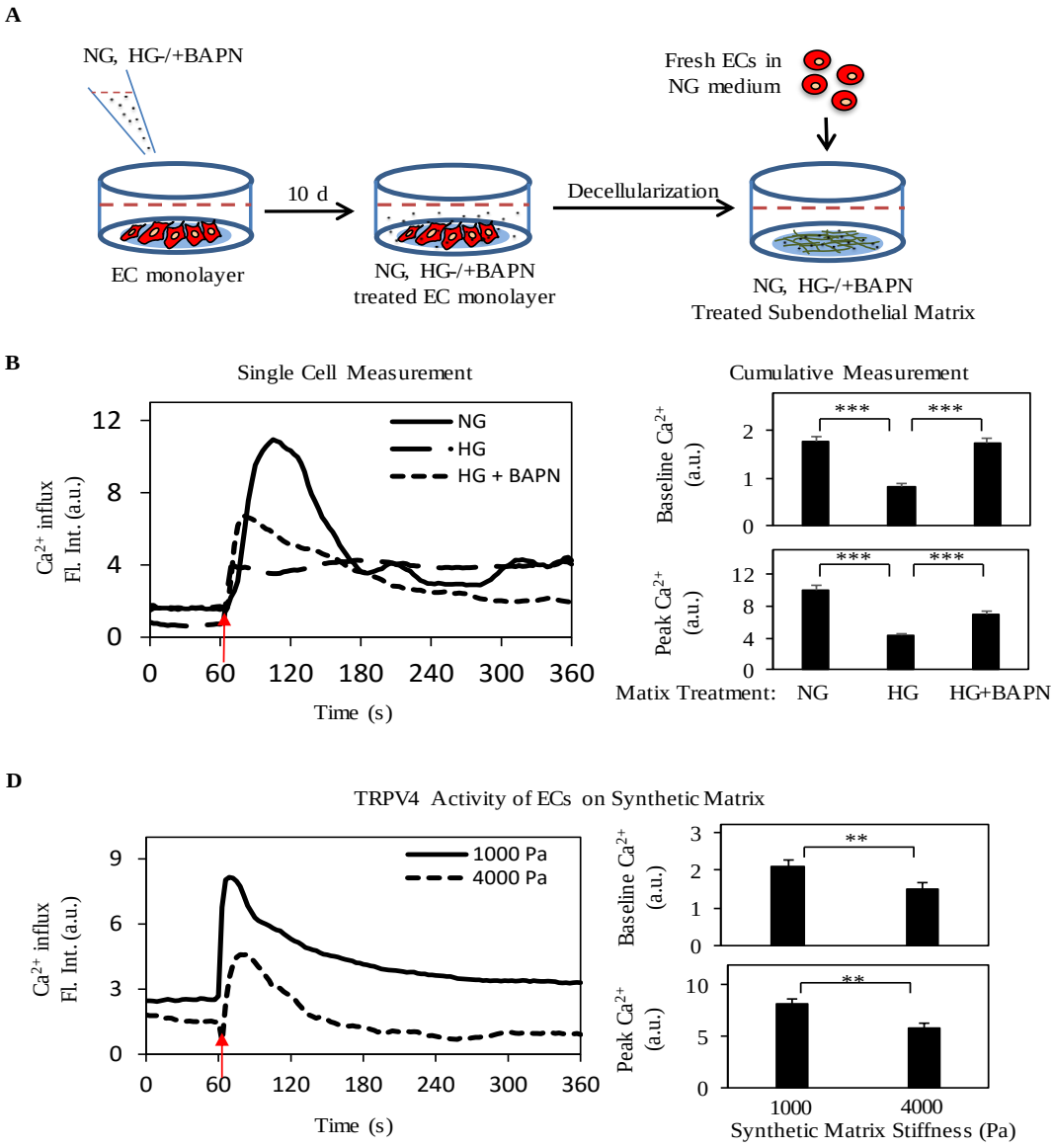
A
NG, HG-/+BAPN
10 d
Decellularization
Fresh ECs in
NG medium
EC monolayer
NG, HG-/+BAPN
treated EC monolayer
NG, HG-/+BAPN
Treated Subendothelial Matrix
B
Single Cell Measurement
Cumulative Measurement
NG
HG
HG + BAPN
Ca2+ influx
Fl. Int. (a.u.)
Time (s)
Baseline Ca2+
(a.u.)
Peak Ca2+
(a.u.)
***
Matix Treatment: NG HG HG+BAPN
D
TRPV4 Activity of ECs on Synthetic Matrix
1000 Pa
4000 Pa
Ca2+ influx
Fl. Int. (a.u.)
Time (s)
Baseline Ca2+
(a.u.)
Peak Ca2+
(a.u.)
**
1000
4000
Synthetic Matrix Stiffness (Pa)

FIGURE 3.5. Subendothelial matrix stiffening alone is sufficient to inhibit TRPV4 activity. (A) Schematic depiction of the experimental procedure to examine the effect of treated, decellularized subendothelial matrix on untreated ECs. (B) TRPV4 activity was measured in NG-treated ECs grown on decellularized subendothelial matrices obtained from preceding NG, HG or HG+BAPN cultures. Ca^{2+} influx measurements indicate that HG-induced subendothelial stiffening alone causes significant suppression of TRPV4 activity, which did not occur on 'normalized' subendothelial matrix obtained from BAPN-treated cultures. (B) Fresh NG-treated ECs were plated on synthetic matrices of normal (1000 Pa) or higher (4000 Pa) stiffness and evaluated for TRPV4 activity. Quantitative measurement of Ca^{2+} influx revealed that ECs on stiffer matrix exhibit a significant decrease in both baseline and peak Ca^{2+} levels. **, $p<0.01$; ***, $p<0.001$.

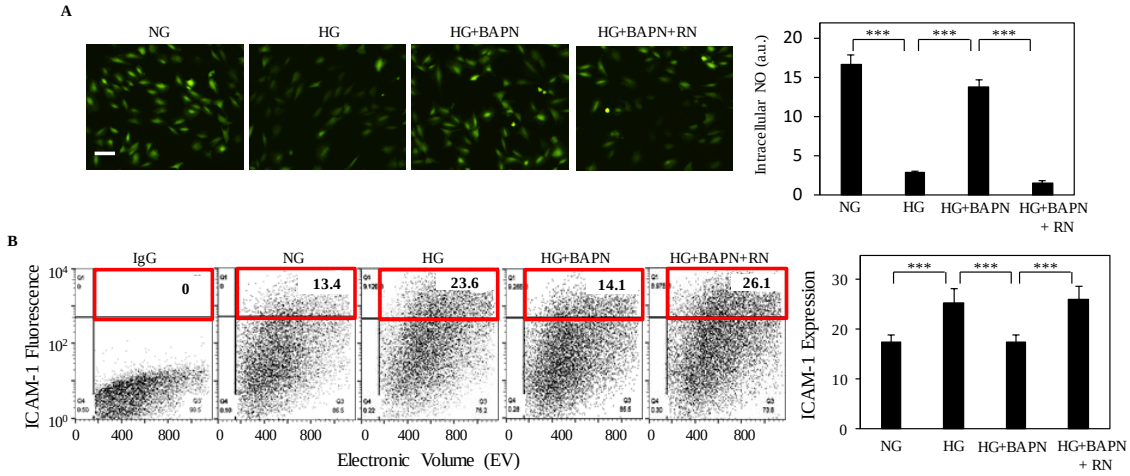

FIGURE 3.6. Increase in TRPV4 activity mediates the anti-inflammatory effects of LOX inhibition on HG-treated ECs. (A) Representative fluorescent images of HRECs labeled with DAF-FM diacetate, a NO-sensitive dye, and their subsequent intensity measurements (n≥25 cells) reveal that inhibition of subendothelial matrix stiffening prevents the loss of constitutive NO production caused by HG treatment. Further, the prevention of NO impairment was lost with TRPV4 inhibition by RN1734. Scale bar: 100 μm. (B) Surface expression of endothelial ICAM-1 was determined by flow cytometry. Quantitative analysis of representative fluorescence vs size (electronic volume) dot plots indicates that HG treatment produces an ~1.5-fold increase in the number of high ICAM-1-expressing ECs (red box and bar graph) than NG treatment and inhibition of subendothelial matrix stiffening prevents ICAM-1 upregulation, but RN treatment diminished the prevention effect of BAPN. RN: RN1737, TRPV4 antagonist. ***, $p<0.001$.

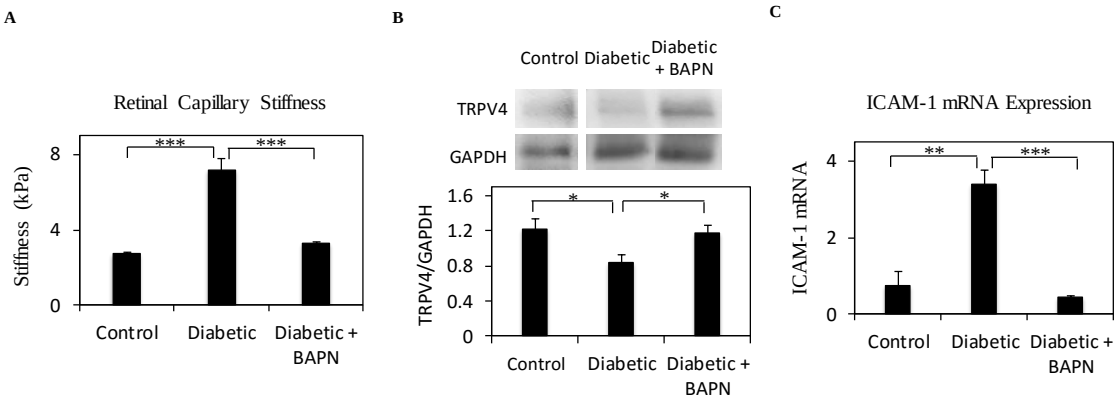

FIGURE 3.7. Inhibition of retinal capillary and subendothelial matrix stiffening prevents retinal endothelial TRPV4 impairment and retinal EC activation. (A) Quantitative analysis of multiple ($n \geq 10$) force indentation measurements revealed a 2.6-fold (***, $p<0.001$) increase in retinal capillary stiffness in diabetic mouse retinal capillaries than in non-diabetic control condition. Further, inhibition of LOX activity with BAPN significantly prevented capillary stiffening in diabetic retinal capillaries. (B) Representative Western blot bands and their densitometric analyses (bar graphs) together reveal that TRPV4 expression is significantly impaired (**, $p<0.01$) in diabetic mouse retinal capillaries when compared with control retinal capillaries, and this impairment was prevented with LOX inhibition using BAPN. Bar graphs indicate average ± SEM from retinal capillaries of three retinas per condition. TRPV4 levels were normalized with respect to the corresponding levels of GAPDH (loading control). (C) Real-time RT-PCR analysis shows that diabetic retinal capillaries exhibit ~3-fold increase (**, $p<0.01$) in ICAM-1 mRNA expression than non-diabetic controls and this increase in ICAM-1 mRNA was inhibited by BAPN treatment. ICAM-1 mRNA levels were normalized with respect to NG levels. BAPN: β-amino-propionitrile (3 mg/kg). *, $p<0.05$; **, $p<0.01$; ***, $p<0.001$.

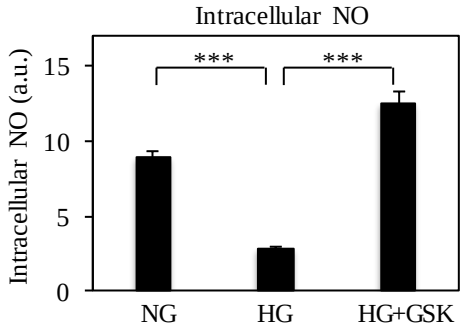

FIGURE 3.8. Pharmacological enhancement of TRPV4 activity reverses the effect of subendothelial matrix stiffness on endothelial NO production. (A) Pharmacological enhancement of TRPV4 activity (using GSK1016790A) in HG-treated ECs resulted in ~5.5-fold increase (***, $p<0.001$) in production of constitutive endothelial NO, as indicated by fluorescent intensity measurement of multiple ($n\geq25$) ECs labeled with the NO-sensitive dye DAF-FM diacetate. ***, $p<0.001$.

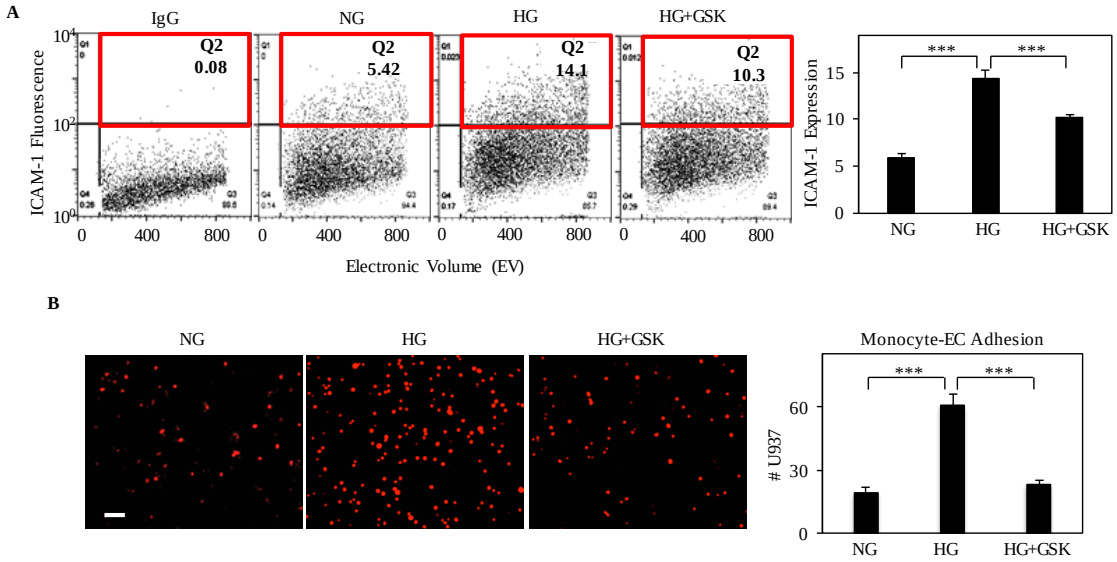

FIGURE 3.9. Pharmacological enhancement of TRPV4 activity reverses the effect of subendothelial matrix stiffness on retinal EC activation. (A) Surface expression of endothelial ICAM-1 was determined by flow cytometry. Quantitative analysis of representative fluorescence vs size (electronic volume) dot plots indicates that HG treatment produces an ~2.5-fold increase in the number of high ICAM-1-expressing ECs (red box and bar graph) than NG treatment and this increase was suppressed with pharmacological enhancement of TRPV4 activity using GSK1016790A. (B) The GSK-induced enhancement of NO production in HG-treated ECs resulted in ~60% decrease (***, $p<0.001$) in monocyte-EC adhesion. Bar graph indicates average ± SEM from multiple ($n\geq10$) images of monocyte-EC co-cultures. ***, $p<0.001$.

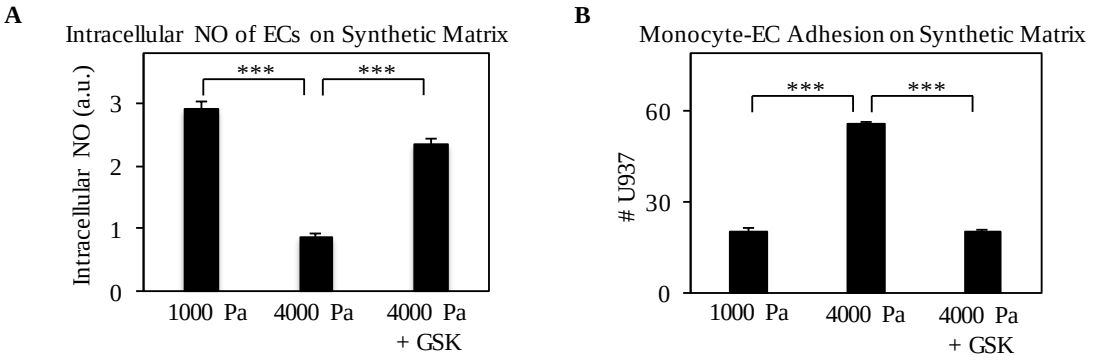

FIGURE 3.10. Pharmacological enhancement of TRPV4 activity reverses the effect of matrix stiffness-dependent retinal EC activation. (A) Pharmacological enhancement of TRPV4 activity (using GSK1016790A) in ECs grown on stiff (4000 Pa) synthetic matrix resulted in 2.7-fold increase (***, $p<0.001$) in production of constitutive endothelial NO. (B) The GSK-induced enhancement of NO production in ECs grown on stiff (4000 Pa) synthetic matrix resulted in ~65% decrease (***, $p<0.001$) in monocyte-EC adhesion. ***, $p<0.001$.

References

1. Yang, X., Scott, H. A., Monickaraj, F., Xu, J., Ardekani, S., Nitta, C. F., Cabrera, A., McGuire, P. G., Mohideen, U., Das, A., and Ghosh, K. (2016) Basement membrane stiffening promotes retinal endothelial activation associated with diabetes. *FASEB journal : official publication of the Federation of American Societies for Experimental Biology* **30**, 601-611

2. Thodeti, C. K., Matthews, B., Ravi, A., Mammoto, A., Ghosh, K., Bracha, A. L., and Ingber, D. E. (2009) TRPV4 channels mediate cyclic strain-induced endothelial cell reorientation through integrin-to-integrin signaling. *Circulation research* **104**, 1123-1130

3. Liedtke, W. (2007) TRPV channels' role in osmotransduction and mechanotransduction. *Handbook of experimental pharmacology*, 473-487

4. Scott, H. A., Yang, X., Ardekani, S., Cabrera, A., Wilson, R., Messaoudi-Powers, I., and Ghosh, K. TRPV4-mediated Biphasic Matrix-dependent Mechanical Control of Endothelial Activation. *Journal of cell science* **Submitted**

5. Adapala, R. K., Thoppil, R. J., Luther, D. J., Paruchuri, S., Meszaros, J. G., Chilian, W. M., and Thodeti, C. K. (2013) TRPV4 channels mediate cardiac fibroblast differentiation by integrating mechanical and soluble signals. *Journal of molecular and cellular cardiology* **54**, 45-52

6. Adapala, R. K., Thoppil, R. J., Ghosh, K., Cappelli, H. C., Dudley, A. C., Paruchuri, S., Keshamouni, V., Klagsbrun, M., Meszaros, J. G., Chilian, W. M., Ingber, D. E., and Thodeti, C. K. (2016) Activation of mechanosensitive ion channel TRPV4 normalizes tumor vasculature and improves cancer therapy. *Oncogene* **35**, 314-322

7. Jardin, I., Dionisio, N., Lopez, J. J., Salido, G. M., and Rosado, J. A. (2013) Pharmacology of TRP channels in the vasculature. *Current vascular pharmacology* **11**, 480-489

8. Adapala, R. K., Talasila, P. K., Bratz, I. N., Zhang, D. X., Suzuki, M., Meszaros, J. G., and Thodeti, C. K. (2011) PKCalpha mediates acetylcholine-induced activation of TRPV4-dependent calcium influx in endothelial cells. *American journal of physiology. Heart and circulatory physiology* **301**, H757-765

9. Ito, H., Akiyama, H., Iguchi, H., Iyama, K., Miyamoto, M., Ohsawa, K., and Nakamura, T. (2001) Molecular cloning and biological activity of a novel lysyl

oxidase-related gene expressed in cartilage. *The Journal of biological chemistry* **276**, 24023-24029

10. Bondareva, A., Downey, C. M., Ayres, F., Liu, W., Boyd, S. K., Hallgrimsson, B., and Jirik, F. R. (2009) The lysyl oxidase inhibitor, beta-aminopropionitrile, diminishes the metastatic colonization potential of circulating breast cancer cells. *PloS one* **4**, e5620

11. Chronopoulos, A., Tang, A., Beglova, E., Trackman, P. C., and Roy, S. (2010) High glucose increases lysyl oxidase expression and activity in retinal endothelial cells: mechanism for compromised extracellular matrix barrier function. *Diabetes* **59**, 3159-3166

12. Palamakumbura, A. H., and Trackman, P. C. (2002) A fluorometric assay for detection of lysyl oxidase enzyme activity in biological samples. *Anal Biochem* **300**, 245-251

13. Fogelgren, B., Polgar, N., Szauter, K. M., Ujfaludi, Z., Laczko, R., Fong, K. S., and Csiszar, K. (2005) Cellular fibronectin binds to lysyl oxidase with high affinity and is critical for its proteolytic activation. *The Journal of biological chemistry* **280**, 24690-24697

14. Yang, X., Scott, H. A., Ardekani, S., Williams, M., Talbot, P., and Ghosh, K. (2014) Aberrant cell and basement membrane architecture contribute to sidestream smoke-induced choroidal endothelial dysfunction. *Investigative ophthalmology & visual science* **55**, 3140-3147

15. Beacham, D. A., Amatangelo, M. D., and Cukierman, E. (2007) Preparation of extracellular matrices produced by cultured and primary fibroblasts. *Curr Protoc Cell Biol* **Chapter 10**, Unit 10 19

16. Wang, Y. L., and Pelham, R. J., Jr. (1998) Preparation of a flexible, porous polyacrylamide substrate for mechanical studies of cultured cells. *Methods in enzymology* **298**, 489-496

17. Yeung, T., Georges, P. C., Flanagan, L. A., Marg, B., Ortiz, M., Funaki, M., Zahir, N., Ming, W., Weaver, V., and Janmey, P. A. (2005) Effects of substrate stiffness on cell morphology, cytoskeletal structure, and adhesion. *Cell motility and the cytoskeleton* **60**, 24-34

18. Mendoza, S. A., Fang, J., Gutterman, D. D., Wilcox, D. A., Bubolz, A. H., Li, R., Suzuki, M., and Zhang, D. X. (2010) TRPV4-mediated endothelial Ca2+ influx and vasodilation in response to shear stress. *American journal of physiology. Heart and circulatory physiology* **298**, H466-476

19. Köhler, R., and Hoyer, J. (2007) Role of TRPV4 in the Mechanotransduction of Shear Stress in Endothelial Cells. In *TRP Ion Channel Function in Sensory Transduction and Cellular Signaling Cascades* (Liedtke, W., and Heller, S., eds) pp. 377-388, Circ Press, Boca Raton, FL

20. Fleming, I., Fisslthaler, B., Dimmeler, S., Kemp, B. E., and Busse, R. (2001) Phosphorylation of Thr(495) regulates Ca(2+)/calmodulin-dependent endothelial nitric oxide synthase activity. *Circulation research* **88**, E68-75

21. Miyamoto, K., Khosrof, S., Bursell, S. E., Rohan, R., Murata, T., Clermont, A. C., Aiello, L. P., Ogura, Y., and Adamis, A. P. (1999) Prevention of leukostasis and vascular leakage in streptozotocin-induced diabetic retinopathy via intercellular adhesion molecule-1 inhibition. *Proceedings of the National Academy of Sciences of the United States of America* **96**, 10836-10841

22. Tang, J., and Kern, T. S. (2011) Inflammation in diabetic retinopathy. *Progress in retinal and eye research* **30**, 343-358

23. Rangasamy, S., McGuire, P. G., and Das, A. (2012) Diabetic retinopathy and inflammation: novel therapeutic targets. *Middle East African journal of ophthalmology* **19**, 52-59

24. Kowluru, R. A., Kowluru, A., Mishra, M., and Kumar, B. (2015) Oxidative Stress and Epigenetic Modifications in the Pathogenesis of Diabetic Retinopathy. *Progress in retinal and eye research*

25. Kolluru, G. K., Siamwala, J. H., and Chatterjee, S. (2010) eNOS phosphorylation in health and disease. *Biochimie* **92**, 1186-1198

26. Li, Q., Verma, A., Han, P. Y., Nakagawa, T., Johnson, R. J., Grant, M. B., Campbell-Thompson, M., Jarajapu, Y. P., Lei, B., and Hauswirth, W. W. (2010) Diabetic eNOS-knockout mice develop accelerated retinopathy. *Investigative ophthalmology & visual science* **51**, 5240-5246

27. Monaghan, K., McNaughten, J., McGahon, M. K., Kelly, C., Kyle, D., Yong, P. H., McGeown, J. G., and Curtis, T. M. (2015) Hyperglycemia and Diabetes Downregulate the Functional Expression of TRPV4 Channels in Retinal Microvascular Endothelium. *PloS one* **10**, e0128359

28. Das, A., McGuire, P. G., and Rangasamy, S. (2015) Diabetic Macular Edema: Pathophysiology and Novel Therapeutic Targets. *Ophthalmology*

29. Bandello, F., Preziosa, C., Querques, G., and Lattanzio, R. (2014) Update of intravitreal steroids for the treatment of diabetic macular edema. *Ophthalmic research* **52**, 89-96

30. O'Day, R. F., Barthelmes, D., Zhu, M., Wong, T. Y., McAllister, I. L., Arnold, J. J., and Gillies, M. C. (2014) Intraocular pressure rise is predictive of vision improvement after intravitreal triamcinolone acetonide for diabetic macular oedema: a retrospective analysis of data from a randomised controlled trial. *BMC ophthalmology* **14**, 123

CHAPTER 4

TRPV4-mediated Rho/ROCK Signaling in Diabetes-induced Retinal Endothelial Activation

Preface

This Chapter identifies the mechanotransduction mechanism underlying TRPV4-mediated diabetic retinal EC activation.

Original contribution	:	Data for Figures 4.2 – 4.3A, 4.4, 4.5.
In collaboration	:	Data for Figures 4.1, 4.3B

Introduction

Studies performed in Chapter 2 demonstrated that endothelial activation is a hallmark of retinal inflammation associated with diabetic retinopathy (DR), which is mechanically controlled through an increase in subendothelial matrix stiffness. Findings from Chapter 3 revealed that mechanosensitive ion channel Transient Receptor Potential Vanilloid 4 (TRPV4) mediates subendothelial matrix stiffening-dependent retinal endothelial cell (EC) activation associated with high glucose treatment. However, the precise mechanotransduction pathway involved in TRPV4-dependent control of retinal EC remains unknown. Past studies have shown that Rho and its downstream effector Rho-associated Kinase (ROCK) (1) are key molecular players in cell tension (cell stiffness) and mechanotransduction and can be directly activated by matrix stiffening (1, 2). Further, Rho/ROCK activity is known to be suppressed by endothelial nitric oxide (NO) (3). Thus, I here examined the role of TRPV4-mediated Rho/ROCK signaling in diabetic retinal EC activation.

Material and Methods

Cell Culture and Glucose Treatment. Human retinal ECs and human monocytic cells (U937) were purchased from Cell Systems (Kirkland, WA) and ATCC, respectively. Human retinal ECs were grown in MCDB131 medium (Mediatech, VA) supplemented with 10% fetal bovine serum (FBS; Fisherbrand), 2 mM L-Glutamine (Life Technologies), 0.03 mg/mL Endothelial Cell Growth Supplement (Sigma), 1x antimycotic/antibiotic

mixture (Life Technologies), 10 ng/ml human EGF (Millipore), 1 μg/ml hydrocortizone, and 0.09 mg/ml heparin (Sigma). U937 monocytes were grown in RPMI-1640 medium (GE Healthcare) supplemented with 10% FBS, 2 mM L-Glutamine, 1.5 mg/ml sodium bicarbonate (Life Technologies), 1x antimycotic/antibiotic mixture, 1 mM sodium pyruvate (Life Technologies), and 4.5 mg/ml glucose (Sigma).

For *in vitro* studies, EC monolayers were cultured in regular growth medium containing normal glucose (NG, 5.5 mM) or high glucose (HG, 30 mM). After 9 days, culture medium was replaced with low serum (2.5% FBS) medium (with all other components at original concentration) and monolayers allowed to grow overnight prior to specific assay.

Measurement of Retinal Endothelial Cell Stiffness. The stiffness of NG- or HG -treated human retinal EC cultures was measured using a biological-grade atomic force microscope (AFM; Veeco Instruments, NY) operated in tapping mode using a ~5 μm glass bead attached to a 140 μm-long microcantilever (MLCT, Bruker) with bending spring constant of 0.1 N/m. The maximum indentation force applied to sample was ~8 nN. Measurements were made in force-curve mode, and the cantilever deflection was measured through the photodiode difference signal (S_{def}, volts). For each region, ~25 force curves were measured and only the linear region of force curves were considered for EC stiffness analysis. Sample stiffness is calculated as $k_{sample} = F/ z_s$, where F is the applied force and z_s the sample deformation. Average stiffness was obtained from indentations in at least 8 different regions across the retinal EC samples.

G-LISA Activation Assay. To detect the activity of Rho in cultured ECs, cells were grown in medium containing NG or HG for 10d, followed by lysis in RIPA buffer. EC culture lysates were centrifuged and supernatants were subjected to Rho activity measurement using a G-LISA Activation Assay Kit (Cytoskeleton Inc, CO), as per the manufacture's protocol.

Western Blot. To detect ROCK-2 expression in cultured ECs, cells were grown in medium containing NG or HG for 10d, followed by lysis in RIPA buffer. To detect ICAM-1 expression in cultured ECs, cells were grown in medium containing NG or HG for 10d, followed by Y27632 (Y27; 20 μM, 0.5h; Reagent Direct) ± RN1734 (25 μM, 5h; Sigma-Aldrich) in HG-treated ECs. Then treated ECs were lysed in RIPA buffer. EC culture lysates were centrifuged and supernatants were subjected to Western Blotting using nitrocellulose membrane, which was probed with antibodies against ROCK-2 (Santa Cruz Biotech) and ICAM-1 (Santa Cruz Biotech) followed by appropriate HRP-conjugated secondary antibodies (Vector Labs). GAPDH (Sigma) was used as the loading control. Western Blot protein bands were visualized using a camera-based imaging system (Biospectrum AC Imaging System) that automatically adjusts exposure time to avoid pixel saturation. ImageJ was used to perform densitometric analysis, and the measurements (within the 10-250 pixel intensity range) were normalized with respect to corresponding loading controls.

Calcium Imaging. Retinal ECs grown in NG or HG medium for 10 days were detached and re-plated on the corresponding decellularized subendothelial matrices in low serum medium containing NG or HG. Next day, one group of |HG-treated ECs were treated with Y27 (20 μM) for 30 minutes. ECs were then loaded with fluorescent Ca^{2+}-sensitive dye Fluo-4 AM (1 μM; Life Technologies) in Ca^{2+} buffer which contains 136 mM Sodium Chloride, 4.7 mM potassium chloride, 1.2 mM magnecium sulfate, 1.1 mM calcium chloride, 1.2 mM potassium phosphate monobasic, 5 mM sodium bicarbonate, 5.5 mM glucose and 20mM HEPES (Sigma). After excess dye was rinsed off and cells recovered in Ca^{2+} Buffer for 30 minutes. To detect TRPV4 activity, dye-loaded cells were imaged with time-lapse function every 3 seconds using Nikon Eclipse Ti microscope and after 1 min of time-lapse imaging, cells were stimulated with TRPV4 agonist GSK-1016790A (300 nM; Sigma-Aldrich) and imaged for an additional 5 min. Intracellular Ca^{2+} was quantified by measuring net intracellular fluorescence intensity ($n \geq 20$ cells per condition; using ImageJ), as previously described (4).

Intracellular Nitric Oxide (NO) Production. Retinal ECs grown in NG or HG medium for 10 days were detached and re-plated on the corresponding decellularized subendothelial matrices in low serum medium containing NG or HG. After overnight incubation, one group of HG-treated cells were treated with selective TRPV4 antagonist RN1734 (RN; 25 μM, 5h). The HG and HG+RN-treated cells were then be treated with a ROCK inhibitor Y27 (20 μM, 30 minutes). Cells were then loaded with fluorescent NO-sensitive dye DAF-FM diacetate (2 μM; Life Technologies), as per manufacturer's protocol. After excess dye

was rinsed off and cells recovered in the respective medium, the medium was replaced with Krebs–Henseleit buffer. Dye-loaded cells were imaged using Nikon Eclipse Ti microscope and intracellular fluorescence intensities were quantified using ImageJ (n ≥20 cells per condition).

Monocyte-EC Adhesion. ECs were cultured in NG or HG medium for 10 days prior to Y27±RN treatment as described above. Fluorescently-labeled U937 cells (125,000 cells/cm^2) were then added to the EC monolayers for 30 minutes at 37ºC. Following rinsing with PBS, adherent monocytes were fixed with 1% PFA, imaged using Nikon Eclipse Ti microscope fitted with a Nikon DS-Qi1Mc camera, and counted using ImageJ (≥10 images per condition).

Statistics. All data were obtained from multiple replicates (n ≥ 3) and expressed as mean±SEM or histogram, as indicated in the respective experiments. Statistical significance was determined using analysis of variance (ANOVA; GraphPad Instat®), followed by Tukey's post-hoc analysis. Results were considered significant if $p<0.05$.

Results

HG treatment increases EC stiffness

Chapter 2 showed that diabetes leads to retinal capillary stiffening (Fig. 2.2C). Since capillary contains both ECs and basement membrane, here I looked to see whether HG-

treatment also simultaneously increased EC stiffness. A biological-grade AFM was used to obtain the stiffness measurements of NG- or HG -treated human retinal ECs in tapping mode The maximum indentation force applied to sample was ~8 nN and the indentation curves were recorded. The AFM force indentations revealed that HG-treated ECs are ~5-fold stiffer ($p<0.01$) compared to NG-treated ECs (Fig. 4.1A).

Rho/ROCK2 is upregulated in HG-treated ECs

Rho/ROCK signaling is known to regulate cell contractility which is proportional to cell stiffness. Thus, I looked to see whether HG-induced EC stiffening was associated with upregulation of Rho/ROCK activity. Here I showed that HG treatment caused a ~50% increase of Rho activity in cultured human retinal ECs (Fig. 4.2A). This increase in Rho activity led to ~40% increase in ROCK2 expression in HG-treated ECs compared to NG-treated ECs (Fig. 4.2B).

Predictably, this HG-induced EC stiffening was associated with ~50% decrease in TRPV4 expression and activity (Fig. 4.2C).

Pharmacological enhancement of TRPV4 activity inhibits Rho activity and EC stiffening in HG-treated ECs

eNOS-derived NO is also know to inhibit Rho/ROCK activation (3), and TRPV4 is known to enhance eNOS activation (5, 6). To determine whether HG-induced Rho activation and EC stiffening is mediated through TRPV4 impairment, I enhanced TRPV4 activity in HG-treated ECs using a pharmacological TRPV4 agonist GSK1016790A (GSK). G-LISA

assay revealed that the HG-induced increase in Rho activation is significantly suppressed by enhancement of TRPV4 activity (Fig. 4.3A). Further, pharmacological enhancement of TRPV4 activity also inhibited EC stiffening in HG-treated cells (Fig. 4.3B). Together, these findings indicate that TRPV4 is an upstream regulator for Rho/ROCK activation.

Inhibition of ROCK2 restores TRPV4 activity in HG-treated ECs

Since EC stiffness is always in dynamic equilibrium with subendothelial matrix stiffness, increase in EC stiffness feeds back to enhance subendothelial matrix stiffness (7, 8). Thus, Rho/ROCK activation may in turn play a role in TRPV4 activation as well. To determine whether HG-induced Rho/ROCK activation actively contributes to TRPV4 activation, I suppressed ROCK2 activity in HG-treated cells using a pharmacological ROCK inhibitor Y27. HG treatment caused significant downregulation of TRPV4 activity in cultured human retinal ECs, as judged by ~60% decrease ($p<0.001$) in baseline and ~50% decrease ($p<0.001$) in peak Ca^{+} influx levels (Fig. 4.4). Further, activity of TRPV4 in HG-treated retinal ECs was restored with suppression of ROCK activity by Y27.

Inhibition of Rho/ROCK restores NO production in HG-treated ECs via an increase in TRPV4

To determine the role of Rho/ROCK activity in HG-induced EC activation, ECs under HG condition were treated with Y27. To confirm the effect is mediated through TRPV4, the HG+Y27-treated cells were treated with RN1734, a TRPV4 antagonist. Quantitative analyses of ECs labeled with NO-sensitive dye revealed that, HG-treated ECs

exhibit ~65% decrease in intracellular NO levels compared to NG-treated ECs, and this decrease in NO levels was restored with suppression of ROCK activity by Y27 (Fig. 4.5). However, with suppression of TRPV4 activity by a TRPV4 antagonist, the restoration of NO levels was diminished.

Inhibition of Rho/ROCK suppresses activation of HG-treated ECs via an increase in TRPV4

Importantly, quantitatively analyses of cells labeled with ICAM-1 antibody revealed that HG-treated ECs exhibit a ~4.5-fold increase in ICAM-1 expression than NG-treated cells and suppression of ROCK activity significantly inhibited ICAM-1 expression in HG-treated cells (Fig. 4.6A). Further, expression of ICAM-1in HG+Y27-treated ECs was significantly increased by TRPV4 inhibition with RN1734. Consistent with ICAM-1 expression, suppression of ROCK activity significantly inhibited the increased monocyte-EC adhesion in HG-treated cells and inhibition of TRPV4 activity in HG+Y27-treated ECs upregulated monocyte-EC adhesion (Fig. 4.6B). Together, these findings suggest that HG-induced EC activation is mediated through TRPV4, and there is a feedback mechanism between TRPV4 and Rho/ROCK signaling pathways.

Discussion

My previous studies (described in Chapters 2 and 3) identified subendothelial matrix stiffening and associated loss of mechanosensitive TRPV4 as critical determinants

of retinal EC activation associated with high glucose and diabetes. This study was performed to identify the mechanotransduction pathway by which TRPV4 impairment promotes retinal EC activation. The current findings demonstrate that there is a subendothelial matrix stiffness-dependent feedback loop between mechanosensitive Ca^{2+} ion channel TRPV4 and mechanotransducer Rho/ROCK in controlling NO-mediated endothelial-monocyte adhesion.

Since my previous studies (Chapter 3) revealed that HG-induced matrix stiffening impairs TRPV4, endothelial NO levels and enhances monocyte-EC adhesion, here I asked whether this TRPV4-dependent control of EC activation was mediated by Rho/ROCK. Rho/ROCK, the major mechanotransduction pathway that controls cell tension and stiffness, has previously been shown to be inhibited by eNOS-derived NO (3). Further, TRPV4 is known to enhance eNOS activation through a calcium-dependent pathway (5, 6). Thus, it is plausible that NO-dependent control of Rho/ROCK is mediated upstream by the TRPV4 signaling. Indeed, my current findings reveal that HG-induced upregulation of Rho activity and EC stiffness are significantly inhibited upon pharmacological enhancement of TRPV4 activity.

Past studies have shown that matrix stiffening directly increases Rho (1). Further, this matrix stiffening-dependent Rho increase is via integrins (9-11). Rho exerts its effects via its downstream target, Rho-associated Kinase (ROCK). Of the two isoforms of ROCK viz. ROCK1 and ROCK2, the former appears to be more important for immunological functions, whereas the latter is more important for endothelial and vascular smooth muscle function (12, 13).

In addition to subendothelial matrix stiffness, Rho/ROCK can also be regulated by eNOS-derived NO levels (3). Specifically, increase in eNOS activation has been shown to negatively regulate Rho activity both *in vitro* (3) and *in vivo* (14). Importantly, Rho/ROCK is upregulated in various pathological conditions marked by matrix stiffening (7, 8, 15). Indeed, work by our group and others have shown that Rho activity and ROCK2 gene expression are significantly upregulated in diabetic mouse retinas (16, 17) that have stiffer capillaries. These *in vivo* findings correlated strongly with the current *in vitro* findings, which showed that HG treatment significantly increases Rho activity and ROCK expression in cultured retinal ECs. Further, consistent with the ability of Rho/ROCK to increase actomyosin-dependent cell contractility, we found that HG-treated ECs also became significantly stiffer, which agrees well with capillary stiffening observed in earlier studies (Chapter 2).

Since a dynamic equilibrium needs to be achived between EC stiffness and subendothelial matrix stiffness, increase in EC stiffness can feed back to enhance subendothelial matrix stiffness (7, 8). Thus, Rho/ROCK activation may in turn play a role in TRPV4 activation as well. Indeed, my current findings reveal that HG-induced downregulation of TRPV4 is significantly reversed upon pharmacological inhibition of Rho/ROCK activity.

Findings from Chapter 3 revealed that TRPV4 activity positively regulates endothelial NO production. Since TRPV4 enhancement increases Rho activity and EC stiffness, and Rho/ROCK also inhibits both TRPV4 and endothelial NO, it is likely that there is a feedback loop between mechanosensitive Ca^{2+} ion channel TRPV4 and

mechanotransducer Rho/ROCK in controlling NO-mediated endothelial-monocyte adhesion. The current findings confirmed this hypothesis because the increased Rho activity can be significant suppressed by TRPV4 enhancement, inhibition of Rho/ROCK activity significant restored endothelial NO production caused by TRPV4 impairment, and significant increase in endothelial NO production caused by Rho/ROCK inhibition was prevented by TRPV4 suppression. Since endothelial NO suppresses ICAM-1 expression and monocyte-EC adhesion, the aforementioned effects of Rho/ROCK/TRPV4 regulation on endothelial NO production correlated predictably and inversely with these functional responses. These new findings provide a crucial mechanistic understanding of the mechanotransduction pathway underlying the effects of diabetes-induced subendothelial matrix stiffening on retinal endothelial activation and inflammation associated with diabetic retinopathy.

Conclusion

This report showed that HG treatment caused significant retinal EC stiffening and activation *in vitro*, which is consistent with diabetic retinal capillary stiffening and inflammation *in vivo*. These inflammatory effects of HG correlated with significant decrease in expression and activity of TRPV4, and upregulation of Rho activity and ROCK-2 expression in retinal EC cultures. Notably, enhancement of TRPV4 activity alone caused significant decrease in Rho activity. Further, inhibition of ROCK-2 activity alone caused significant recovery of TRPV4 activity, endothelial NO production and suppression

of monocyte-EC adhesion. More importantly, pharmacological enhancement of TRPV4 alone suppressed the Rho-mediated EC stiffening and the inflammatory effects *in vitro*, which indicates there is a feedback loop between TRPV4 and Rho/ROCK. Thus, TRPV4 activity is both a target and an effector of Rho/ROCK signaling. These findings identify a crucial role of Rho/ROCK-mediated TRPV4 signaling in diabetic retinal inflammation and implicate Rho/ROCK and TRPV4 as the novel anti-inflammatory target for management of early DR.

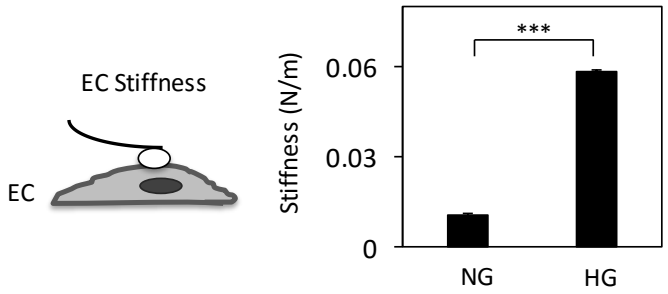

FIGURE 4.1. HG treatment increases EC stiffness. Stiffness of human retinal ECs was measured by an atomic force microscope (AFM) fitted with a ~5 μm glass bead tip (schematic). Quantitative analysis of multiple ($n \geq 13$) force indentation measurements revealed a 5-fold (***, $p<0.001$) increase in retinal EC stiffness under HG condition than in NG condition. NG: Normal Glucose, 5.5 mM; HG: High Glucose, 30 mM. ***, $p<0.001$.

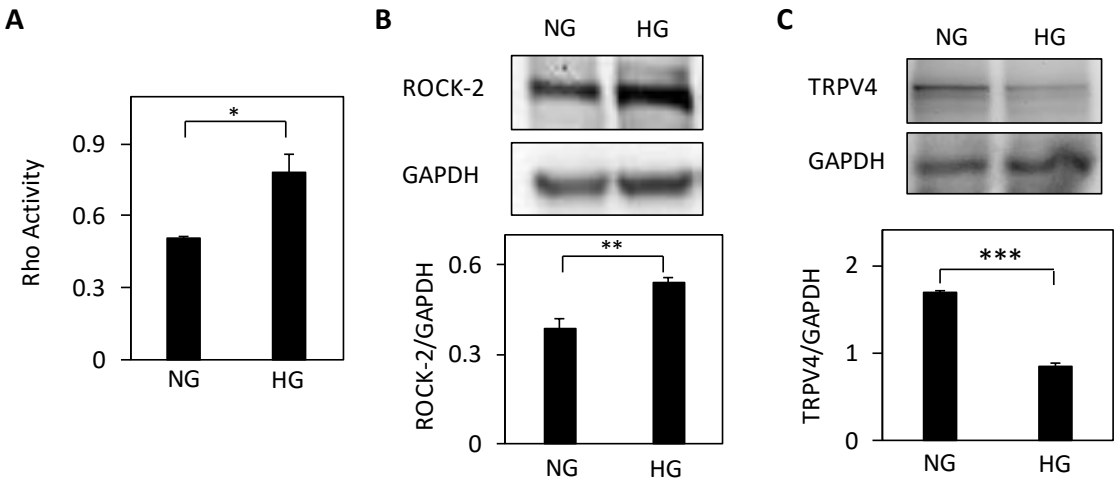

FIGURE 4.2. Rho/ROCK2 and TRPV4 is upregulated in HG-treated ECs. (A) Rho activity was measured with a G-LISA Activation Assay Kit. Quantitative analysis of multiple ($n \geq 3$) samples revealed a 50% (*, $p<0.05$) increase in Rho activity under HG condition than in NG condition. (B) Representative Western blot bands and their densitometric analyses (bar graphs) together reveal that ROCK-2 expression is ~40% higher (***, $p<0.001$) in HG-treated ECs when compared with NG-treated ECs. Bar graphs indicate average ± SEM. ROCK-2 levels were normalized with respect to the corresponding levels of GAPDH (loading control). (C) Representative Western blot bands and their densitometric analyses (bar graphs) together reveal that TRPV4 expression is significantly higher (***, $p<0.001$) in HG-treated ECs when compared with NG-treated ECs. Bar graphs indicate average ± SEM. TRPV4 levels were normalized with respect to the corresponding levels of GAPDH (loading control). *, $p<0.05$; **, $p<0.01$; ***, $p<0.001$.

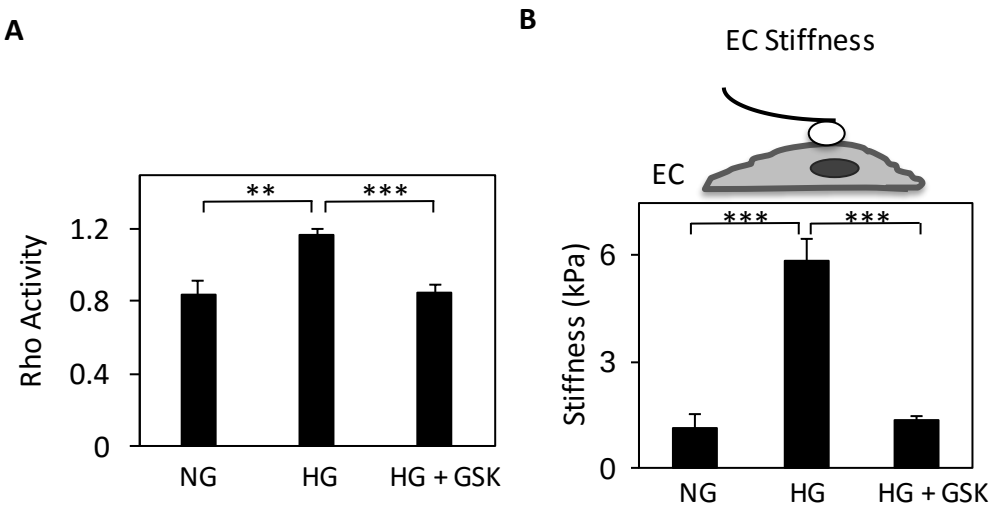

FIGURE 4.3. Pharmacological enhancement of TRPV4 activity inhibits Rho activity and EC stiffening in HG-treated ECs. (A) Rho activity was measured with a G-LISA Activation Assay Kit. Quantitative analysis of multiple (n≥3) samples revealed that HG-induced increase in Rho activity was inhibited by pharmacological enhancement of TRPV4 activity. (B) Stiffness of human retinal ECs was measured by an atomic force microscope (AFM) fitted with a ~5 μm glass bead tip (schematic). Quantitative analysis of multiple (n≥13) force indentation measurements revealed HG-induced EC stiffening was inhibited with TRPV4 enhancement. GSK: GSK1016790A, TRPV4 agonist. **, $p<0.01$; ***, $p<0.001$.

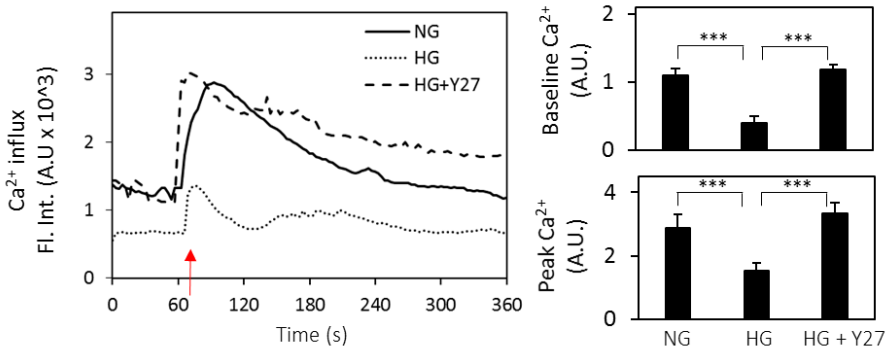

FIGURE 4.4. Inhibition of ROCK2 restores TRPV4 activity in HG-treated ECs. Calcium microfluorimetry was performed in Fluo4-AM-loaded human retinal ECs cultured in medium containing NG, HG ±Y27632 (ROCK inhibitor). Line graph from a representative cell and bar graph (average ± SEM) from multiple (n≥20) cells reveal that HG treatment significantly inhibits TRPV4 activity, as indicated by a ~60% and ~50% decrease (***, $p<0.001$) in baseline Ca^{2+} and peak Ca^{2+} influx levels, respectively. Arrow indicates the moment selective TRPV4 agonist GSK1016790A was added to cells. Y27: Y27632, ROCK inhibitor. ***, $p<0.001$.

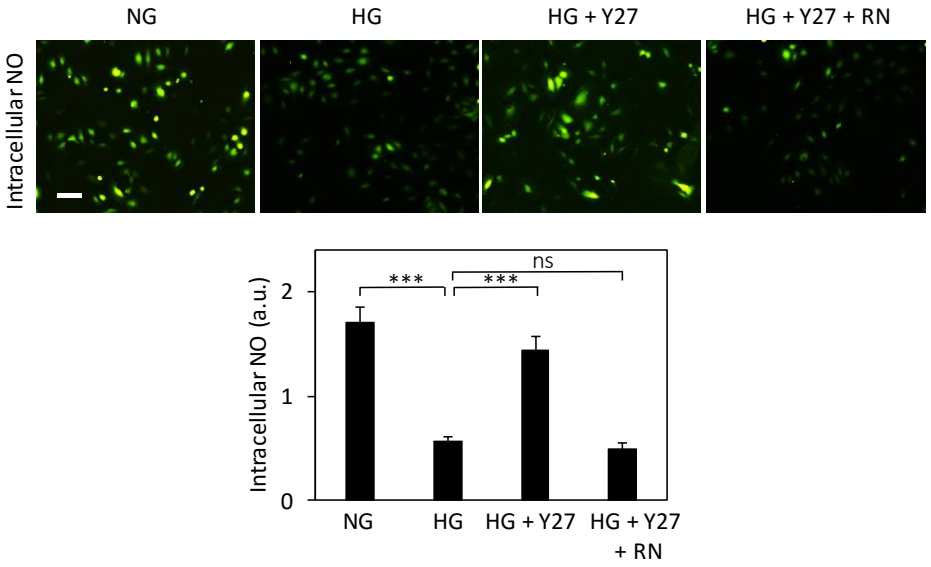

FIGURE 4.5. Inhibition of Rho/ROCK restores NO production in HG-treated ECs via an increase in TRPV4. (A) Human retinal ECs labeled with DAF-FM diacetate, a NO-sensitive dye, and subsequent intensity measurements (n≥25 cells) reveal that inhibition of ROCK activity prevents the loss of constitutive NO production caused by HG treatment. Further, the prevention of NO impairment was lost with TRPV4 inhibition by RN. RN: RN1737, TRPV4 antagonist. ***, $p<0.001$; ns, no significance.

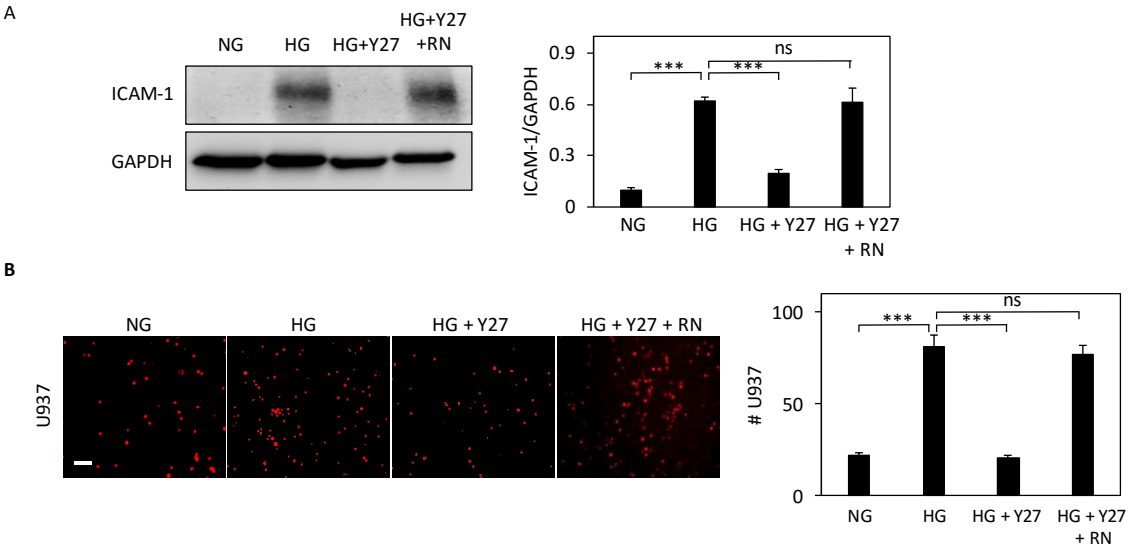

FIGURE 4.6. Inhibition of Rho/ROCK suppresses activation of HG-treated ECs via an increase in TRPV4. (A) Western blot bands and their densitometric analyses (bar graph) together reveal that HG treatment produces an ~4.5-fold increase in ICAM-1 expression than NG treatment and inhibition of ROCK activity prevents ICAM-1 upregulation, but RN treatment diminished the prevention effect of Y27. ICAM-1 levels were normalized with respect to the corresponding levels of GAPDH (loading control). (B) Fluorescently-labeled U937 cells were added to EC monolayers for 30 min. Subsequent cell count of adherent U937 cells (bar graph) revealed that the Y27-induced suppression of ICAM-1 expression in HG-treated ECs resulted in ~75% decrease (***, $p<0.001$) in monocyte-EC adhesion, and RN treatment enhanced monocyte-EC adhesion in HG+Y27-treated cells. Bar graph indicates average ± SEM from multiple ($n\geq10$) images of monocyte-EC co-cultures. ***, $p<0.001$; ns, no significance.

References

1. Huynh, J., Nishimura, N., Rana, K., Peloquin, J. M., Califano, J. P., Montague, C. R., King, M. R., Schaffer, C. B., and Reinhart-King, C. A. (2011) Age-related intimal stiffening enhances endothelial permeability and leukocyte transmigration. *Science translational medicine* **3**, 112ra122

2. Burridge, K., and Wennerberg, K. (2004) Rho and Rac take center stage. *Cell* **116**, 167-179

3. Suzuki, H., Kimura, K., Shirai, H., Eguchi, K., Higuchi, S., Hinoki, A., Ishimaru, K., Brailoiu, E., Dhanasekaran, D. N., Stemmle, L. N., Fields, T. A., Frank, G. D., Autieri, M. V., and Eguchi, S. (2009) Endothelial nitric oxide synthase inhibits G12/13 and rho-kinase activated by the angiotensin II type-1 receptor: implication in vascular migration. *Arteriosclerosis, thrombosis, and vascular biology* **29**, 217-224

4. Thodeti, C. K., Matthews, B., Ravi, A., Mammoto, A., Ghosh, K., Bracha, A. L., and Ingber, D. E. (2009) TRPV4 channels mediate cyclic strain-induced endothelial cell reorientation through integrin-to-integrin signaling. *Circulation research* **104**, 1123-1130

5. Jardin, I., Dionisio, N., Lopez, J. J., Salido, G. M., and Rosado, J. A. (2013) Pharmacology of TRP channels in the vasculature. *Current vascular pharmacology* **11**, 480-489

6. Adapala, R. K., Talasila, P. K., Bratz, I. N., Zhang, D. X., Suzuki, M., Meszaros, J. G., and Thodeti, C. K. (2011) PKCalpha mediates acetylcholine-induced activation of TRPV4-dependent calcium influx in endothelial cells. *American journal of physiology. Heart and circulatory physiology* **301**, H757-765

7. Huveneers, S., Daemen, M. J., and Hordijk, P. L. (2015) Between Rho(k) and a hard place: the relation between vessel wall stiffness, endothelial contractility, and cardiovascular disease. *Circulation research* **116**, 895-908

8. Ghosh, K., Thodeti, C. K., Dudley, A. C., Mammoto, A., Klagsbrun, M., and Ingber, D. E. (2008) Tumor-derived endothelial cells exhibit aberrant Rho-mediated mechanosensing and abnormal angiogenesis in vitro. *Proceedings of the National Academy of Sciences of the United States of America* **105**, 11305-11310

9. Matthews, B. D., Overby, D. R., Mannix, R., and Ingber, D. E. (2006) Cellular adaptation to mechanical stress: role of integrins, Rho, cytoskeletal tension and mechanosensitive ion channels. *Journal of cell science* **119**, 508-518

10. Paszek, M. J., Zahir, N., Johnson, K. R., Lakins, J. N., Rozenberg, G. I., Gefen, A., Reinhart-King, C. A., Margulies, S. S., Dembo, M., Boettiger, D., Hammer, D. A., and Weaver, V. M. (2005) Tensional homeostasis and the malignant phenotype. *Cancer Cell* **8**, 241-254

11. Galbraith, C. G., Yamada, K. M., and Sheetz, M. P. (2002) The relationship between force and focal complex development. *The Journal of cell biology* **159**, 695-705

12. Burridge, K., and Wennerberg, K. (2004) Rho and Rac Take Center Stage. *Cell* **116**, 167-179

13. Liu, P. Y., and Liao, J. K. (2008) A method for measuring Rho kinase activity in tissues and cells. *Methods Enzymol* **439**, 181-189

14. Reimann, K., Krishnamoorthy, G., and Wangemann, P. (2013) NOS inhibition enhances myogenic tone by increasing rho-kinase mediated Ca2+ sensitivity in the male but not the female gerbil spiral modiolar artery. *PloS one* **8**, e53655

15. Huang, S., and Ingber, D. E. (2005) Cell tension, matrix mechanics, and cancer development. *Cancer Cell* **8**, 175-176

16. Monickaraj, F., McGuire, P. G., Nitta, C. F., Ghosh, K., and Das, A. (2015) Cathepsin D: an Mvarphi-derived factor mediating increased endothelial cell permeability with implications for alteration of the blood-retinal barrier in diabetic retinopathy. *FASEB journal : official publication of the Federation of American Societies for Experimental Biology*

17. Arita, R., Hata, Y., Nakao, S., Kita, T., Miura, M., Kawahara, S., Zandi, S., Almulki, L., Tayyari, F., Shimokawa, H., Hafezi-Moghadam, A., and Ishibashi, T. (2009) Rho kinase inhibition by fasudil ameliorates diabetes-induced microvascular damage. *Diabetes* **58**, 215-226

CHAPTER 5

CONCLUSION

The goal of this research was to understand the role of cell- and subendothelial matrix-dependent mechanical cues in retinal vascular inflammation associated with diabetes and to identify novel molecular targets for effective suppression of diabetic retinal vascular inflammation. As reported in Chapter 2, lysyl oxidase (LOX) is a key molecular determinant of retinal subendothelial matrix stiffening associated with diabetes. Further, high glucose-induced subendothelial matrix stiffening alone is necessary and sufficient to promote diabetic retinal EC activation, which can be prevented by LOX inhibition. However, the molecular mechanism behind this subendothelial matrix stiffness-induced retinal EC activation and inflammation remains unknown.

With the hope to identify the mechanosensitive mechanism implicated in this subendothelial matrix stiffening-dependent retinal EC activation, Chapter 3 explored the role of mechanosensitive TRPV4 channel, a member of the transmembrane TRP family of Ca^{2+} channels, which is ubiquitously expressed in ECs. Here I showed that (i) high glucose-induced subendothelial matrix stiffening significantly impairs TRPV4 expression and activity, (ii) TRPV4 impairment alone is sufficient to promote high glucose-induced retinal EC activation, (iii) LOX inhibition prevents high glucose-induced impairment of TRPV4 and, consequently, anti-inflammatory nitric oxide. These findings identify a crucial role of

mechanosensitive TRPV4 in diabetic retinal inflammation. However, the mechanotransduction mechanism underlying the TRPV4-mediated diabetic retinal EC activation remains to be examined.

Finally, Chapter 4 showed that the TRPV4-dependent diabetic EC activation is mediated, at least in part, via the canonical Rho/ROCK mechanotransduction pathway that directly controls EC stiffness. Additionally, there is a feedback mechanism between TRPV4 and Rho/ROCK signaling pathways and it is likely to exacerbate retinal capillary stiffening and inflammation associated with DR. Together, these findings identify a crucial role of TRPV4-mediated Rho/ROCK signaling in diabetic retinal inflammation and implicate TRPV4 as the novel anti-inflammatory target for management of early DR.

Working Model

The findings from my studies indicate a complex mechanochemical signaling mechanism that links matrix stiffening and retinal inflammation in diabetes. Specifically, we showed that diabetes enhances LOX. Although these studies do not focus on the underlying mechanism in diabetes-induced LOX upregulation, past studies have shown that hypoxia-inducible factor-1 (HIF-1) was significantly upregulated under diabetic condition (1, 2), and LOX can be regulated by HIF-1 at transcriptional level (3). Thus, I speculate that diabetes/HG-induced LOX upregulation is mediated through upregulation of HIF-1 (Schematic 5.1A).

My findings also show that LOX upregulation leads to subendothelial matrix stiffening. LOX is a copper-dependent amine oxidase that crosslinks collagen and increases matrix stiffness (4) (Schematic 5.1B). This HG-induced subendothelial matrix stiffening significantly impairs TRPV4 expression and activity. However, whether subendothelial matrix stiffness control TRPV4 expression and activity remains unclear. Integrins are the major transmembrane cell surface receptors that mediate cell adhesion to matrix molecules (5). Additionally, they transmit external forces (such as matrix stiffness-dependent resistance force) rapidly to TRPV4 via a "hardwired" framework. It is this *physical* association between integrins and TRPV4 that confers the latter its mechanosensitivity (6) (Schematic 5.1C). Thus, I speculate that the matrix stiffening-dependent TRPV4 impairment is mediated through integrin activity.

Next, TRPV4 is known to enhance eNOS activation through calcium-dependent pathway (7, 8). Calcium influx induced by TRPV4 activation caused increase in cytoplasmic calcium levels and activates calmodulin (CaM). CaM binds to the CaM-binding domain in eNOS, causes alignment of the oxygenase and reductase domains of eNOS, and then leads to efficient NO synthesis. Additionally, CaM activates CaM kinase II (CaMKII), which phosphorylate eNOS on S1179 and promote nitric oxide (NO) synthesis (Schematic 5.1D). Thus, impaired TRPV4 activation inhibits eNOS-derived NO production and decreased endothelial NO levels in retinal ECs.

eNOS produces constitutively low levels of NO that inhibits activation of inhibitory κB kinase (IKK), the prerequisite enzyme complex necessary to induce NF-κB nuclear translocation (activation) in ECs (9-11) (Schematic 5.1E). Decreased endothelial NO

causes activation of NF-κB and leads to downstream transcription of pro-inflammatory factors (TNF-α, IL-6) and cell adhesion molecule (ICAM-1) (Schematic 5.1F). This increase in ICAM-1 leads to increased monocyte-EC adhesion via binding of ICAM-1 (on ECs) and $\alpha_m\beta_2$ integrin (on monocytes) (Schematic 5.1G).

More importantly, eNOS-derived NO is also know to inhibit Rho/ROCK activation via inhibition of $G_{12/13}$, family of heterotrimeric G proteins (12) (Schematic 5.1H). $G_{12/13}$ stimulate Rho guanine nucleotide exchange factors (GEFs). Thus, inhibition of NO enhances $G_{12/13}$ and upregulates GEF that, in turn, promotes Rho-GDP (inactive) transformation to Rho-GTP (active). This increase in Rho activity leads to an increase in cytoskeleton tension (cell stiffening) via activation of its downstream effector, Rho-associated Kinase (ROCK) (13). ROCK activates myosin to generate contractility that increases cell stiffness. Together, increase in both retinal EC and endothelial matrix stiffness result to retinal capillary stiffening.

Finally, since EC stiffness is always in dynamic equilibrium with matrix stiffness, increase in EC stiffness feeds back to enhance matrix stiffness through increasing contractility force (14, 15). The increase in cell contractility pulls on the endothelial matrix through integrin, which physically causes an increase in local density and stiffness of endothelial matrix. This further impairs TRPV4 and downstream endothlial NO levels. The existence of this feedback mechanism between TRPV4 and Rho/ROCK signaling pathways is likely to exacerbate retinal capillary stiffening and inflammation associated with DR. Therefore, future *in vivo* studies that aim to enhance TRPV4 through a nanotechnological approach may be come a more effective in managing DR.

Future Directions

Although HIF-1 is known to be upregulated under diabetic/HG condition and LOX is a directly transcriptional target of HIF-1, the link between diabetes/HG and HIF-1-dependent LOX expression has not been explicitly demonstrated. To confirm the role of diabetes-induced HIF-1 upregulation in LOX overexpression, 8-10 weeks old STZ-diabetic adult mice (C57BL/6) will be divided into two groups: no treatment (vehicle only), treatment with HIF-1 inhibitor EZN-2698, an antisense oligonucleotide that can specifically bind to HIF-1α mRNA with high affinity and cause down-regulation of HIF-1α protein levels (16). Treatments will begin at the onset of diabetes and continue for the duration of the experiment. After 3 months of diabetes, mice will be sacrificed and whole retinas will be harvested for assessment of LOX expression (Western Blot). Age-matched (untreated) nondiabetic mice will serve as controls. To confirm the role of HG-induced HIF-1 upregulation in LOX overexpression, human retinal ECs under HG condition will be treated with a HIF-1 inhibitor EZN-2698. Culture medium and cell lysates will be collected for measurements of LOX activity (Amplex Red assay) and expression (Western Blot), respectively.

Retinas of diabetic animals and humans contain high levels of oxidative stress, advanced glycation end-products (AGEs), and fibronectin in capillary basement membrane (17-19). Notably, these biochemical factors are implicated in enhancing LOX expression and/or activity. Specifically, past studies have shown that (a) reactive oxygen species

(ROS) enhance LOX expression in ECs and dermal fibroblasts (20, 21), (b) AGEs enhance LOX expression and activity in aortic ECs and ovarian tissues (22, 23), and (c) fibronectin interacts with both LOX and collagen IV (the major structural protein in basement membrane) and regulates LOX activity (24). Since these factors are overexpressed in the retina of diabetic mice, it will be important to investigate whether they contribute to the observed increase in retinal LOX expression and capillary stiffening.

To investigate the role of oxidative stress and AGEs on retinal LOX upregulation and capillary stiffening, 8-10 weeks old STZ-diabetic adult mice (C57BL/6) will be divided into three groups: no treatment (vehicle only), treatment with NADPH (superoxide) inhibitor apocynin (37 mg/Kg in feed(25, 26)), and treatment with AGE inhibitor aminoguanidine (1 g/L through drinking water(27)). To investigate the role of fibronectin on retinal LOX upregulation and capillary stiffening, 8-10 weeks old STZ-diabetic adult mice (C57BL/6) will be divided into three groups: no treatment (vehicle only), and treatment with antisense oligonucleotide against fibronectin (28-30) or scrambled oligonucleotides. Treatments will begin at the onset of diabetes and continue for the duration of the experiment. Age-matched (untreated) nondiabetic mice will serve as controls. Mice will be sacrificed after 3 months of diabetes and whole retinas will be harvested for assessment of LOX activity, and superoxide (Amplex Red assay) or AGEs (Western Blot). Intact retinal capillaries will be isolated for measurement of (1) LOX and ICAM-1 mRNA, (2) LOX activity, (3) superoxide, AGEs, or fibronectin and (4) retinal capillary stiffness (AFM). Levels of oxidative stress, AGEs, or fibronectin will be correlated with LOX and retinal capillary stiffness.

Acute mechanical activation of integrins is known to rapidly activate TRPV4 (6). However, the role of chronic integrin activation, which is likely occurring on the stiffer subendothelial matrix, in TRPV4 impairment remains unknown. This is important to know because it would reveal whether the impaired TRPV4 expression and activity that observed in the stiffer retinal capillaries and EC cultures is mediated upstream by abnormal integrin-matrix interactions. To investigate this, I will focus on two specific integrin-matrix interactions: α2β1-collagen IV and α5β1-fibronectin, because collagen IV is a key capillary basement membrane molecule that retinal ECs bind to (using α2β1) under physiological conditions while fibronectin (α5β1 integrin) is abundantly expressed in retinal capillaries in diabetes. Cultured human retinal ECs will be grown on 1000 Pa (normal) or 4000 Pa (stiff) synthetic matrices surface-coated with equimolar doses (5 $\mu g/cm^2$) of either collagen IV or fibronectin. TRPV4 expression and activity will be measured by Western Blot and Ca^{2+} microfluorimetry, as shown in Chapter 3, while integrin activity will be measured by adding distinct 'activation-specific' antibodies against the individual integrin and comparing antibody binding (and thus, integrin activation state) using flow cytometry, as previously reported (15, 31).

Diabetes-induced capillary lesions develop slowly, and require 6-8 months of diabetes to become statistically greater than normal (32). Thus, it is important to know the long term effect (in mice – 8 mos of diabetes) of LOX inhibition and TRPV4 activation in DR. STZ-diabetic C57BL/6 mice will be divided into three groups (n= 20/group): no treatment (vehicle only), treatment with LOX inhibitor (BAPN), and treatment with TRPV4 agonist (GSK1016790A). Treatments will begin at the onset of overt diabetes and

continue for the duration of the experiment. Age-matched (untreated) nondiabetic mice will serve as controls. LOX and TRPV4 expression will be measured in retinal capillaries isolated from these mice after 8 months of diabetes and correlated with retinal capillary stiffness (measured by AFM). To assess vascular leakage (hyperpermeability), mice will receive intravenous FITC-dextran injections and sacrificed 20 min later (following perfusion) for quantification of FITC-dextran leakage into retinal tissue (32-35). For assessment of diabetes-induced capillary lesions viz. acellular (degenerate) capillaries and pericyte loss, isolated retinal capillaries will be stained with Periodic acid–Schiff and subjected to quantitative image analyses (32-35).

Together with my current findings, completing these future studies will not only identify other previously-unrecognized mechanochemical mechanisms underlying DR pathogenesis, but also further confirm the important role of LOX and TRPV4 in retinal inflammation associated with early DR. Therefore, these studies implicate LOX and TRPV4 as new anti-inflammatory targets for DR therapy.

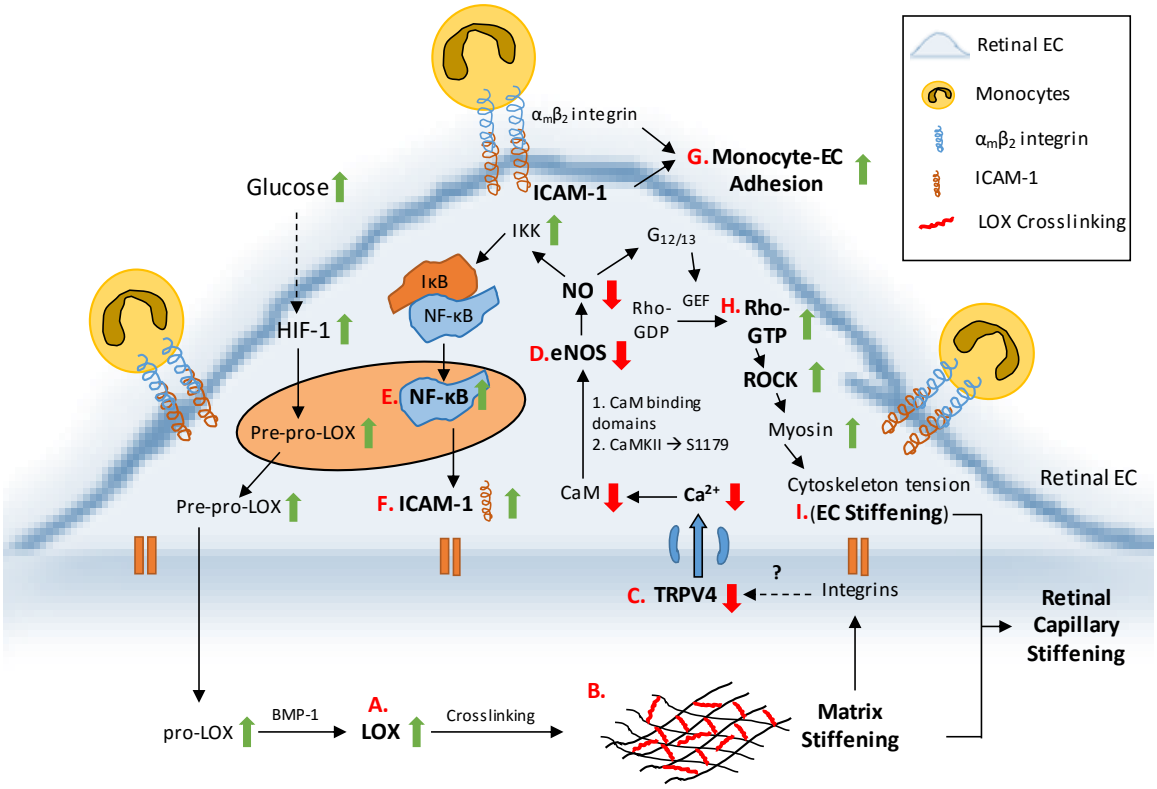

Schematic 5.1: Illustration of mechanisms in subendothelial matrix stiffness-dependent EC activation. HIF-1: hypoxia inducible factor-1; CaM: calmodulin; CaMKII: calmodulin kinase II; IKK: inhibitory κB kinase; GEF: guanine nucleotide exchange factor.

References

1. Yan, H. T., and Su, G. F. (2014) Expression and significance of HIF-1 alpha and VEGF in rats with diabetic retinopathy. *Asian Pac J Trop Med* **7**, 237-240

2. Yan, J., Zhang, Z., and Shi, H. (2012) HIF-1 is involved in high glucose-induced paracellular permeability of brain endothelial cells. *Cell Mol Life Sci* **69**, 115-128

3. Erler, J. T., Bennewith, K. L., Nicolau, M., Dornhofer, N., Kong, C., Le, Q. T., Chi, J. T., Jeffrey, S. S., and Giaccia, A. J. (2006) Lysyl oxidase is essential for hypoxia-induced metastasis. *Nature* **440**, 1222-1226

4. Barker, H. E., Cox, T. R., and Erler, J. T. (2012) The rationale for targeting the LOX family in cancer. *Nature reviews. Cancer* **12**, 540-552

5. Mammoto, A., Mammoto, T., and Ingber, D. E. (2008) Rho signaling and mechanical control of vascular development. *Current opinion in hematology* **15**, 228-234

6. Matthews, B. D., Thodeti, C. K., Tytell, J. D., Mammoto, A., Overby, D. R., and Ingber, D. E. (2010) Ultra-rapid activation of TRPV4 ion channels by mechanical forces applied to cell surface beta1 integrins. *Integr Biol (Camb)* **2**, 435-442

7. Jardin, I., Dionisio, N., Lopez, J. J., Salido, G. M., and Rosado, J. A. (2013) Pharmacology of TRP channels in the vasculature. *Current vascular pharmacology* **11**, 480-489

8. Adapala, R. K., Talasila, P. K., Bratz, I. N., Zhang, D. X., Suzuki, M., Meszaros, J. G., and Thodeti, C. K. (2011) PKCalpha mediates acetylcholine-induced activation of TRPV4-dependent calcium influx in endothelial cells. *American journal of physiology. Heart and circulatory physiology* **301**, H757-765

9. Cirino, G., Fiorucci, S., and Sessa, W. C. (2003) Endothelial nitric oxide synthase: the Cinderella of inflammation? *Trends in pharmacological sciences* **24**, 91-95

10. Kolluru, G. K., Siamwala, J. H., and Chatterjee, S. (2010) eNOS phosphorylation in health and disease. *Biochimie* **92**, 1186-1198

11. Reynaert, N. L., Ckless, K., Korn, S. H., Vos, N., Guala, A. S., Wouters, E. F., van der Vliet, A., and Janssen-Heininger, Y. M. (2004) Nitric oxide represses inhibitory kappaB kinase through S-nitrosylation. *Proceedings of the National Academy of Sciences of the United States of America* **101**, 8945-8950

12. Suzuki, H., Kimura, K., Shirai, H., Eguchi, K., Higuchi, S., Hinoki, A., Ishimaru, K., Brailoiu, E., Dhanasekaran, D. N., Stemmle, L. N., Fields, T. A., Frank, G. D.,

Autieri, M. V., and Eguchi, S. (2009) Endothelial nitric oxide synthase inhibits G12/13 and rho-kinase activated by the angiotensin II type-1 receptor: implication in vascular migration. *Arteriosclerosis, thrombosis, and vascular biology* **29**, 217-224

13. Huynh, J., Nishimura, N., Rana, K., Peloquin, J. M., Califano, J. P., Montague, C. R., King, M. R., Schaffer, C. B., and Reinhart-King, C. A. (2011) Age-related intimal stiffening enhances endothelial permeability and leukocyte transmigration. *Science translational medicine* **3**, 112ra122

14. Huveneers, S., Daemen, M. J., and Hordijk, P. L. (2015) Between Rho(k) and a hard place: the relation between vessel wall stiffness, endothelial contractility, and cardiovascular disease. *Circulation research* **116**, 895-908

15. Ghosh, K., Thodeti, C. K., Dudley, A. C., Mammoto, A., Klagsbrun, M., and Ingber, D. E. (2008) Tumor-derived endothelial cells exhibit aberrant Rho-mediated mechanosensing and abnormal angiogenesis in vitro. *Proceedings of the National Academy of Sciences of the United States of America* **105**, 11305-11310

16. Onnis, B., Rapisarda, A., and Melillo, G. (2009) Development of HIF-1 inhibitors for cancer therapy. *J Cell Mol Med* **13**, 2780-2786

17. Antonetti, D. A., Klein, R., and Gardner, T. W. (2012) Diabetic retinopathy. *The New England journal of medicine* **366**, 1227-1239

18. Das, A., McGuire, P. G., and Rangasamy, S. (2015) Diabetic Macular Edema: Pathophysiology and Novel Therapeutic Targets. *Ophthalmology* **122**, 1375-1394

19. Das, A., Stroud, S., Mehta, A., and Rangasamy, S. (2015) New treatments for diabetic retinopathy. *Diabetes, obesity & metabolism* **17**, 219-230

20. Guadall, A., Orriols, M., Alcudia, J. F., Cachofeiro, V., Martinez-Gonzalez, J., and Rodriguez, C. (2011) Hypoxia-induced ROS signaling is required for LOX up-regulation in endothelial cells. *Front Biosci (Elite Ed)* **3**, 955-967

21. Majora, M., Wittkampf, T., Schuermann, B., Schneider, M., Franke, S., Grether-Beck, S., Wilichowski, E., Bernerd, F., Schroeder, P., and Krutmann, J. (2009) Functional consequences of mitochondrial DNA deletions in human skin fibroblasts: increased contractile strength in collagen lattices is due to oxidative stress-induced lysyl oxidase activity. *The American journal of pathology* **175**, 1019-1029

22. Adamopoulos, C., Piperi, C., Gargalionis, A. N., Dalagiorgou, G., Spilioti, E., Korkolopoulou, P., Diamanti-Kandarakis, E., and Papavassiliou, A. G. (2015) Advanced glycation end products upregulate lysyl oxidase and endothelin-1 in

human aortic endothelial cells via parallel activation of ERK1/2-NF-kappaB and JNK-AP-1 signaling pathways. *Cellular and molecular life sciences : CMLS*

23. Papachroni, K. K., Piperi, C., Levidou, G., Korkolopoulou, P., Pawelczyk, L., Diamanti-Kandarakis, E., and Papavassiliou, A. G. (2010) Lysyl oxidase interacts with AGE signalling to modulate collagen synthesis in polycystic ovarian tissue. *Journal of cellular and molecular medicine* **14**, 2460-2469

24. Fogelgren, B., Polgar, N., Szauter, K. M., Ujfaludi, Z., Laczko, R., Fong, K. S., and Csiszar, K. (2005) Cellular fibronectin binds to lysyl oxidase with high affinity and is critical for its proteolytic activation. *The Journal of biological chemistry* **280**, 24690-24697

25. Du, Y., Cramer, M., Lee, C. A., Tang, J., Muthusamy, A., Antonetti, D. A., Jin, H., Palczewski, K., and Kern, T. S. (2015) Adrenergic and serotonin receptors affect retinal superoxide generation in diabetic mice: relationship to capillary degeneration and permeability. *FASEB journal : official publication of the Federation of American Societies for Experimental Biology* **29**, 2194-2204

26. Du, Y., Veenstra, A., Palczewski, K., and Kern, T. S. (2013) Photoreceptor cells are major contributors to diabetes-induced oxidative stress and local inflammation in the retina. *Proceedings of the National Academy of Sciences of the United States of America* **110**, 16586-16591

27. Berdal, M., and Jenssen, T. (2014) Effects of AGE Inhibition with Aminoguanidine in a Diabetic db/db Mouse Wound Model. *Journal of Diabetes Mellitus* **4**, 107-114

28. Oshitari, T., Polewski, P., Chadda, M., Li, A. F., Sato, T., and Roy, S. (2006) Effect of combined antisense oligonucleotides against high-glucose- and diabetes-induced overexpression of extracellular matrix components and increased vascular permeability. *Diabetes* **55**, 86-92

29. Roy, S., Sato, T., Paryani, G., and Kao, R. (2003) Downregulation of fibronectin overexpression reduces basement membrane thickening and vascular lesions in retinas of galactose-fed rats. *Diabetes* **52**, 1229-1234

30. Roy, S., Zhang, K., Roth, T., Vinogradov, S., Kao, R. S., and Kabanov, A. (1999) Reduction of fibronectin expression by intravitreal administration of antisense oligonucleotides. *Nature biotechnology* **17**, 476-479

31. Thodeti, C. K., Matthews, B., Ravi, A., Mammoto, A., Ghosh, K., Bracha, A. L., and Ingber, D. E. (2009) TRPV4 channels mediate cyclic strain-induced endothelial cell reorientation through integrin-to-integrin signaling. *Circulation research* **104**, 1123-1130

32. Robinson, R., Barathi, V. A., Chaurasia, S. S., Wong, T. Y., and Kern, T. S. (2012) Update on animal models of diabetic retinopathy: from molecular approaches to mice and higher mammals. *Disease models & mechanisms* **5**, 444-456

33. Veenstra, A., Liu, H., Lee, C. A., Du, Y., Tang, J., and Kern, T. S. (2015) Diabetic Retinopathy: Retina-Specific Methods for Maintenance of Diabetic Rodents and Evaluation of Vascular Histopathology and Molecular Abnormalities. *Current protocols in mouse biology* **5**, 247-270

34. Liu, H., Tang, J., Du, Y., Lee, C. A., Golczak, M., Muthusamy, A., Antonetti, D. A., Veenstra, A. A., Amengual, J., von Lintig, J., Palczewski, K., and Kern, T. S. (2015) Retinylamine Benefits Early Diabetic Retinopathy in Mice. *The Journal of biological chemistry* **290**, 21568-21579

35. Rajashekhar, G., Ramadan, A., Abburi, C., Callaghan, B., Traktuev, D. O., Evans-Molina, C., Maturi, R., Harris, A., Kern, T. S., and March, K. L. (2014) Regenerative therapeutic potential of adipose stromal cells in early stage diabetic retinopathy. *PloS one* **9**, e84671